United States Nuclear Regulatory Commission

Protecting People and the Environment

NUREG-2160

Post-Test Examination Results from Integral, High-Burnup, Fueled LOCA Tests at Studsvik Nuclear Laboratory

Office of Nuclear Regulatory Research

AVAILABILITY OF REFERENCE MATERIALS IN NRC PUBLICATIONS

NRC Reference Material

As of November 1999, you may electronically access NUREG-series publications and other NRC records at NRC's Public Electronic Reading Room at http://www.nrc.gov/reading-rm.html. Publicly released records include, to name a few, NUREG-series publications; *Federal Register* notices; applicant, licensee, and vendor documents and correspondence; NRC correspondence and internal memoranda; bulletins and information notices; inspection and investigative reports; licensee event reports; and Commission papers and their attachments.

NRC publications in the NUREG series, NRC regulations, and Title 10, "Energy," in the *Code of Federal Regulations* may also be purchased from one of these two sources.

1. The Superintendent of Documents
   U.S. Government Printing Office
   Mail Stop SSOP
   Washington, DC 20402–0001
   Internet: bookstore.gpo.gov
   Telephone: 202-512-1800
   Fax: 202-512-2250
2. The National Technical Information Service
   Springfield, VA 22161–0002
   www.ntis.gov
   1–800–553–6847 or, locally, 703–605–6000

A single copy of each NRC draft report for comment is available free, to the extent of supply, upon written request as follows:
Address: U.S. Nuclear Regulatory Commission
Office of Administration
Publications Branch
Washington, DC 20555-0001
E-mail: DISTRIBUTION.RESOURCE@NRC.GOV
Facsimile: 301–415–2289

Some publications in the NUREG series that are posted at NRC's Web site address http://www.nrc.gov/reading-rm/doc-collections/nuregs are updated periodically and may differ from the last printed version. Although references to material found on a Web site bear the date the material was accessed, the material available on the date cited may subsequently be removed from the site.

Non-NRC Reference Material

Documents available from public and special technical libraries include all open literature items, such as books, journal articles, transactions, *Federal Register* notices, Federal and State legislation, and congressional reports. Such documents as theses, dissertations, foreign reports and translations, and non-NRC conference proceedings may be purchased from their sponsoring organization.

Copies of industry codes and standards used in a substantive manner in the NRC regulatory process are maintained at—
The NRC Technical Library
Two White Flint North
11545 Rockville Pike
Rockville, MD 20852–2738

These standards are available in the library for reference use by the public. Codes and standards are usually copyrighted and may be purchased from the originating organization or, if they are American National Standards, from—
American National Standards Institute
11 West 42nd Street
New York, NY 10036–8002
www.ansi.org
212–642–4900

Legally binding regulatory requirements are stated only in laws; NRC regulations; licenses, including technical specifications; or orders, not in NUREG-series publications. The views expressed in contractor-prepared publications in this series are not necessarily those of the NRC.

The NUREG series comprises (1) technical and administrative reports and books prepared by the staff (NUREG–XXXX) or agency contractors (NUREG/CR–XXXX), (2) proceedings of conferences (NUREG/CP–XXXX), (3) reports resulting from international agreements (NUREG/IA–XXXX), (4) brochures (NUREG/BR–XXXX), and (5) compilations of legal decisions and orders of the Commission and Atomic and Safety Licensing Boards and of Directors' decisions under Section 2.206 of NRC's regulations (NUREG–0750).

DISCLAIMER: This report was prepared as an account of work sponsored by an agency of the U.S. Government. Neither the U.S. Government nor any agency thereof, nor any employee, makes any warranty, expressed or implied, or assumes any legal liability or responsibility for any third party's use, or the results of such use, of any information, apparatus, product, or process disclosed in this publication, or represents that its use by such third party would not infringe privately owned rights.

United States Nuclear Regulatory Commission

Protecting People and the Environment

NUREG-2160

Post-Test Examination Results from Integral, High-Burnup, Fueled LOCA Tests at Studsvik Nuclear Laboratory

Manuscript Completed: April 2013
Date Published: August 2013

Michelle E. Flanagan
U.S. Nuclear Regulatory Commission

Peter Askeljung
Anders Puranen
Hot Cell Laboratory, Studsvik Nuclear AB, Sweden

Office of Nuclear Regulatory Research

ABSTRACT

This report presents and discusses the results of the U.S. Nuclear Regulatory Commission's integral loss-of-coolant accident (LOCA) testing program conducted at Studsvik Nuclear AB in Sweden. In this program, refabricated, high burnup irradiated fuel rodlets were subjected to LOCA conditions. In total, six single-rod LOCA tests were conducted in the Hot Cell Laboratory at Studsvik Nuclear AB. This report documents the test conditions, rodlet response, and post-test examinations for all six tests. The purpose of this document is to make this information available for comparison to related or complementary experimental programs. The observations of fuel fragmentation, relocation, and dispersal in this experimental program may be of particular interest for comparison to related or complementary experimental programs.

FOREWORD

The purpose of this document is to make available the results of the U.S. Nuclear Regulatory Commission's integral loss-of-coolant accident (LOCA) testing program conducted at Studsvik Nuclear AB in Sweden for comparison to related or complementary experimental programs. Recently, discussion about the results of LOCA testing in the area of fuel fragmentation, relocation and dispersal has grown common and rigorous throughout the international community. Therefore, the observations of fuel fragmentation, relocation, and dispersal in this experimental program may be of particular interest for comparison to related or complementary experimental programs.

CONTENTS

ABSTRACT III

FOREWORD V

CONTENTS VII

FIGURES IX

TABLES XV

ABBREVIATIONS AND ACRONYMS XVII

1. GENERAL INFORMATION ABOUT THE STUDSVIK LOCA TEST SERIES, EXPERIMENTAL PROCEDURES, AND EXAMINATIONS 1-1

2. SPECIFIC RESULTS OF EACH TEST 2-1

2.1 TEST 189 2-2
2.1.1 Initial State *2-2*
2.1.2 Transient Information *2-2*
2.1.3 In-Cell Measurements *2-4*
2.1.4 Metallography and Hot-Vacuum Extraction *2-6*
2.1.5 Gamma Scan Results with Comparison to Profilometry and Initial Wire Probe Measurements *2-6*
2.2 TEST 191 2-6
2.2.1 Initial State *2-7*
2.2.2 Transient Information *2-7*
2.2.3 In-Cell Measurements *2-8*
2.2.4 Metallography and Hot-Vacuum Extraction *2-11*
2.2.5 Gamma Scan Results with Comparison to Profilometry and Initial Wire Probe Measurements *2-13*
2.3 TEST 192 2-15
2.3.1 Initial State *2-15*
2.3.2 Transient Information *2-15*
2.3.3 In-Cell Measurements *2-17*
2.3.4 Metallography and Hot-Vacuum Extraction *2-19*
2.3.5 Gamma Scan Results with Comparison to Profilometry and Initial Wire Probe Measurements *2-23*
2.4 TEST 193 2-30
2.4.1 Initial State *2-31*
2.4.2 Transient Information *2-31*
2.4.3 In-Cell Measurements *2-32*
2.4.4 Metallography and Hot-Vacuum Extraction *2-35*
2.4.5 Gamma Scan Results with Comparison to Profilometry and Initial Wire Probe Measurements *2-39*
2.5 TEST 196 2-40
2.5.1 Initial State *2-41*
2.5.2 Transient Information *2-41*
2.5.3 In-Cell Measurements *2-43*

2.5.4 Metallography and Hot-Vacuum Extraction *2-45*
2.5.5 Gamma Scan Results with Comparison to Profilometry and Initial Wire Probe Measurements *2-47*
2.6 TEST 198 2-50
2.6.1 Initial State *2-51*
2.6.2 Transient Information *2-51*
2.6.3 In-Cell Measurements *2-53*
2.6.4 Metallography and Hot-Vacuum Extraction *2-55*
2.6.5 Gamma Scan Results with Comparison to Profilometry and Initial Wire Probe Measurements *2-58*

3. REVIEW OF TEST RESULTS FOR SPECIFIC PARAMETER COMPARISONS 3-1

3.1 INITIAL STATE 3-1
3.2 TRANSIENT 3-1
3.3 IN-CELL MEASUREMENTS 3-2

4. CONCLUSIONS 4-1

5. REFERENCES 5-1

FIGURES

Figure 1-1 Schematic of the apparatus used for the Studsvik LOCA tests..... 1-1
Figure 1-2 A detailed drawing of the rodlet components and dimensions..... 1-2
Figure 2-1 Fill pressure adjustment at 300 °C for Test 189, which provides an indication of gas communication 2-3
Figure 2-2 Temperature and pressure history for Test 189..... 2-3
Figure 2-3 Rod segment from Test 189 (a) in test rig after transient and (b) a closeup of the rupture opening after the transient..... 2-4
Figure 2-4 A wire probe is inserted into the fuel rod to measure the voided cladding length..... 2-4
Figure 2-5 Rod segment from Test 189 showing no significant rod bending (a) in plane with the rupture or (b) out of plane with the rupture..... 2-5
Figure 2-6 Profilometry measurements of segment 189 post-transient. The rupture length is also indicated. 2-5
Figure 2-7 Images of fuel collected from Test 189..... 2-6
Figure 2-8 Fill pressure adjustment at 300 °C for Test 191, which provides an indication of gas communication 2-8
Figure 2-9 Temperature and pressure history for Test 191..... 2-8
Figure 2-10 Rod segment from Test 191 (a) in test rig after transient and (b) a closeup of the rupture opening after the transient..... 2-9
Figure 2-11 Rod segment from Test 191 showing (a) no significant rod bending out of plane with the rupture and (b) & (c) noticeable bending in plane with the rupture..... 2-9
Figure 2-12 Profilometry measurements of segment 191 post-transient. The rupture length is also indicated. 2-10
Figure 2-13 Images of fuel collected from Test 191..... 2-10
Figure 2-14 Photo of test segment from Test 191, indicating the location of metallography and hydrogen measurements..... 2-11
Figure 2-15 Macrograph of cross section from the rupture region of rodlet tested in LOCA Test 191 2-12
Figure 2-16 Two high-resolution images of the cladding outer diameter from the metallography examination in the rupture region of the rodlet tested in LOCA Test 191 at (a) 45° and (b) 225° 2-12
Figure 2-17 Two high-resolution images of the cladding inner diameter from the metallography examination in the rupture region of the rodlet tested in LOCA Test 191 at (a) 0° and (b) 135° 2-13
Figure 2-18 Photo of test segment from Test 191, indicating the relative length of gamma scan results 2-13
Figure 2-19 Gamma scan results for Test 191 with comparison to profilometry and initial wire probe measurements..... 2-14
Figure 2-20 Fill pressure adjustment at 300 °C for Test 192, which provides an indication of gas communication 2-16
Figure 2-21 Temperature and pressure history for Test 192..... 2-16
Figure 2-22 Rod segment from Test 192 (a) in test rig after transient and (b) a closeup of the rupture opening after the transient..... 2-17
Figure 2-23 Rod segment from Test 192 showing no significant rod bending (a) out of plane with the rupture or (b) in plane with the rupture..... 2-17

Figure 2-24 Profilometry measurements of segment 192 post-transient. The rupture length is also indicated. 2-18
Figure 2-25 Images of fuel collected from Test 192 2-18
Figure 2-26 Photo of test segment from Test 192, indicating the location of metallography and hydrogen measurements 2-19
Figure 2-27 Macrograph of cross section from the rupture region of rodlet tested in LOCA Test 192 2-20
Figure 2-28 Two high-resolution images of the cladding outer diameter from the metallography examination in the rupture region of the rodlet tested in LOCA Test 192 at (a) 45° and (b) 135° 2-20
Figure 2-29 Two high-resolution images of the cladding inner diameter from the metallography examination in the rupture region of the rodlet tested in LOCA Test 192 at (a) 0° and (b) 315° 2-21
Figure 2-30 Macrograph of cross section from 50 mm below the rupture region of rodlet tested in LOCA Test 192 2-22
Figure 2-31 Two high-resolution images of the cladding outer diameter from the metallography examination 50 mm below the rupture region of the rodlet tested in LOCA Test 192 at (a) 90° and (b) 315° 2-22
Figure 2-32 Two high-resolution images of the cladding inner diameter from the metallography examination 50 mm below the rupture region of the rodlet tested in LOCA Test 192 at (a) 45°and (b) 225° 2-23
Figure 2-33 Hydrogen measurements from 192 relative to segment strain profile and rupture length 2-23
Figure 2-34 Photo of test segment from Test 192, indicating the relative length of gamma scan results and location of additional M/C examinations in the remaining fueled regions 2-24
Figure 2-35 Gamma scan results for Test 192 with comparison to profilometry and initial wire probe measurements 2-25
Figure 2-36 Fuel fragments collected from the top end of rod 192 after gentle shaking just before gamma scan 2-26
Figure 2-37 Comparison of fuel fragment size distribution from two regions of segment 192 2-27
Figure 2-38 Macrograph of transverse cross section 35 mm from the bottom of the rodlet tested in LOCA Test 192 2-28
Figure 2-39 A high-resolution image of the fuel cladding gap from the M/C examination 35 mm from the bottom of the rodlet tested in LOCA Test 192 2-28
Figure 2-40 Macrograph of axial cross section covering a span approximately 50–75 mm from the segment bottom of the rodlet tested in LOCA Test 192 2-29
Figure 2-41 High-resolution images of the cladding (a and b) inner and (c and d) outer diameter taken from the axial M/C shown above. These images were near the bottom (left) of the axial M/C, approximately 55 mm from the original segment bottom and approximately 100 mm below the rupture opening of the rodlet tested in LOCA Test 192. 2-30
Figure 2-42 Fill pressure adjustment at 300 °C for Test 193, which provides an indication of gas communication 2-31
Figure 2-43 Temperature and pressure history for Test 193 2-32
Figure 2-44 Rod segment from Test 193 (a) in test rig after transient and (b) a closeup of the rupture opening after the transient 2-33

Figure 2-45 Rod segment from Test 193 showing no significant rod bending (a) in plane with the rupture and (b) minor bending out of plane with the rupture 2-33
Figure 2-46 Profilometry measurements of segment 193 post-transient. The rupture length is also indicated. 2-34
Figure 2-47 Images of fuel collected from Test 193 2-34
Figure 2-48 Photo of test segment from Test 193, indicating the location of metallography 2-35
Figure 2-49 Macrograph of cross section from the rupture region of rodlet tested in LOCA Test 193 2-36
Figure 2-50 Two high-resolution images of the cladding outer diameter from the metallography examination in the rupture region of the rodlet tested in LOCA Test 193 at (a) 90° and (b) 270° 2-36
Figure 2-51 Two high-resolution images of the cladding inner diameter from the metallography examination in the rupture region of the rodlet tested in LOCA Test 193 at (a) 135° and (b) 270° 2-37
Figure 2-52 Macrograph of cross section from 35 mm above the rupture region of rodlet tested in LOCA Test 193 2-37
Figure 2-53 Two high-resolution images of the cladding outer diameter from the metallography examination 35 mm above the rupture region of the rodlet tested in LOCA Test 193 at (a) 45° and (b) 270° 2-38
Figure 2-54 Two high-resolution images of the cladding inner diameter from the metallography examination 35 mm above the rupture region of the rodlet tested in LOCA Test 193 at (a) 135° and (b) 270° 2-38
Figure 2-55 Etched cross section revealing hydrogen microstructure in the cladding in the rupture region of Test 193 2-39
Figure 2-56 Photo of test segment from Test 193, indicating the relative length of gamma scan results 2-39
Figure 2-57 Gamma scan results for Test 193 with comparison to profilometry and initial wire probe measurements 2-40
Figure 2-58 Fill pressure adjustment at 300 °C for Test 196, which provides an indication of gas communication 2-42
Figure 2-59 Temperature and pressure history for Test 196 2-42
Figure 2-60 Rod segment from Test 196 (a) in test rig after transient and (b) a closeup of the rupture opening after the transient 2-43
Figure 2-61 Rod segment from Test 196 showing no significant rod bending 2-43
Figure 2-62 Profilometry measurements of segment 196 post-transient. The rupture length is also indicated. 2-44
Figure 2-63 Images of fuel collected from Test 196 2-44
Figure 2-64 Photo of test segment from Test 196, indicating the location of metallography and hydrogen measurements 2-45
Figure 2-65 Macrograph of cross section from the rupture region of rodlet tested in LOCA Test 196 2-46
Figure 2-66 Two high-resolution images of the cladding outer diameter from the metallography examination in the rupture region of the rodlet tested in LOCA Test 196 at (a) 90° and (b) 270° 2-46
Figure 2-67 Two high-resolution images of the cladding inner diameter from the metallography examination in the rupture region of the rodlet tested in LOCA Test 196 at (a) 45° and (b) 270° 2-47

Figure 2-68 Hydrogen measurements from 196 relative to segment strain profile and rupture length 2-47
Figure 2-69 Photo of test segment from Test 196, indicating the relative length of gamma scan results 2-48
Figure 2-70 Gamma scan results for Test 196 with comparison to profilometry and initial wire probe measurements 2-48
Figure 2-71 Fuel fragments collected from the bottom of rod 196 after gentle shaking just before gamma scan 2-49
Figure 2-72 Comparison of fuel fragment size distribution from two regions of segment 196 2-50
Figure 2-73 Fill pressure adjustment at 300 °C for Test 198, which provides an indication of gas communication 2-52
Figure 2-74 Temperature and pressure history for Test 198 2-52
Figure 2-75 Rupture opening after the transient simulation for Test 198 2-53
Figure 2-76 Rod segment from Test 198 showing no significant rod bending 2-53
Figure 2-77 Profilometry measurements of segment 198 post-transient. The rupture length is also indicated. 2-54
Figure 2-78 Images of fuel collected from Test 198 2-54
Figure 2-79 Photo of test segment from Test 198, indicating the location of metallography and hydrogen measurements 2-55
Figure 2-80 Macrograph of cross section from the rupture region of rodlet tested in LOCA Test 198 2-55
Figure 2-81 Two high-resolution images of the cladding outer diameter from the metallography examination in the rupture region of the rodlet tested in LOCA Test 198 at (a) 90° and (b) 270° 2-56
Figure 2-82 Two high-resolution images of the cladding inner diameter from the metallography examination in the rupture region of the rodlet tested in LOCA Test 198 at (a) 90° and (b) 225° 2-56
Figure 2-83 Macrograph of cross section from 50 mm below the rupture region of rodlet tested in LOCA test 198 2-57
Figure 2-84 Two high-resolution images of the cladding outer diameter from the metallography examination 50 mm below the rupture region of the rodlet tested in LOCA Test 198 at (a) 90° and (b) 180° 2-57
Figure 2-85 Two high-resolution images of the cladding inner diameter from the metallography examination 50 mm below the rupture region of the rodlet tested in LOCA Test 198 at (a) 90° and (b) 225° 2-57
Figure 2-86 Hydrogen measurements from Test 198 relative to segment strain profile and rupture length 2-58
Figure 2-87 Photo of test segment from Test 198, indicating the relative length of gamma scan results and location of an additional M/C examination in the remaining fueled region 2-59
Figure 2-88 Gamma scan results for Test 198 with comparison to profilometry and initial wire probe measurements 2-60
Figure 2-89 Macrograph of axial cross section covering a span approximately 80–105 mm from the segment bottom of the rodlet tested in LOCA Test 198 2-61
Figure 2-90 High-resolution images of the cladding (a and b) inner and (c and d) outer diameter taken from the axial M/C shown above. These images

were near the bottom (left) of the axial M/C, approximately 85 mm from the original segment bottom of the rodlet tested in LOCA Test 198. 2-62
Figure 3-1 Pressure drop after rupture in the top plenum, plotted as a function of time, for all six tests 3-2
Figure 3-2 Approximate percentage of fuel loss during each test, color-coded by when fuel loss occurred. Note: Measured mass loss was compared to an estimated initial fuel mass of 150 g for the 300-mm segment. 3-3
Figure 3-3 Fragment size distribution for each test 3-4

TABLES

Table 2-1 Measurements and Values That Characterize the Initial State, Transient, and In-Cell Measurements of the Six LOCA Tests Run at Studsvik in the NRC's LOCA Research Program 2-1
Table 2-2 Measurements and Values That Characterize the Initial State, Transient, and In-Cell Measurements of Test 189 2-2
Table 2-3 Measurements and Values That Characterize the Initial State, Transient, and In-Cell Measurements of Test 191 2-7
Table 2-4 Fragment Size Distribution Results from Test 191 2-11
Table 2-5 Measurements and Values That Characterize the Initial State, Transient, and In-Cell Measurements of Test 192 2-15
Table 2-6 Fragment Size Distribution Results from Test 192 2-19
Table 2-7 Hydrogen Measurements for Test 192 2-23
Table 2-8 Fragment Size Distribution Results for Fuel Fragments Collected from the Top End of Rod 192 after Gentle Shaking Just before Gamma Scan 2-26
Table 2-9 Measurements and Values That Characterize the Initial State, Transient, and In-Cell Measurements of Test 193 2-30
Table 2-10 Fragment Size Distribution Results from Test 193 2-35
Table 2-11 Measurements and Values That Characterize the Initial State, Transient, and In-Cell Measurements of Test 196 2-41
Table 2-12 Fragment Size Distribution Results from Test 196 2-45
Table 2-13 Hydrogen Measurements for Test 196 2-47
Table 2-14 Fragment Size Distribution Results for Fuel Fragments Collected from the Bottom End of Rod 196 after Gentle Shaking Just before Gamma Scan 2-50
Table 2-15 Measurements and Values That Characterize the Initial State, Transient, and In-Cell Measurements of Test 198 2-51
Table 2-16 Fragment Size Distribution Results from Test 198 2-54
Table 2-17 Hydrogen Measurements from Test 198 2-58
Table 3-1 Summary of All "Initial State" Information from the Six LOCA Tests 3-1
Table 3-2 Summary of All "Transient" Information from the Six LOCA Tests 3-2
Table 3-3 Summary of All "In-Cell Measurement" Information from the Six LOCA Tests 3-3

ABBREVIATIONS AND ACRONYMS

C	Celsius
cm	centimeter
CP-ECR	Equivalent cladding reacted, as calculated by the Cathcart-Pawel Oxidation equation
F	Fahrenheit
GWd/MTU	gigawatt days per metric ton uranium
IR	infrared radiation
kW/m	kilowatt per meter
LHGR	linear heat generation rate
LOCA	loss-of-coolant accident
M/C	metallography and ceramography
PIE	postirradiation examination
PWR	pressurized-water reactor
wppm	weight parts per million

1. GENERAL INFORMATION ABOUT THE STUDSVIK LOCA TEST SERIES, EXPERIMENTAL PROCEDURES, AND EXAMINATIONS

The U.S. Nuclear Regulatory Commission (NRC) commissioned six single-rod, out-of-pile, integral loss-of-coolant accident (LOCA) tests at the Hot Cell Laboratory of Studsvik Nuclear AB to assess the mechanical performance of ballooned and ruptured high-burnup fuel rods. In each of these tests, a pressurized, high-burnup, fueled rod segment was subjected to a temperature transient in a steam environment to induce ballooning, rupture, and high-temperature steam oxidation. The apparatus used for the Studsvik LOCA tests is shown below in Figure 1-1.

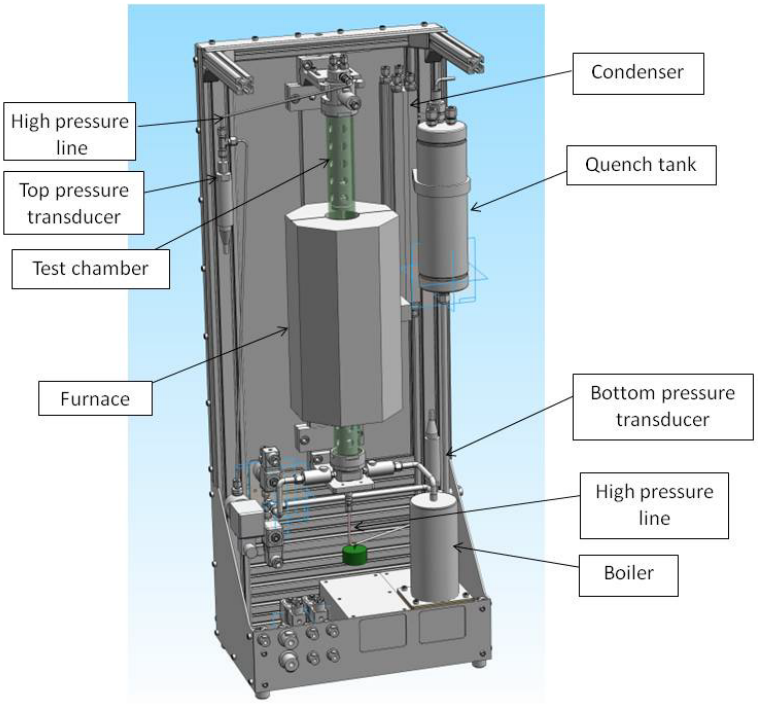

Figure 1-1 Schematic of the apparatus used for the Studsvik LOCA tests

The LOCA apparatus was designed to externally heat a 30 centimeters (cm) long, pressurized, irradiated fuel rodlet up to 1,200 degrees Celsius (C) (2192 degrees Fahrenheit (F)) by infrared (IR) radiation. The fuel rodlets are heated in a flowing steam environment from 300 degrees C (572 degrees F) to a target temperature of about 1,200 degrees C at a rate of 5 degrees C/second (s) (41 degrees F/s). The rodlet temperature is measured with a thermocouple attached by a metal clamp 50 millimeters above the axial mid plane. The test segment is pressurized with helium. Internal pressures were consistent with typical end of life rod internal pressure, although likely on the high end, and were chosen to induce ballooning and rupture with rupture strains in the range of 30 percent-50 percent. Rodlet temperatures were held at 1,200 degrees C for either 0, 5, 25, or 85 seconds to achieve various oxidation levels.

Identical pressure transducers were used at the bottom and at the top of the rodlet, measuring the internal pressure throughout the preparation and testing phases. The void volumes of the

rodlet were: 7.3 cm^3 above the rod (approximately 6.1 cm^3 in the upper pressure line and approximately 1.2 cm^3 in the upper rod plenum) and 3.1 cm^3 below the rod (approximately 2.4 cm^3 in the lower pressure line and approximately 0.7 cm^3 in the lower rod plenum). Thus, the total void volume was approximately 10.4 cm^3. A drawing showing the main parts of the rodlet is shown in Figure 1-2. Additional information about the LOCA apparatus and test train design can be found in reference [1].

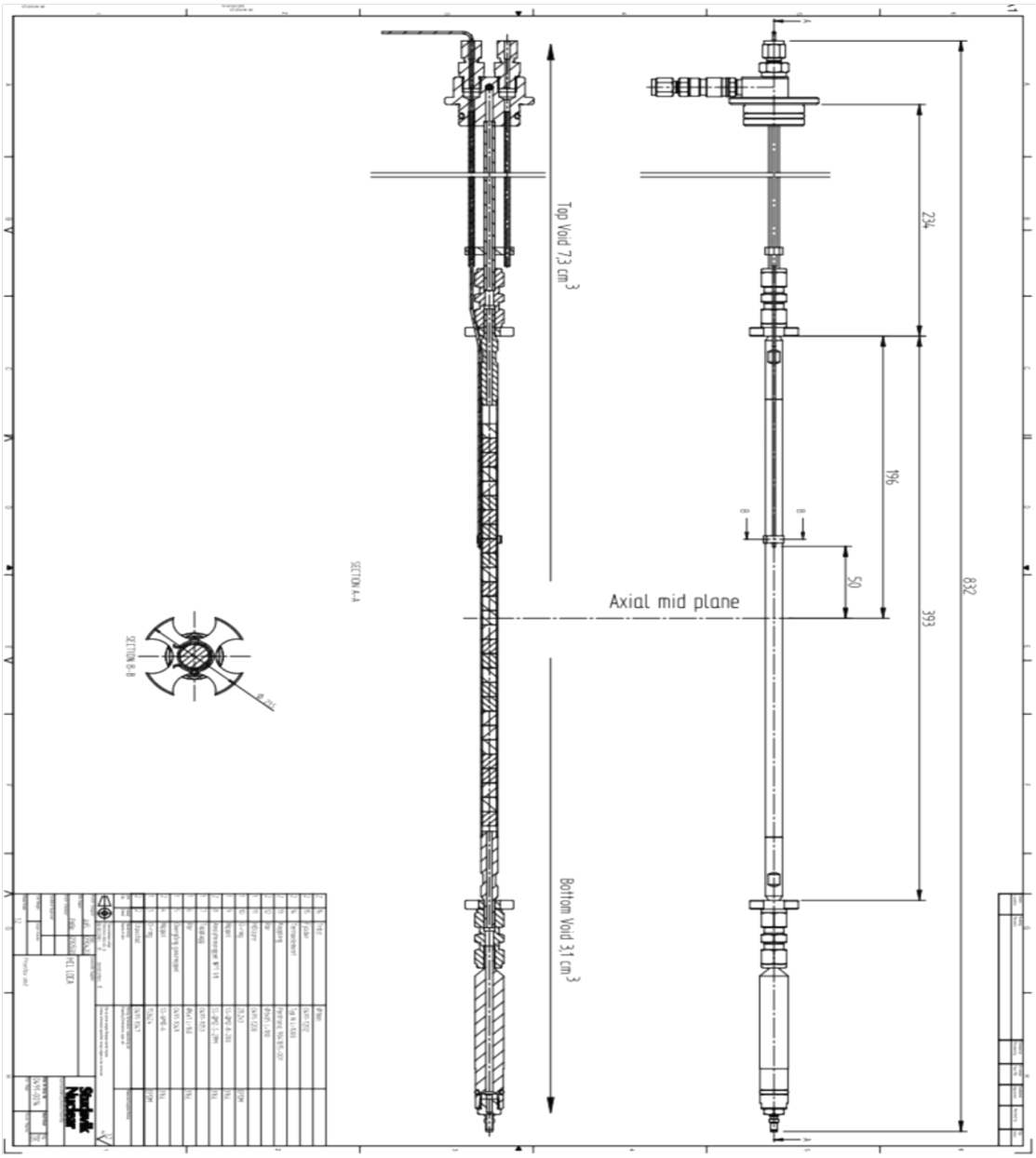

Figure 1-2 A detailed drawing of the rodlet components and dimensions

The LOCA tests performed at Studsvik used segments taken from pressurized-water reactor (PWR) rods. For the first four tests (189, 191-193) the segments were taken from rods with a rod average burnup level between 68-69 gigawatt days per metric ton uranium (GWd/MTU).

For the last two, 196 and 198, the segments were taken from rods with a rod average burnup level of 55 GWd/MTU, respectively. Two of the tests (189, 196) were terminated just after rupture, while the four other tests each experienced some degree of high-temperature steam oxidation, followed by quench.

Following the LOCA simulation, four-point bend tests were conducted to measure the residual mechanical behaviour of the ballooned and ruptured region. The results of the four-point bend tests on the first four LOCA tests have been reported elsewhere [2]. After the four-point bend test, a shake test was performed to determine the mobility of fuel fragments that remained in the fuel rod. The shake test consisted of an inversion of the two halves of the broken fuel rod, followed by minor shaking to dislodge any loose fuel fragments. The shake test was conducted approximately 2 days after the LOCA simulation.

During these tests, significant fuel loss was observed at various stages of the experimental procedures and multiple measurements and observations were made to characterize the fuel loss. Wire probe measurements were performed to measure the length of cladding that was "empty" of fuel for each segment. Mass measurements were made before and after the LOCA simulation, after the four-point bend test and after the shake test to determine the fuel loss at each stage by comparison to the mass at the previous step (the exception is Test 189, which did not have an initial rodlet mass and therefore fuel mass loss was determined by weighing the collected fuel). Photos were taken to document the appearance of the fuel and cladding at all stages. Fragment size measurements were completed by processing fuel fragments through a series of six sieves to determine the distribution of the fuel fragments by size (the exception is Test 189, which was sent for disposal before sieving analysis). Some of the observations of fuel relocation and loss have been reported in previous conference papers and reports [3-4].

Axial locations of interest were identified for each test segment, and multiple metallography samples were prepared, along with measurement of the hydrogen content by hot vacuum extraction.

Almost 1 year after the last LOCA tests were completed, emerging questions prompted additional postirradiation examination (PIE) investigations. The wire probe measurements performed after the shaking test indicated a long length of empty cladding, but also a significant amount of residual fuel material in some test segments. To investigate the length and condition of the remaining fueled segments, gamma scans were performed on many of the remaining fueled portions of each test segment. This report documents the test condition, rodlet response, and post-test examinations for all six LOCA tests.

2. SPECIFIC RESULTS OF EACH TEST

In this section, specific information about each test will be presented and discussed. Table 2-1 summarizes basic information for all six loss-of-coolant (LOCA) tests run in the U.S. Nuclear Regulatory Commission's (NRC's) LOCA program at Studsvik. In the following subsections, the initial state, transient information and in-cell measurements will be discussed for each test.

Table 2-1 Measurements and Values That Characterize the Initial State, Transient, and In-Cell Measurements of the Six LOCA Tests Run at Studsvik in the NRC's LOCA Research Program

	Test	Adjacent H (wppm)	Average Oxide (μm)	Rod Average Burn Up (GWd/MTU)	Rod Internal Pressure at 300°C (bar)
Initial State	189	176	20	68.2	110
	191	187, 271	20-30	69.3	110
	192	176, 288	25-30	68.2	82
	193	187	20	69.3	82
	196	149	20	55.2	82
	198	225	20	55.2	82

	Test	Peak Cladding Temperature (°C)	Rupture Temp (°C)	Rupture Pressure (bar)	Time (s) to 50% of rupture P for top/bottom gauges	CP-ECR (%)	Quench
Transient	189	950	700	109	35 / 7	0	No
	191	1185	680	104	21 / 10	13	Yes
	192	1185	700	81	13 / 15	11	Yes
	193	1185	728	81	45 / 8	17	Yes
	196	950	686	81	5 / 2	0	No
	198	1185	693	81	3 / 2	15	Yes

	Test	Max Strain (%)	Length >10% Strain (mm)	Wire Probe Measurement (mm) (Top/Bottom)	Rupture Dimensions (mm) (Width/Length)
In-cell Measurements	189	48	105	82 / 66	10.5 / 23.9
	191	50	70	70 / 55	17.5 / 21.6
	192	56	85	85 / 73	9 / 22.7
	193	50	100	113 / 91	13.8 / 17.8
	196	25	95	90 / 66	0.2 / 1.5
	198	25	115	55 / 76	1.6 / 11

2.1 Test 189

Table 2-2 summarizes measurements and values that characterize the initial state, transient, and in-cell measurements of Test 189. The initial state, transient information, and in-cell measurements will be described further in the following sections.

Table 2-2 Measurements and Values That Characterize the Initial State, Transient, and In-Cell Measurements of Test 189

Initial State	Adjacent H (wppm)	Average Oxide (μm)	Rod Average Burn Up (GWd/MTU)		Rod Internal Pressure at 300°C (bar)	
	176	20	68.2		110	
Transient	Peak Cladding Temperature (°C)	Rupture Temp (°C)	Rupture Pressure (bar)	Time (s) to reach 50% of rupture P for top/bottom gauges	CP-ECR (%)	Quench
	950	700	109	35 / 7	0	No
In-Cell Measurements	Max Strain (%)	Length >10% Strain (mm)	Wire Probe Measurement (mm) (Top/Bottom)		Rupture Dimensions (mm) (Width/Length)	
	48	105	82 / 66		10.5 / 23.9	

2.1.1 Initial State

For Test 189, a segment of high burnup Westinghouse ZIRLO™ was used. The segment was taken from a rod that was irradiated at a U.S. pressurized-water reactor (PWR) power plant and had a rod average burnup of 68.2 gigawatt days per metric ton uranium (GWd/MTU). The particular father rods used in Tests 189-193 had a unique operating history characterized by an end-of-life power that is greater than typical operating practice, namely a mean linear heat generation rate (LHGR) of approximately 24 kilowatts per meter (kW/m) for cycle one, 23 kW/m for cycle two, 5 kW/m for cycle three, and 15 kW/m for cycle four. The 300-millimeter segment was taken from the middle section of the fuel rod, approximately 1,400 millimeters from the bottom of the full length rod. A hydrogen content of 176 weight parts per million (wppm) was measured just above the segment. The eddy current measurements indicate that the oxide layer thickness was relatively constant over the length of this segment, and average about 20 micrometers.

2.1.2 Transient Information

To begin the transient, the rodlet was heated and maintained at 300 degrees Celsius (C) (572 degrees Fahrenheit (F)) for approximately 15 minutes to achieve thermal equilibrium. Before initiating the temperature ramp, the desired fill pressure was established at 300 degrees C. For Test 189, the rodlet was pressurized to 110 bar (at 300 degrees C). The pressure adjustment procedure provides an indication of gas communication by observing the response time of the lower pressure transducer, as shown in Figure 2-1. Recall that while the gas line is open, the top pressure transducer indicates the gas line pressure and the bottom should reflect the ability of gas to move the 300 millimeter segment length to equilibrate pressure. Once the desired fill pressure was established, the gas line was closed and the rodlet

was heated at 5 degrees C/second (s) (41 degrees F/s) through ballooning and rupture. This was a “ramp-to-rupture” test and therefore the furnace was shut off to terminate the test at 950 degrees C (1,742 degrees F) and there was no quench. Rupture is estimated to have taken place when the rod internal pressure reached 109 bar and the cladding temperature reached 700 degrees C (1,292 degrees F). The depressurization rate was relatively slow for Test 189; the top pressure gauge recorded a 50 percent reduction in pressure (relative to 109 bar) after 35 seconds and the bottom pressure gauge recorded a 50 percent reduction in pressure after 7 seconds. No significant oxidation was accumulated during this test. The temperature and pressure history for Test 189 is shown in Figure 2-2.

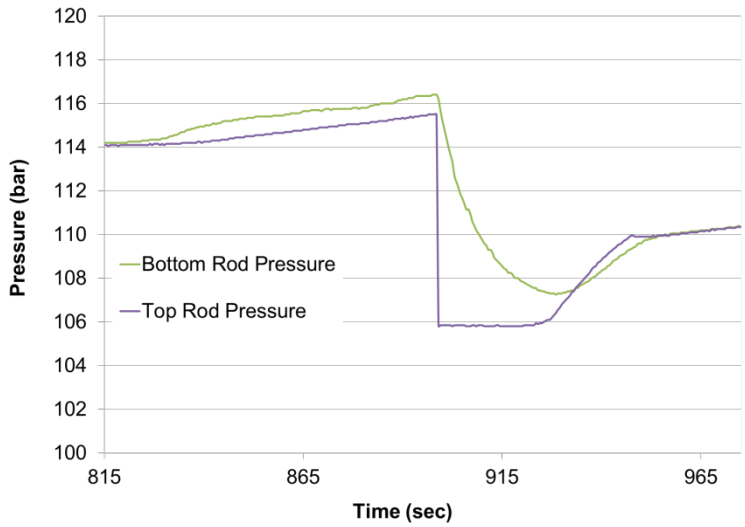

Figure 2-1 Fill pressure adjustment at 300 °C for Test 189, which provides an indication of gas communication

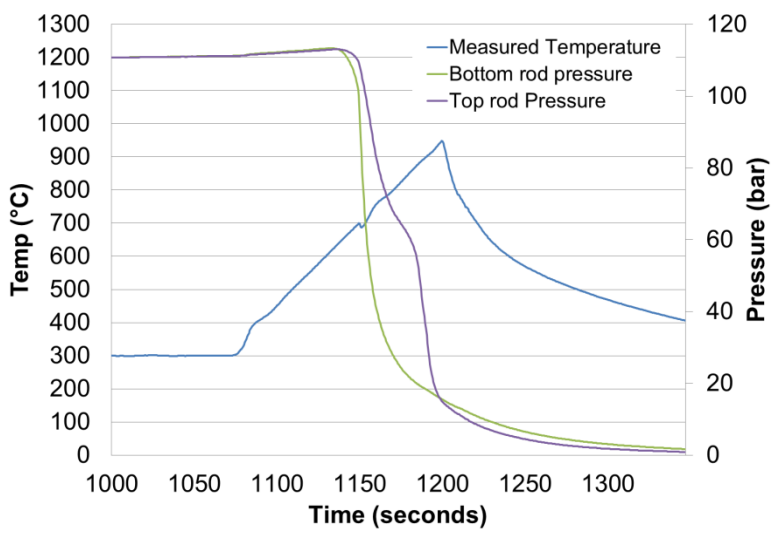

Figure 2-2 Temperature and pressure history for Test 189

2.1.3 In-Cell Measurements

After the simulated LOCA transient was complete, the fuel rod was examined. Figure 2-3 provides two photos of the fuel rod after the transient. The rupture opening was measured to be 10.5 millimeters wide and 23.9 millimeters in length. It is significant to note that when the rupture opening was examined after the transient, no fuel could be seen in the region. In fact, a wire probe was used to measure the length of voided cladding after all experimental steps (LOCA transient, bending, and shaking) and the probe traveled unobstructed approximately 66 millimeter above and approximately 82 millimeter below the rupture center. The technique to measure the voided cladding is illustrated below in Figure 2-4.

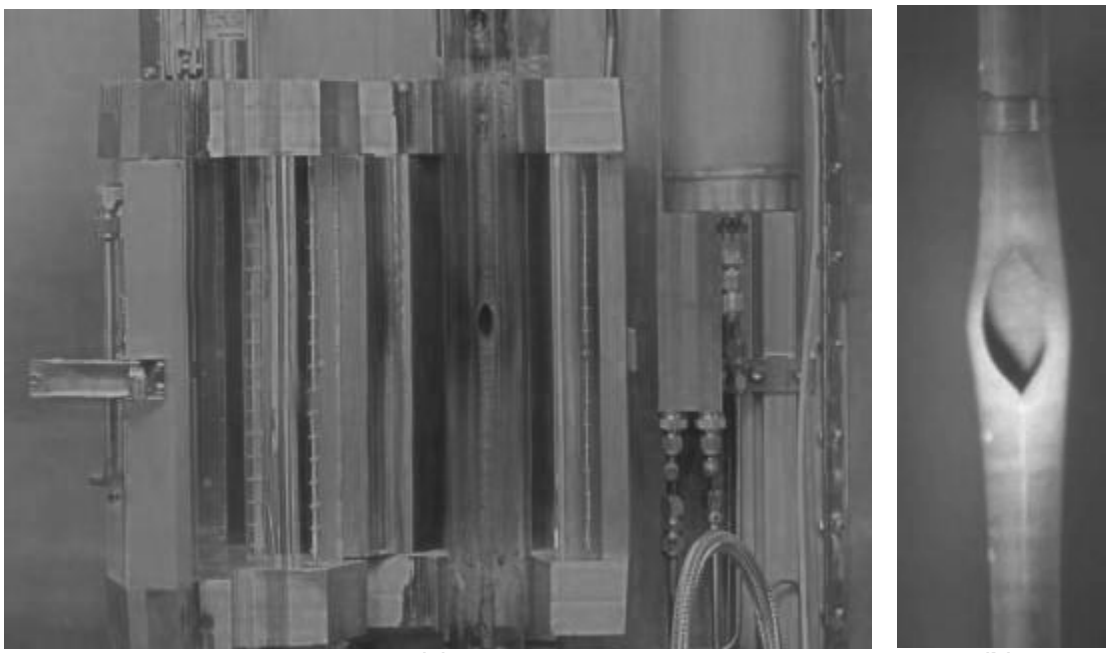

(a) (b)

Figure 2-3 Rod segment from Test 189 (a) in test rig after transient and (b) a closeup of the rupture opening after the transient

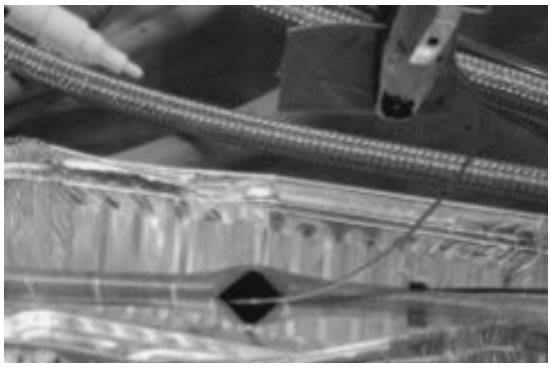

Figure 2-4 A wire probe is inserted into the fuel rod to measure the voided cladding length

The rod did not experience distortion or bending during the LOCA transient, which can be seen in Figure 2-5. Profilometry measurements were made, and they are shown in Figure 2-6. In Figure 2-6, the initial diameter and rupture length are also indicated. The mid-wall rupture strain value for Test 189 was calculated to be 48 percent.

(a)

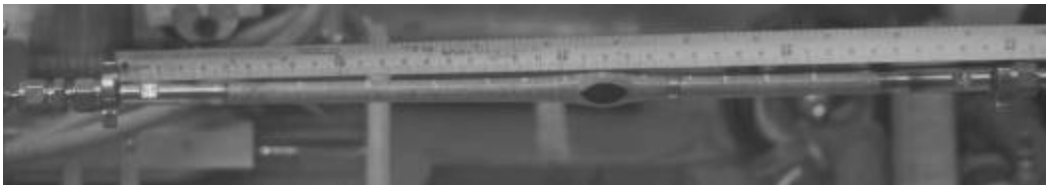

(b)

Figure 2-5 Rod segment from Test 189 showing no significant rod bending (a) in plane with the rupture or (b) out of plane with the rupture

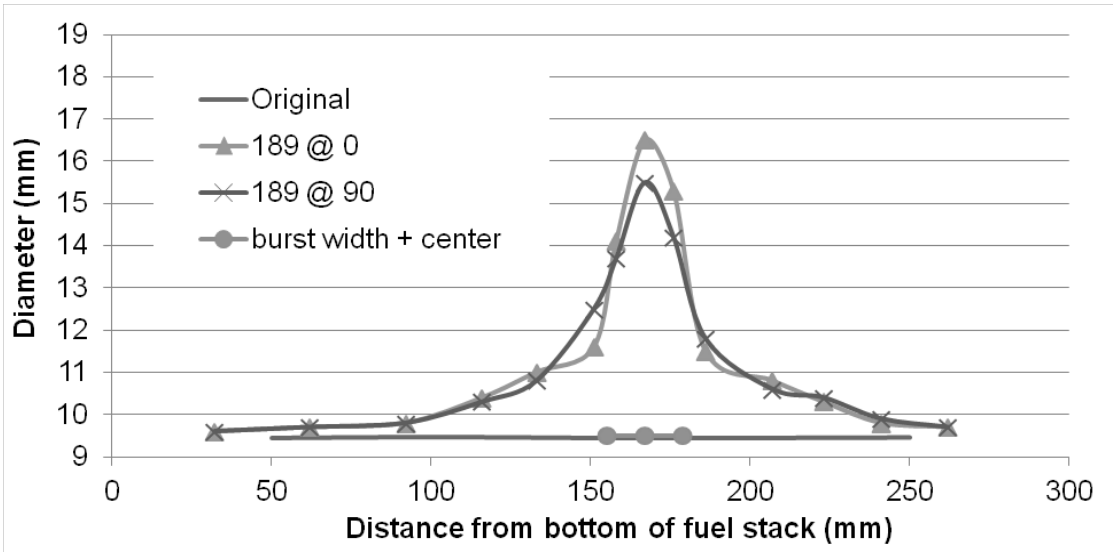

Figure 2-6 Profilometry measurements of segment 189 post-transient. The rupture length is also indicated.

Following the simulated LOCA transient of Test 189, a large amount of fuel was collected from the LOCA test train. Additional fuel fragments were collected during the four-point bend test and after minor shaking of the bent segment. The pre-test rod mass was not measured, so it is possible that the total fuel loss was not accounted for by weighing and totalling the mass of collected fuel fragments. All of the readily collected fuel was weighed, but it is likely some additional fuel fragments remained within the test train, quench tank, or in the hot-cell itself.

In total, it appears that about half of the fuel fell out of this rod during the simulated LOCA transient test and during shaking. The collected fuel in LOCA test chamber totalled 41 grams. Fuel which was lost during the four-point bend test and after minor shaking was also collected and weighed. The mass of fuel that was collected after the bend test and after shaking was 20 grams. In total, 61 grams of fuel were collected. Figure 2-7 provides an image of the collected fuel fragments.

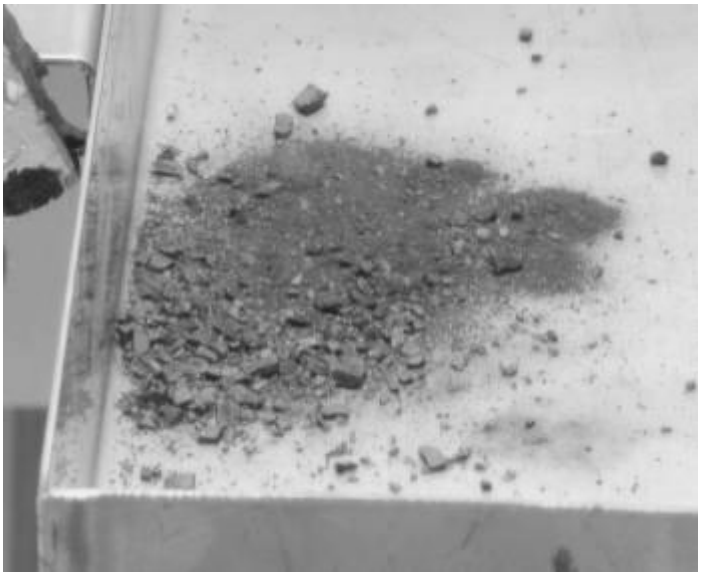

Figure 2-7 Images of fuel collected from Test 189

The fuel dispersed and collected from Test 189 was sent to disposal before sieve analysis; therefore, there is no quantitative information regarding fragment size distribution for this rodlet.

2.1.4 Metallography and Hot-Vacuum Extraction

No metallography or hot-vacuum extraction measurements were made of the rodlet from Test 189.

2.1.5 Gamma Scan Results with Comparison to Profilometry and Initial Wire Probe Measurements

No gamma scans were performed on the rodlet from Test 189 because it was sent for disposal before the decision to conduct gamma scanning.

2.2 Test 191

Table 2-3 summarizes measurements and values that characterize the initial state, transient, and in-cell measurements of Test 191. The initial state, transient information, and in-cell measurements will be described further in the following sections. Metallography, hydrogen measurements, and gamma scan results will also be provided.

Table 2-3 Measurements and Values That Characterize the Initial State, Transient, and In-Cell Measurements of Test 191

Initial State	Adjacent H (wppm)	Average Oxide (μm)	Rod Average Burn Up (GWd/MTU)		Rod Internal Pressure at 300°C (bar)	
	187, 271	20-30	69.3		110	
Transient	Peak Cladding Temperature (°C)	Rupture Temp (°C)	Rupture Pressure (bar)	Time (s) to reach 50% of rupture P for top/bottom gauges	CP-ECR (%)	Quench
	1185	680	104	21 / 10	13	Yes
In-Cell Measurements	Max Strain (%)	Length >10% Strain (mm)	Wire Probe Measurement (mm) (Top/Bottom)		Rupture Dimensions (mm) (Width/Length)	
	50	70	70 / 55		17.5 / 21.6	

2.2.1 Initial State

For Test 191, a segment of high burnup Westinghouse ZIRLO™ was used. The segment was taken from a rod which was irradiated at a U.S. PWR power plant and had a rod average burnup of 69.3 GWd/MTU. Again, the operating history for this rod was non-typical and defined by a mean LHGR of approximately 24 kW/m for cycle one, 23 kW/m for cycle two, 5 kW/m for cycle three, and 15 kW/m for cycle four. The 300-millimeter segment was taken from the middle section of the fuel rod, approximately 1,800 millimeters from the bottom of the full length rod. The measured hydrogen content just below and above the segment was 187 and 271 weight parts per million (wppm), respectively. The eddy current measurements indicate that the oxide layer thickness increased slightly over the length of this segment, and range from about 20 micrometers to 30 micrometers.

2.2.2 Transient Information

To begin the transient, the rodlet was heated and maintained at 300 degrees C for approximately 15 minutes to achieve thermal equilibrium. Before initiating the temperature ramp, the desired fill pressure was established at 300 degrees C. For Test 191, the rodlet was pressurized to 110 bar (at 300 degrees C). The pressure adjustment procedure provides an indication of gas communication by observing the response time of the lower pressure transducer, as shown in Figure 2-8. Recall that while the gas line is open, the top pressure transducer is indicating the gas line pressure and the bottom should reflect the ability of gas to move the 300 millimeters to equilibrate pressure.

The rodlet was then heated at 5 degrees C/s until the rodlet temperature reached 1,160 degrees C (2120 degrees F) (previous benchmarks [1] indicated that the control thermocouple location is a relatively cold location and that a majority of the cladding circumference sees a slightly higher temperature. The set point of 1,160 degrees C was selected, based on prior measurements, to provide cladding temperature in the range of 1185 plus or minus 20 degrees C). The rodlet was held at 1,160 degrees C for 25 seconds. The calculated Cathcart-Pawel equivalent cladding reacted (CP-ECR) (based on measured rupture strain reported below) was approximately 13 percent.

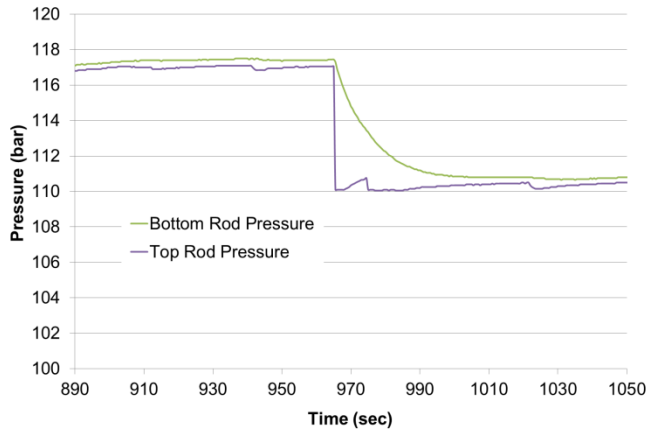

Figure 2-8 Fill pressure adjustment at 300 °C for Test 191, which provides an indication of gas communication

Rupture is estimated to have taken place when the rod internal pressure reached 104 bar and the cladding temperature reached 680 degrees C. The depressurization rate was relatively slow for Test 191; the top pressure gauge recorded a 50 percent reduction in pressure (relative to 104 bar) after 21 seconds and the bottom pressure gauge recorded a 50 percent reduction in pressure after 10 seconds. The temperature and pressure history for Test 191 is shown in Figure 2-9.

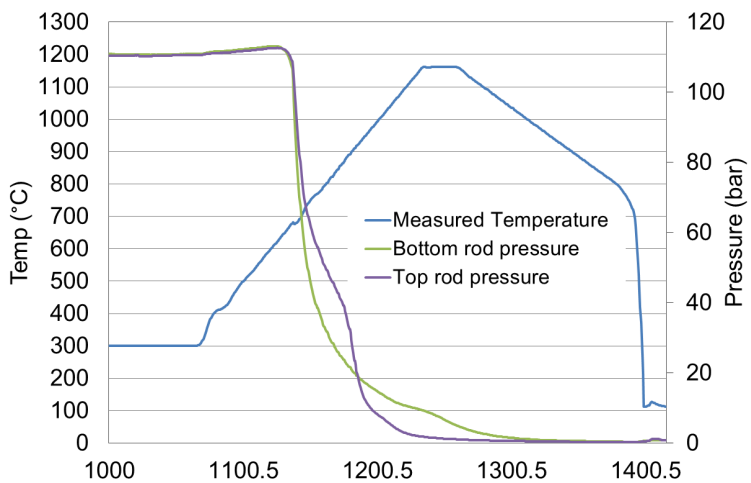

Figure 2-9 Temperature and pressure history for Test 191

2.2.3 In-Cell Measurements

After the simulated LOCA transient was complete, the fuel rod was examined. Figure 2-10 provides two photos of the fuel rod after the test. The rupture opening was measured to be 17.5 millimeters wide and 21.6 millimeters in length along the axial direction. In Figure 2-10 (b), inside the rupture opening, it appears that the pellet-pellet interfaces can be seen on the inside cladding wall.

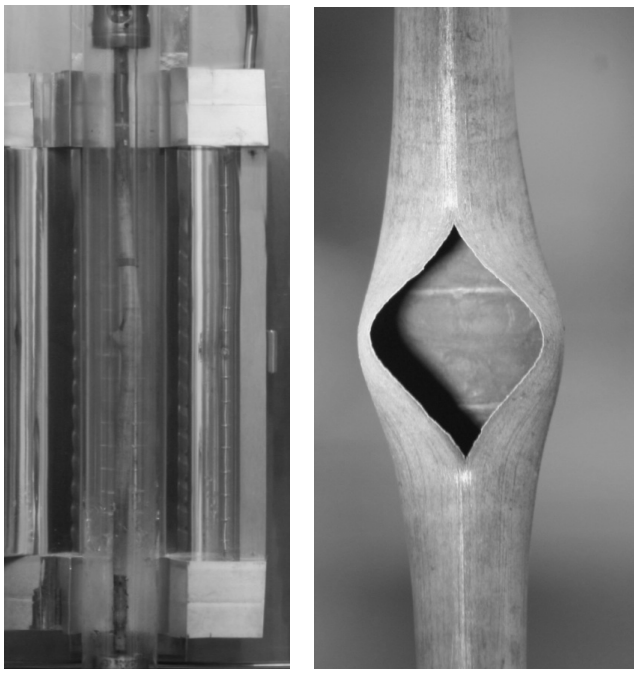

(a) (b)

Figure 2-10 Rod segment from Test 191 (a) in test rig after transient and (b) a closeup of the rupture opening after the transient

The rod experienced distortion (or bending) during the LOCA transient, which can be seen in Figure 2-11. The bending was in plane with the rupture (Figure 2-11 b & c) and the segment remained straight out of plane with the rupture (Figure 2-11 a). The distortion of this fuel rod was addressed with a small modification to the test train; the modification proved effective as later test segments did not experience significant bending.

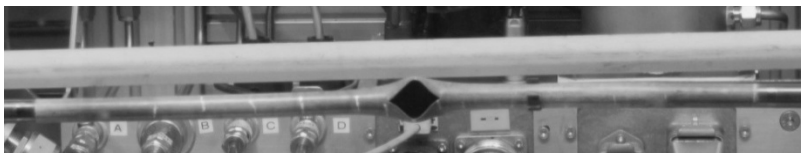

(a)

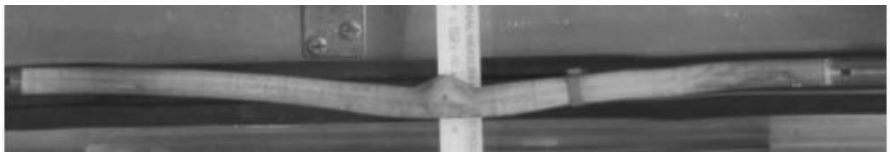

(b)

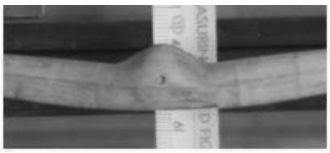

(c)

Figure 2-11 Rod segment from Test 191 showing (a) no significant rod bending out of plane with the rupture and (b) & (c) noticeable bending in plane with the rupture

Profilometry measurements were made and they are shown in Figure 2-12. In Figure 2-12, the initial diameter and rupture length are also indicated. The mid-wall rupture strain value for Test 191 was calculated to be 56 percent.

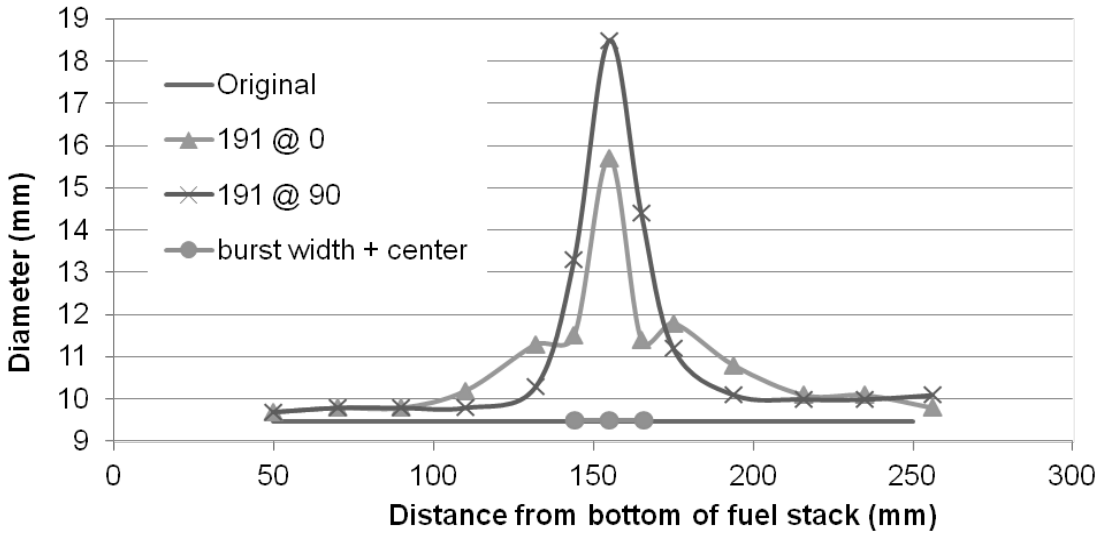

Figure 2-12 Profilometry measurements of segment 191 post-transient. The rupture length is also indicated.

In total, it appears that about half of the fuel fell out of this rod during the simulated LOCA transient test and during shaking. During the wire probe measurement, completed after all experimental steps (LOCA transient, bending and shaking), the probe traveled unobstructed approximately 55 millimeters above and approximately 70 millimeters below the rupture center. The mass loss measured following the LOCA test was 52 grams. The mass loss measured following the bend test and after shaking was 7 grams. In total, 59 grams of fuel was lost. Figure 2-13 provides an image of the collected fuel fragments.

Figure 2-13 Images of fuel collected from Test 191

The fragment size distribution of the fuel dispersed and collected from Test 191 was investigated using sieve analysis. The measured mass of each sieve group is provided in Table 2-4, along with the mass percentage of each group relative to the total fuel analyzed.

Table 2-4 Fragment Size Distribution Results from Test 191

Size	Weight fuel (g)	% of total
< 0.125 mm	9.2	18%
0.125 - 0.25	6.3	12%
0.25 - 0.5 mm	8.2	16%
0.5 - 1 mm	10.9	21%
1 - 2 mm	9.9	19%
2 - 4 mm	6.3	12%
> 4 mm	0	0%
Sum:	50.8	100%

2.2.4 Metallography and Hot-Vacuum Extraction

One metallography examination was made of the rodlet used in Test 191. The metallography sample shown in Figure 2-15 was taken from the rupture opening as indicated in Figure 2-14. Select, high-resolution images from the outer cladding diameter and inner cladding diameter are included in Figure 2-16 and Figure 2-17, respectively.

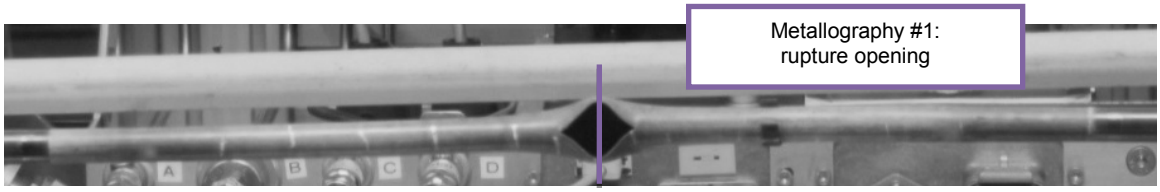

Figure 2-14 Photo of test segment from Test 191, indicating the location of metallography and hydrogen measurements

Figure 2-15 Macrograph of cross section from the rupture region of rodlet tested in LOCA Test 191

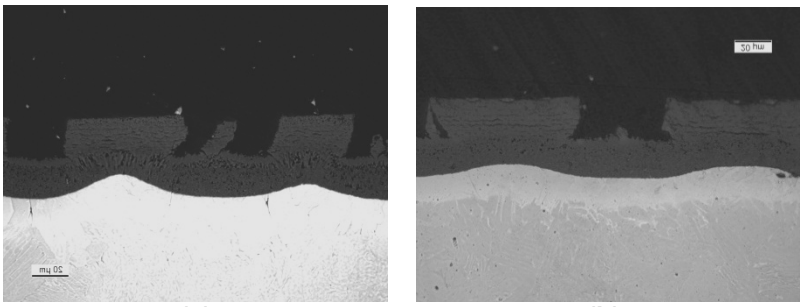

(a) **(b)**

Figure 2-16 Two high-resolution images of the cladding outer diameter from the metallography examination in the rupture region of the rodlet tested in LOCA Test 191 at (a) 45° and (b) 225°

Here, it is useful to recall that the calculated CP-ECR was 13 percent, with a hold time at 1,185 degrees C (2,165 degrees Fahrenheit) of 25 seconds. In Figure 2-16, the initial oxide thickness can be seen to have cracked and separated in this high strain (56 percent) area, and the transient oxidation layer is seen beneath the damaged initial oxide layer. In Figure 2-17, it appears that some fuel fragments remain on the inner diameter and that the initial fuel-cladding bonding layer has also cracked and separated. An inner diameter transient oxidation layer is seen, which appears to approximately the same thickness at the outer transient oxidation layer. These observations are expected at this location because it is in the rupture node and exposed to a steam environment after rupture.

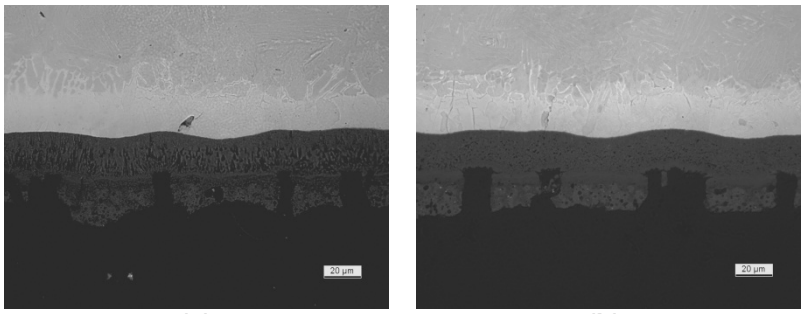

(a) (b)

Figure 2-17 Two high-resolution images of the cladding inner diameter from the metallography examination in the rupture region of the rodlet tested in LOCA Test 191 at (a) 0° and (b) 135°

No hydrogen measurements were made of the rodlet used in Test 191.

2.2.5 Gamma Scan Results with Comparison to Profilometry and Initial Wire Probe Measurements

Almost 1 year after the last LOCA tests were completed, emerging questions prompted new postirradiation examination (PIE) investigations. The wire probe measurements performed just after the LOCA tests indicated a long length of empty cladding, but also a significant amount of residual fuel material in some test segments. To investigate the length and condition of the remaining fueled segments, gamma scans were performed. Recall that the rodlet used in Test 191 fractured in the rupture node during the four-point bend test. The two halves of the rodlet were gamma scanned separately and the scans in combination covered almost the entire length of the rodlet, as shown in Figure 2-18.

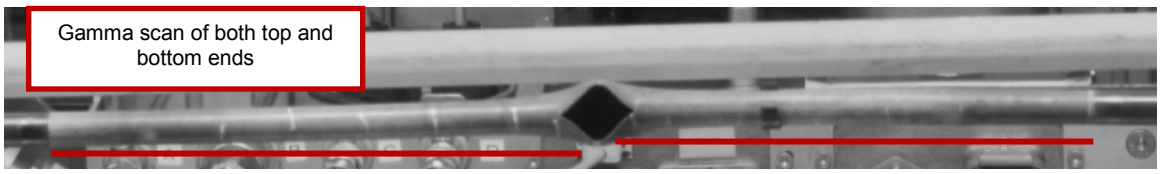

Figure 2-18 Photo of test segment from Test 191, indicating the relative length of gamma scan results

In Figure 2-19, the gamma scan results were plotted together with the profilometry results and the wire probe measurements performed just after the LOCA test (indicated as “post-LOCA” in the figure below) and just after the shaking test (indicated as “final wire probe measurement” in the figure below).

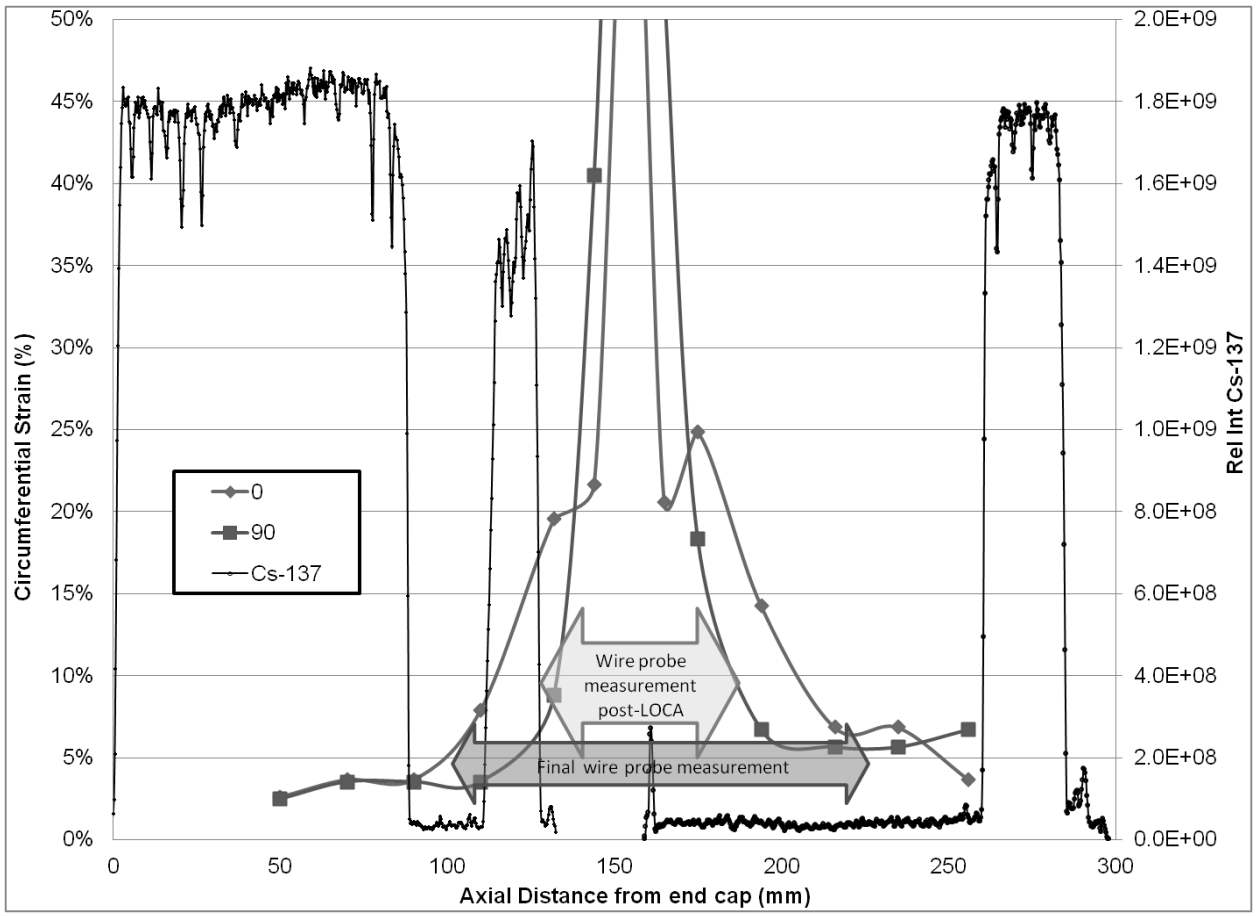

Figure 2-19 Gamma scan results for Test 191 with comparison to profilometry and initial wire probe measurements

As indicated earlier, theses gamma scan results were obtained over 1 year after the LOCA test was performed. In the time between the LOCA test and these gamma scans, the rodlet portions were stored in metal cans in the hot-cell. It is important to note that the gamma scan was performed with the balloon end down and that the bottom end of the rodlet portion was filled with epoxy because of the preparation work for making the metallography sample in the balloon node. The gamma scan indicates fuel material in the 110-120 millimeter range and a gradual decline of the fuel column in the 75-90 millimeter range in Figure 2-19. The fuel material in the 110-120 millimeter range is probably loose material that is trapped by the epoxy filling. However, the balloon end of the top rodlet portion was open during storage and some fuel material was found in the metal can once this rodlet portion was removed for gamma scanning. The mass of fuel material found in the can was 16.7 grams. It is important to note that this fuel had fallen out of the rod before the gamma scan. This additional fuel loss during storage approximately accounts for the difference between the final wire probe measurement and the indication on the gamma scan results of the start of the remaining fuel column on the top rodlet portion.

2.3 Test 192

Table 2-5 summarizes measurements and values that characterize the initial state, transient, and in-cell measurements of Test 192. The initial state, transient information and in-cell measurements will be described further in the following sections. Metallography, hydrogen measurements, and gamma scan results will also be provided.

Table 2-5 Measurements and Values That Characterize the Initial State, Transient, and In-Cell Measurements of Test 192

Initial State	Adjacent H (wppm)	Average Oxide (μm)	Rod Average Burn Up (GWd/MTU)		Rod Internal Pressure at 300°C (bar)	
	176, 288	25-30	68.2		82	
Transient	Peak Cladding Temperature (°C)	Rupture Temp (°C)	Rupture Pressure (bar)	Time (s) to reach 50% of rupture P for top/bottom gauges	CP-ECR (%)	Quench
	1185	700	81	13 / 15	11	Yes
In-Cell Measurements	Max Strain (%)	Length >10% Strain (mm)	Wire Probe Measurement (mm) (Top/Bottom)		Rupture Dimensions (mm) (Width/Length)	
	56	85	85 / 73		9 / 22.7	

2.3.1 Initial State

For Test 192, a segment of high burnup Westinghouse ZIRLO™ was used. The segment was taken from a rod that was irradiated at a U.S. power plant and had a rod average burnup of 68.2 GWd/MTU. Again, the operating history for this rod was defined by a mean LHGR of approximately 24 kW/m for cycle one, 23 kW/m for cycle two, 5 kW/m for cycle three, and 15 kW/m for cycle four. The 300-millimeter segment was taken from the middle section of the fuel rod, approximately 1800 millimeters from the bottom of the full length rod. The hydrogen content was measured just below and above the segment and was determined to be 176 and 288 wppm, respectively. The eddy current measurements indicate that the oxide layer thickness increased slightly over the length of this segment, and ranged from about 25 micrometers to 30 micrometers.

2.3.2 Transient Information

To begin the transient, the rodlet was heated and maintained at 300 degrees C for approximately 15 minutes to achieve thermal equilibrium. Before initiating the temperature ramp, the desired fill pressure was established at 300 degrees C. The pressure adjustment procedure provides an indication of gas communication by observing the response time of the lower pressure transducer, as shown in Figure 2-20. Recall that while the gas line is open, the top pressure transducer indicates the gas line pressure and the bottom should reflect the ability of gas to move the 300 millimeters to equilibrate pressure. Once the desired fill pressure was established, the gas line was closed and the rodlet was heated at 5 degrees C/s until the rodlet temperature reached 1,160°C. The rodlet was held at 1,160°C for 5 seconds. The calculated CP-ECR (based on measured rupture strain reported below) was approximately 11 percent.

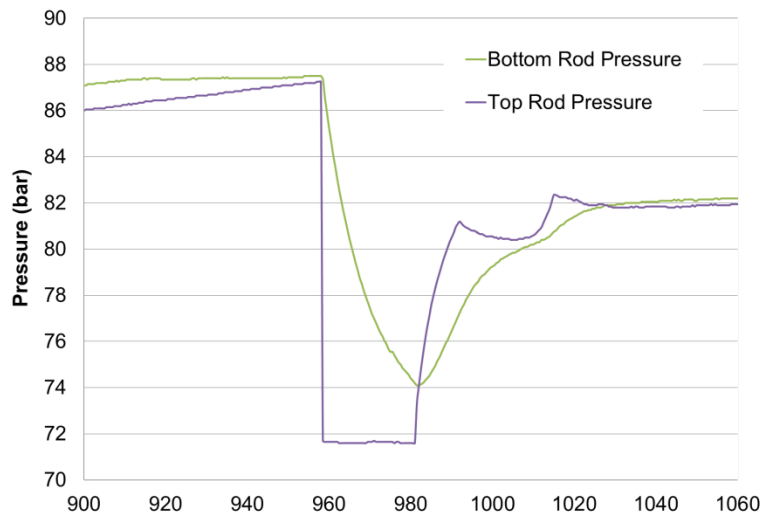

Figure 2-20 Fill pressure adjustment at 300 °C for Test 192, which provides an indication of gas communication

Rupture is estimated to have taken place when the rod internal pressure reached 81 bar and the cladding temperature reached 700 °C. The depressurization rate was relatively slow for Test 192; the top pressure gauge recorded a 50 percent reduction in pressure (relative to 81 bar) after 13 seconds and the bottom pressure gauge recorded a 50 percent reduction in pressure after 15 seconds. The temperature and pressure history for Test 192 is shown in Figure 2-21.

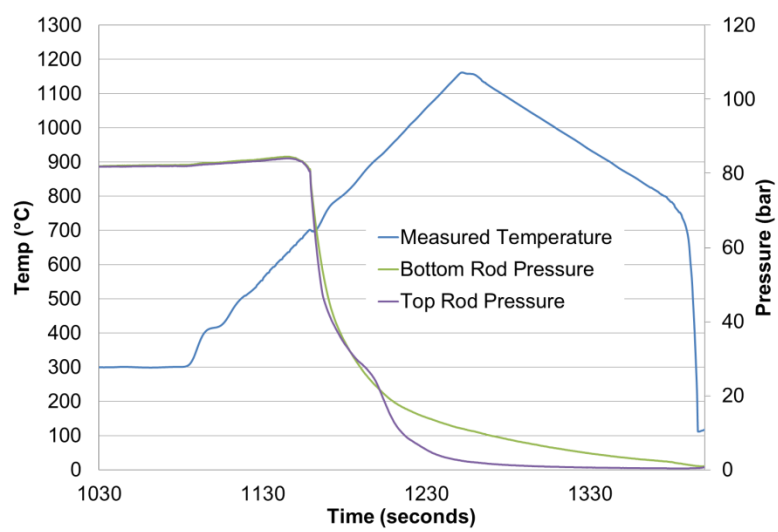

Figure 2-21 Temperature and pressure history for Test 192

2.3.3 In-Cell Measurements

After the simulated LOCA transient was complete, the fuel rod was examined. Figure 2-22 provides two photos of the fuel rod after the test. The rupture opening was measured to be 9.0 millimeters wide and 22.7 millimeters in length along the axial direction.

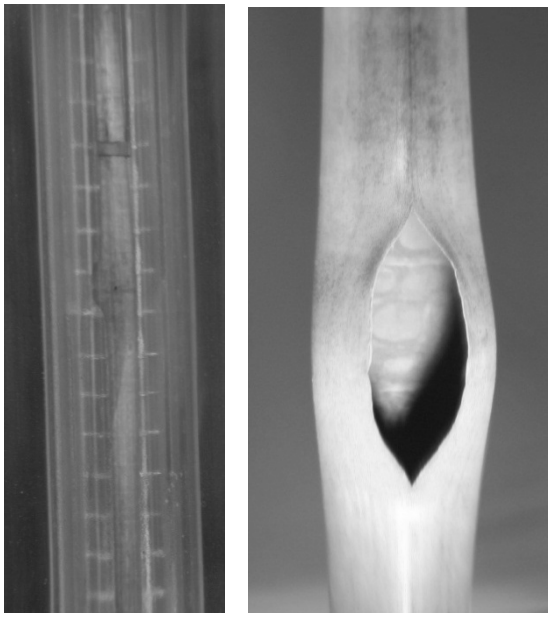

(a) (b)

Figure 2-22 Rod segment from Test 192 (a) in test rig after transient and (b) a closeup of the rupture opening after the transient

The rod did not experience significant distortion (or bending) during the LOCA transient, which can be seen in Figure 2-23. Profilometry measurements were made and they are shown in Figure 2-24. In Figure 2-24, the initial diameter and rupture length are also indicated. The mid-wall rupture strain value for Test 192 was calculated to be 56 percent.

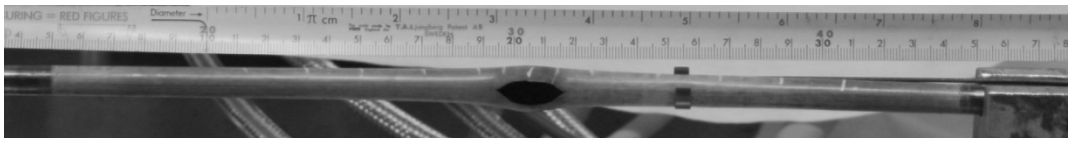

(a)

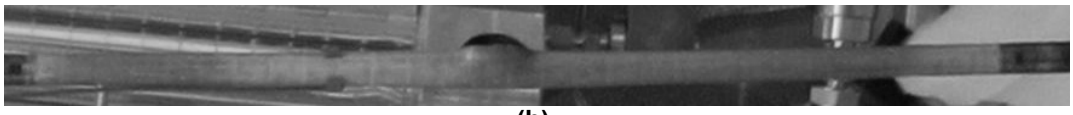

(b)

Figure 2-23 Rod segment from Test 192 showing no significant rod bending (a) out of plane with the rupture or (b) in plane with the rupture

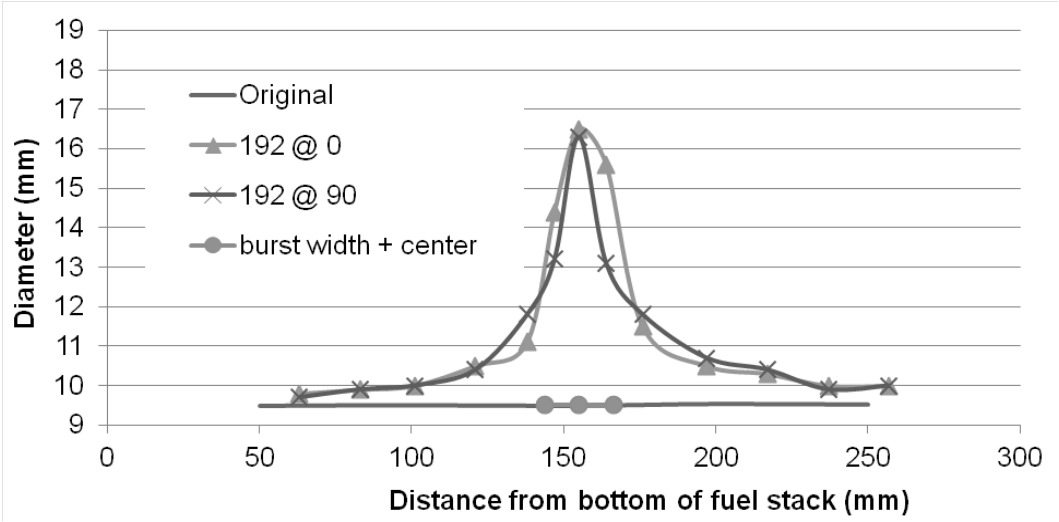

Figure 2-24 Profilometry measurements of segment 192 post-transient. The rupture length is also indicated.

In total, it appears that about half of the fuel fell out of this rod during the simulated LOCA transient test and during shaking. During the wire probe measurement, completed after all experimental steps (LOCA transient, bending and shaking), the probe traveled unobstructed approximately 73 millimeters above and approximately 85 millimeters below the rupture center. The mass loss measured following the LOCA test was 68 grams. The mass loss measured following the bend test and after shaking was16 grams. In total, 84 grams of fuel was lost. Figure 2-25 provides an image of the collected fuel fragments.

Figure 2-25 Images of fuel collected from Test 192

The fragment size distribution of the fuel dispersed and collected from Test 192 was investigated using sieve analysis. The measured mass of each sieve group is provided in Table 2-6, along with the mass percentage of each group relative to the total fuel analyzed.

Table 2-6 Fragment Size Distribution Results from Test 192

Size	Weight fuel (g)	% of total
< 0.125 mm	22.6	32%
0.125 - 0.25	8.0	11%
0.25 - 0.5 mm	9.1	13%
0.5 - 1 mm	10.2	14%
1 - 2 mm	13.3	19%
2 - 4 mm	8.2	11%
> 4 mm	0	0%
Sum:	71.4	100%

2.3.4 Metallography and Hot-Vacuum Extraction

Two metallography examinations and seven hydrogen measurements were made of the rodlet used in Test 192. The locations of metallography and hydrogen measurements are shown in Figure 2-26.

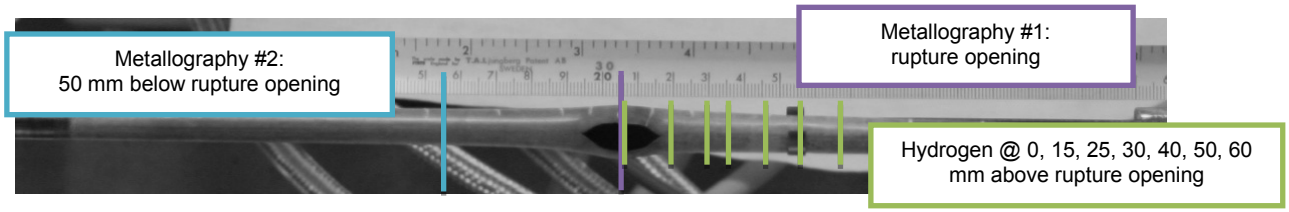

Figure 2-26 Photo of test segment from Test 192, indicating the location of metallography and hydrogen measurements

The metallography sample shown in Figure 2-27 was taken from the rupture opening. Select, high-resolution images from the outer cladding diameter and inner cladding diameter are included in Figure 2-28 and Figure 2-29, respectively.

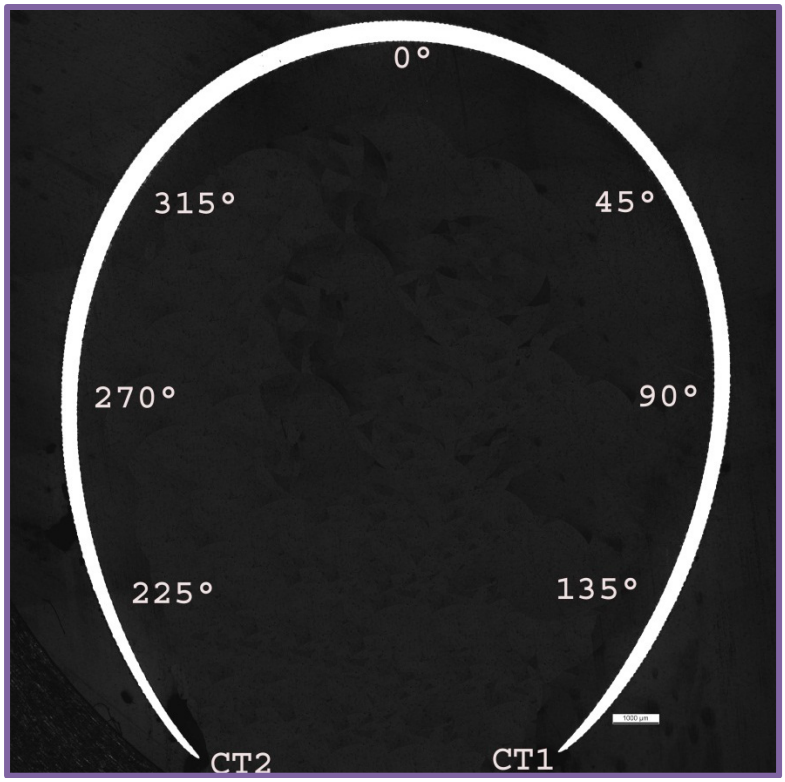

Figure 2-27 Macrograph of cross section from the rupture region of rodlet tested in LOCA Test 192

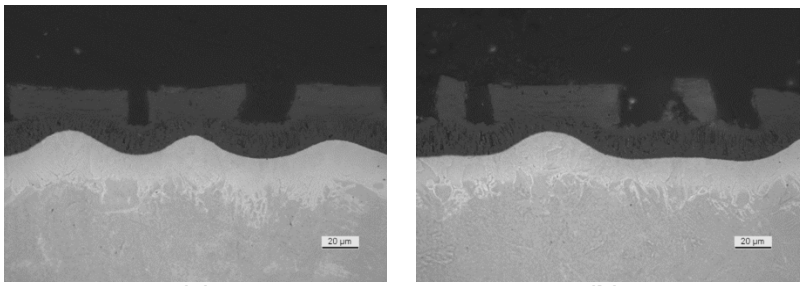

Figure 2-28 Two high-resolution images of the cladding outer diameter from the metallography examination in the rupture region of the rodlet tested in LOCA Test 192 at (a) 45° and (b) 135°

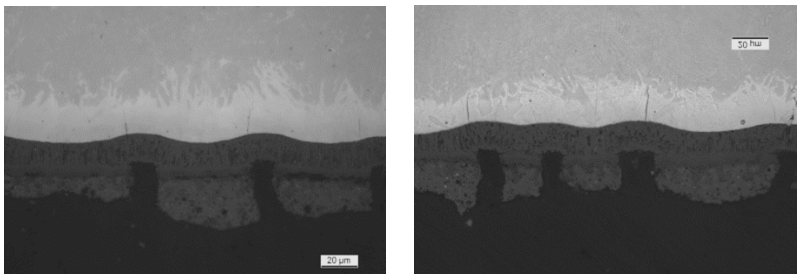

(a) (b)

Figure 2-29 Two high-resolution images of the cladding inner diameter from the metallography examination in the rupture region of the rodlet tested in LOCA Test 192 at (a) 0° and (b) 315°

Here, it is useful to recall that the calculated CP-ECR was 11 percent, with a hold time at 1,185 degrees C of 5 seconds. In Figure 2-28, the initial oxide thickness can be seen to have cracked and separated in this high strain (56 percent) area, and the transient oxidation layer is seen beneath this damaged initial oxide layer. The noticeable scalloping of the oxide layer was often seen in the outer diameter of the LOCA test samples. In Figure 2-29, it appears that some fuel fragments remain on the inner diameter and that the initial fuel-cladding bonding layer has also cracked and separated. An inner diameter transient oxidation layer is seen, which appears to be approximately the same thickness at the outer transient oxidation layer. These observations are expected at this location because it is in the rupture node and therefore exposed to a steam environment after rupture.

The metallography sample shown in Figure 2-30 was taken from a section 50 millimeters below the rupture opening. Select, high-resolution images from the outer cladding diameter and inner cladding diameter are included in Figure 2-31 and Figure 2-32, respectively.

In Figure 2-30, the interior of the cladding contains a large feature in the middle of the cross section. This feature is an artifact of the epoxy casting. This rod was cast with epoxy in two stages and the features in the interior of the cladding reveal the boundary between the two stages of epoxy casting.

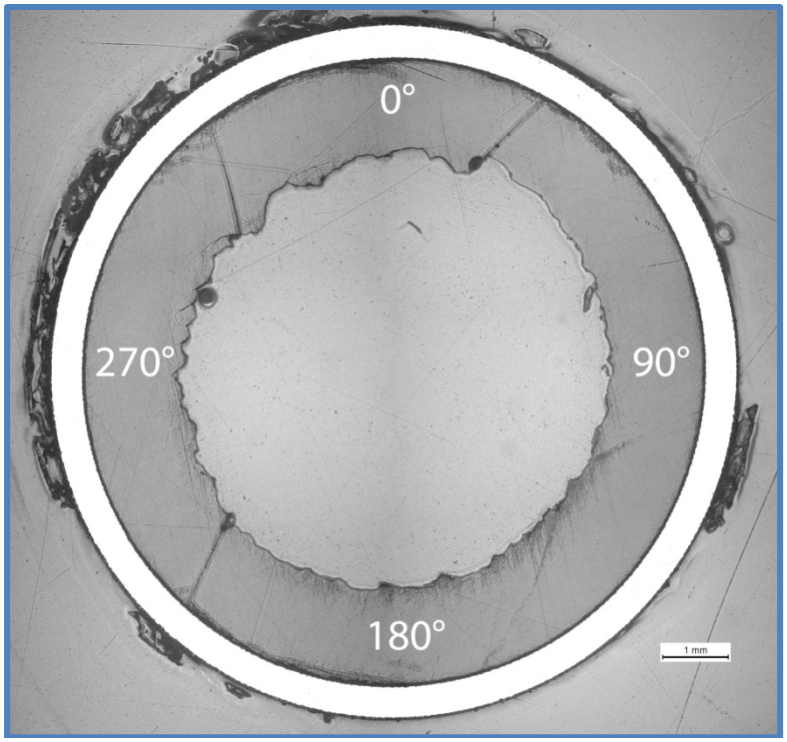

Figure 2-30 Macrograph of cross section from 50 mm below the rupture region of rodlet tested in LOCA Test 192

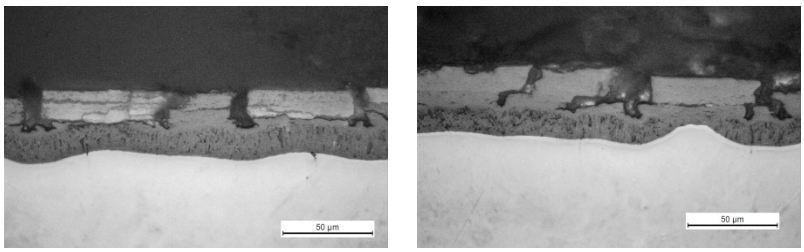

(a) **(b)**

Figure 2-31 Two high-resolution images of the cladding outer diameter from the metallography examination 50 mm below the rupture region of the rodlet tested in LOCA Test 192 at (a) 90° and (b) 315°

In Figure 2-31, the initial oxide thickness can be seen to have slightly cracked and separated in this area, although much less than in the images taken from the rupture node. The strain in this region was approximately 5-7 percent. As in the rupture node, the transient oxidation layer is seen beneath this damaged initial oxide layer. In Figure 2-32, it appears that some fuel fragments remain on the inner diameter and that the initial fuel-cladding bonding layer has also cracked and separated. An inner diameter transient oxidation layer is seen, which appears to approximately the same thickness at the outer transient oxidation layer.

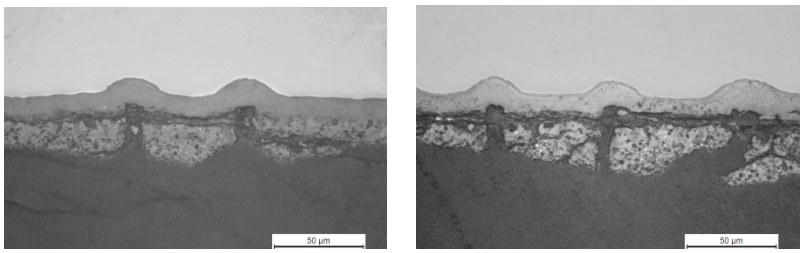

(a) (b)

Figure 2-32 Two high-resolution images of the cladding inner diameter from the metallography examination 50 mm below the rupture region of the rodlet tested in LOCA Test 192 at (a) 45°and (b) 225°

The location and values of hydrogen content, measured by hot vacuum extraction, are provided in Table 2-7 and illustrated, relative to the segment post-LOCA strain profile and rupture length measurements, in
Figure 2-33.

Table 2-7 Hydrogen Measurements for Test 192

Distance above rupture opening (mm)	0	15	25	30	40	50	60
Hydrogen Content (wppm)	212	781	963	938	738	635	453

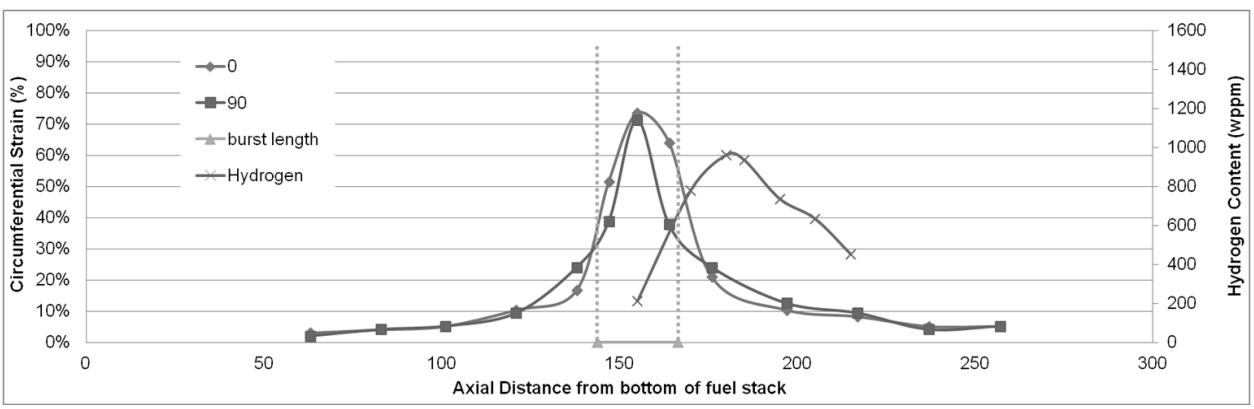

Figure 2-33 Hydrogen measurements from 192 relative to segment strain profile and rupture length

2.3.5 Gamma Scan Results with Comparison to Profilometry and Initial Wire Probe Measurements

Almost 1 year after the last LOCA tests were completed, emerging questions prompted new PIE investigations. The wire probe measurements performed just after the LOCA tests indicated a long length of empty cladding, but also a significant amount of residual fuel material in the end

regions of the test segments. To investigate the length and condition of the remaining fueled regions, gamma scans and additional metallography and ceramography (M/C) examinations were performed. Recall that the rodlet used in Test 192 fractured in the rupture node during the four-point bend test, and multiple cladding segments were removed for metallography and hydrogen analysis. The remaining portions of the rodlet were gamma scanned separately and the scans in combination covered about two-thirds of length of the rodlet, as shown in Figure 2-34. The locations of additional M/C examinations are also shown in Figure 2-34.

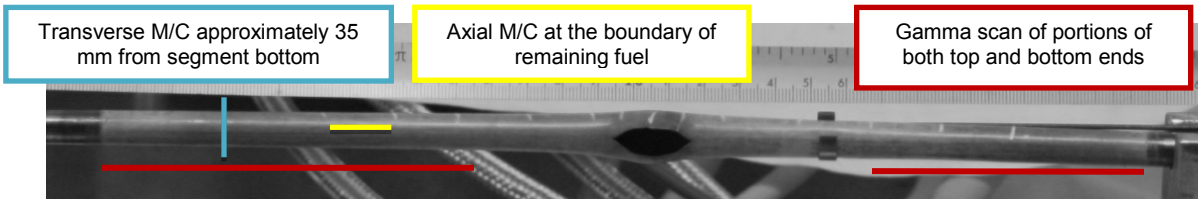

Figure 2-34 Photo of test segment from Test 192, indicating the relative length of gamma scan results and location of additional M/C examinations in the remaining fueled regions

In Figure 2-35, the gamma scan results were plotted together with the profilometry results and the wire probe measurements performed just after the LOCA test (indicated as “post-LOCA” in the figure below) and just after the shaking test (indicated as “final wire probe measurement” in the figure below).

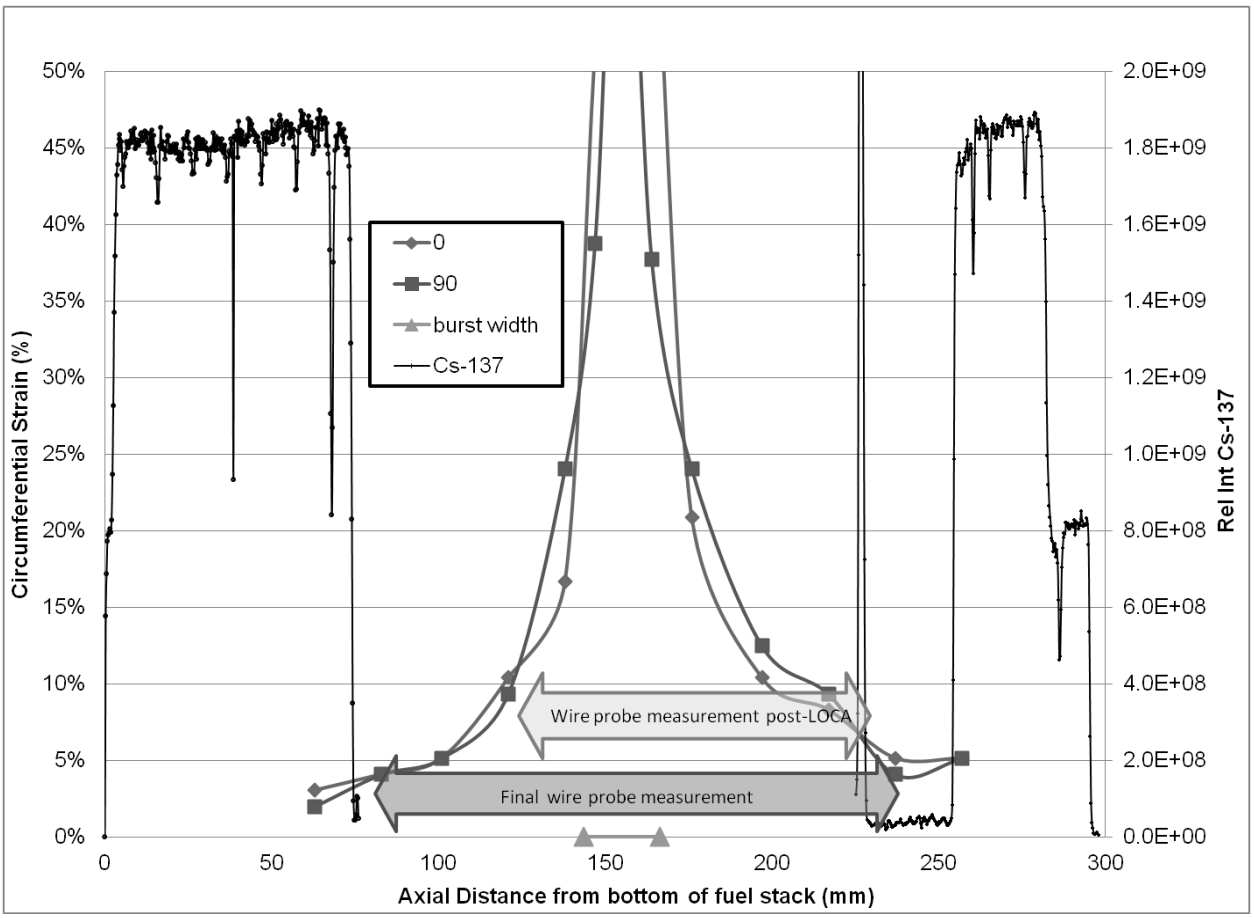

Figure 2-35 Gamma scan results for Test 192 with comparison to profilometry and initial wire probe measurements

As indicated earlier, theses gamma scan results were obtained over 1 year after the LOCA test was performed. In the time between the LOCA test and these gamma scans, the rodlet portions were stored in metal cans in the hot-cell. Some fuel material was found in the metal cans once the rodlet portions were removed for gamma scanning and some additional material fell out after minor shaking. The mass of fuel material found in the can storing the top portion of the rodlet was 5.4 grams (no additional fuel loss was noticed in the can storing the bottom portion of the rodlet). It is important to note that this fuel had fallen out of the rod before the gamma scan. This additional fuel loss during storage approximately accounts for the difference between the final wire probe measurement and the indication on the gamma scan results of the start of the remaining fuel column on the top rodlet portion. An image of the fuel material collected from the top end of rodlet 192 is shown in Figure 2-36.

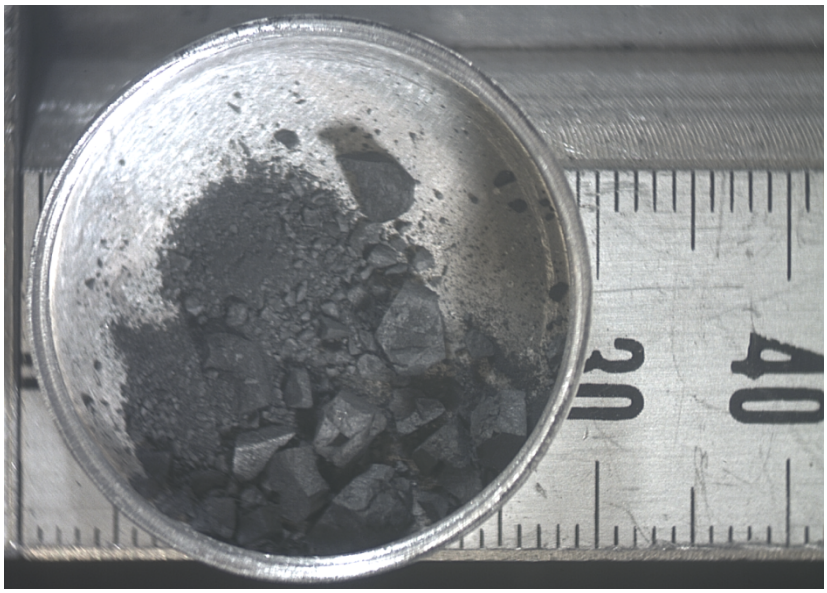

Figure 2-36 Fuel fragments collected from the top end of rod 192 after gentle shaking just before gamma scan

Considering the initial wire probe measurements, the fuel fragments collected after the LOCA test and initial shake test (shown in Figure 2-25 and quantified in Table 2-6) likely originated from the middle 150 millimeter region of the fuel rod that was measured to be empty following the LOCA test. However, the fuel fragments shown in Figure 2-36 collected 1 year later, after gentle shaking just before the gamma scan, likely originated from some span beyond the middle 150 millimeters, possibly in the axial length between the wire probe measurement and the indication of fuel in the gamma scan (approximately 230-255 millimeters in Figure 2-35). Additional sieve analysis was performed to characterize the fragment size distribution of the fragments shown in Figure 2-36. The measured mass of each sieve group is provided in Table 2-8, along with the mass percentage of each group relative to the total fuel analyzed. Figure 2-37 provides a comparison of the fuel fragment size distribution from these two regions of segment 192. The comparison suggests that fragmentation may be less pronounced in regions near the rodlet ends and further from rupture.

Table 2-8 Fragment Size Distribution Results for Fuel Fragments Collected from the Top End of Rod 192 after Gentle Shaking Just before Gamma Scan

Size	Weight fuel (g)	% of total
< 0.125 mm	0.4	7%
0.125 - 0.25	0.2	4%
0.25 - 0.5 mm	0.3	6%
0.5 - 1 mm	0.3	6%
1 - 2 mm	0.9	17%
2 - 4 mm	3.3	61%
> 4 mm	0	0%
Sum:	5.4	100%

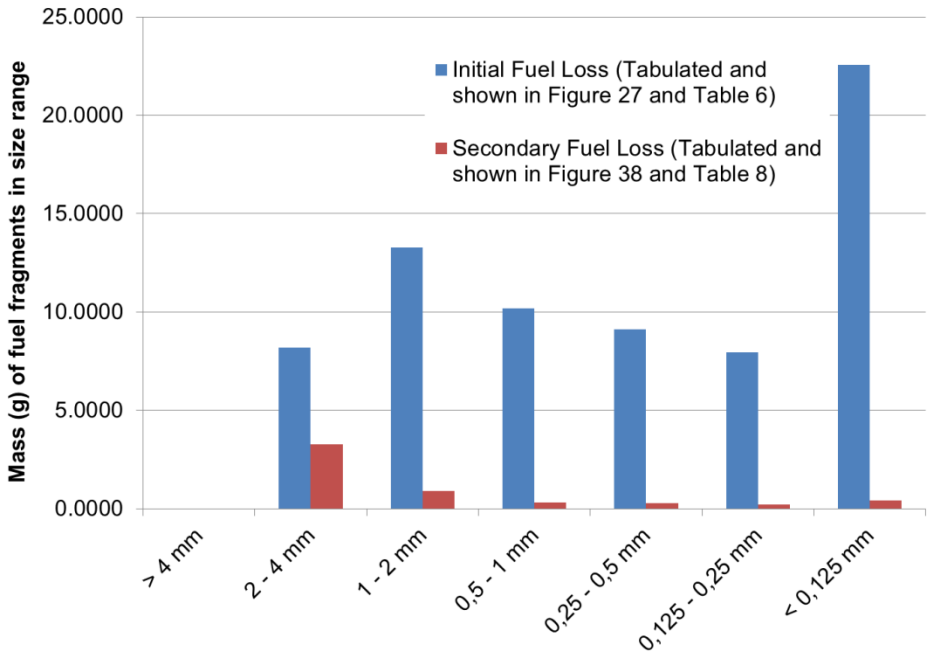

Figure 2-37 Comparison of fuel fragment size distribution from two regions of segment 192

Additional M/C examinations provide an even more detailed characterization of the remaining fueled region than the gamma scan results. The transverse M/C sample shown in Figure 2-38 was taken approximately 35 millimeters from the segment bottom. The image reveals a largely intact pellet cross section. A high-resolution image, shown in Figure 2-39, reveals that some amount of fuel remains attached to the inner cladding wall. Many small fuel fragments can be seen in the space between the cladding and the relatively intact remaining fuel material.

Figure 2-38 Macrograph of transverse cross section 35 mm from the bottom of the rodlet tested in LOCA Test 192

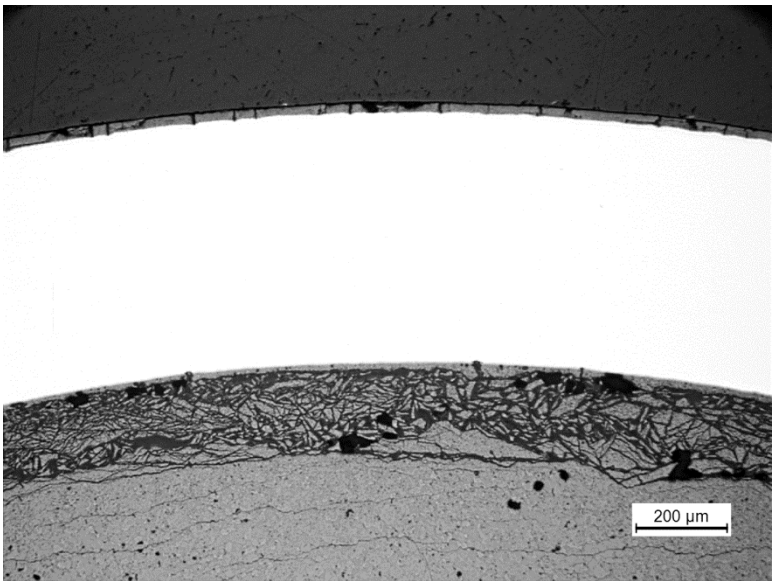

Figure 2-39 A high-resolution image of the fuel cladding gap from the M/C examination 35 mm from the bottom of the rodlet tested in LOCA Test 192

The axial M/C sample shown in Figure 2-40 was taken at the boundary of remaining fuel and empty cladding, covering a span approximately 50-75 millimeters from the segment bottom.

The image reveals that the boundary between fueled an empty cladding is abrupt, and that the fueled region contains cracked, but largely complete, pellet cross sections.

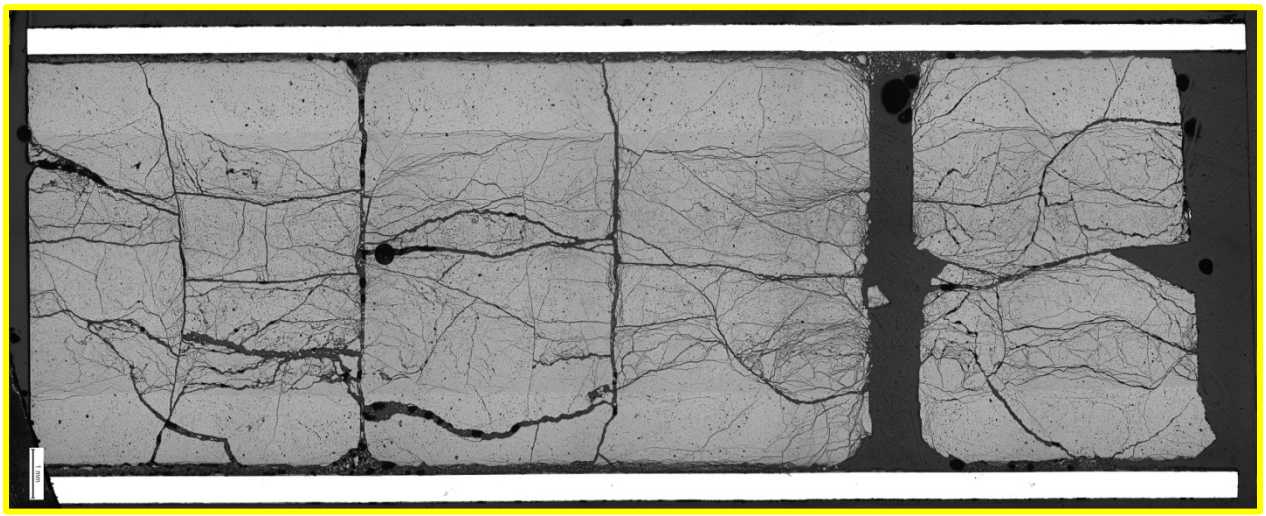

Figure 2-40 Macrograph of axial cross section covering a span approximately 50–75 mm from the segment bottom of the rodlet tested in LOCA Test 192

Select, high-resolution images are included in Figure 2-41 from the inner (a and b) and outer (c and d) cladding diameter. These images were near the bottom (left) of the axial M/C, approximately 55 millimeters from the original segment bottom of the rodlet tested in LOCA Test 192. Again, here it is useful to recall that for Test 192 the calculated CP-ECR was 11 percent, with a hold time at 1,185 degrees C of 5 seconds.

In Figure 2-41 (a and b), fuel fragments remain on the inner diameter and the fuel-clad bond layer appears more intact than in the M/C images in Figure 2-29 and Figure 2-32 taken within and 50 millimeter below the rupture node, respectively. Also, an alpha layer microstructure can be seen on the inner diameter. This region of the test segment remained fueled and was far (approximately 100 millimeters) from the rupture location; therefore, the inner diameter was not exposed to a steam environment during the transient. The oxygen necessary for the inner diameter alpha layer is proposed to have originated from the fuel-cladding bond layer. In Figure 2-41 (c and d), the initial oxide layer, transient oxide layer, and an alpha layer can be seen.

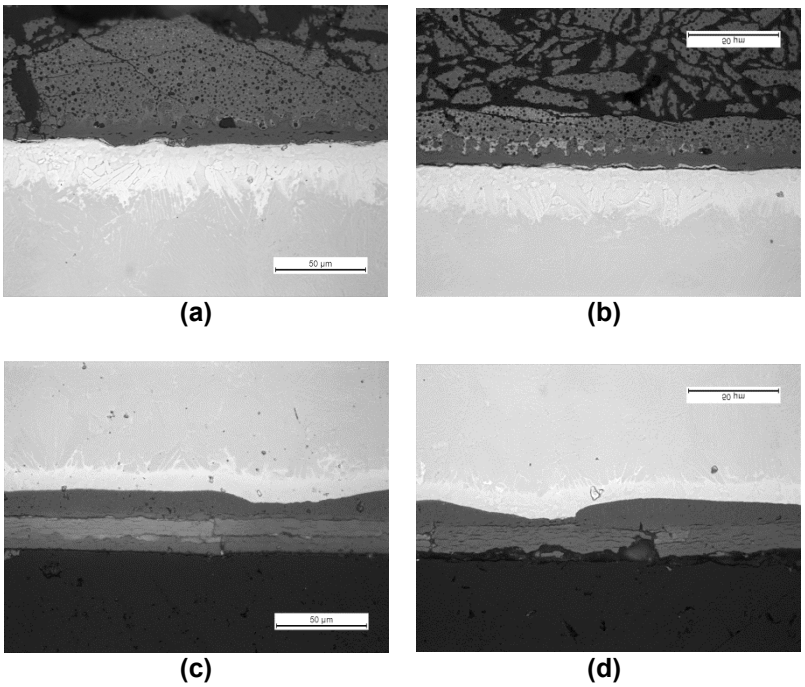

Figure 2-41 High-resolution images of the cladding (a and b) inner and (c and d) outer diameter taken from the axial M/C shown above. These images were near the bottom (left) of the axial M/C, approximately 55 mm from the original segment bottom and approximately 100 mm below the rupture opening of the rodlet tested in LOCA Test 192.

2.4 Test 193

Table 2-9 summarizes measurements and values that characterize the initial state, transient, and in-cell measurements of Test 193. The initial state, transient information and in-cell measurements will be described further in the following sections. Metallography, hydrogen measurements, and gamma scan results will also be provided.

Table 2-9 Measurements and Values That Characterize the Initial State, Transient, and In-Cell Measurements of Test 193

Initial State	Adjacent H (wppm)	Average Oxide (µm)	Rod Average Burn Up (GWd/MTU)		Rod Internal Pressure at 300°C (bar)	
	187	20	69.3		82	
Transient	Peak Cladding Temperature (°C)	Rupture Temp (°C)	Rupture Pressure (bar)	Time (s) to reach 50% of rupture P for top/bottom gauges	CP-ECR (%)	Quench
	1185	728	81	45 / 8	17	Yes
In-Cell Measurements	Max Strain (%)	Length >10% Strain (mm)	Wire Probe Measurement (mm) (Top/Bottom)		Rupture Dimensions (mm) (Width/Length)	
	50	100	113 / 91		13.8 / 17.8	

2.4.1 Initial State

For Test 193, a segment of high burnup Westinghouse ZIRLO™ was used. The segment was taken from a rod that was irradiated at a U.S. PWR power plant and had a rod average burnup of 69.3 GWd/MTU. Again, the operating history for this rod was non-typical and defined by a mean LHGR of approximately 24 kW/m for cycle one, 23 kW/m for cycle two, 5 kW/m for cycle three, and 15 kW/m for cycle four. The 300-millimeter segment was taken from the middle section of the fuel rod, approximately 1400 millimeters from the bottom of the full length rod. A hydrogen content of 187 wppm was measured just above the segment. The eddy current measurements indicate that the oxide layer thickness is relatively constant over the length of this segment, averaging about 20 micrometers thick.

2.4.2 Transient Information

To begin the transient, the rodlet was heated and maintained at 300 degrees C for approximately 15 minutes to achieve thermal equilibrium. Before initiating the temperature ramp, the desired fill pressure was established at 300 degrees C. For Test 193, the rodlet was pressurized to 82 bar (at 300 degrees C). The pressure adjustment procedure provides an indication of gas communication by observing the response time of the lower pressure transducer, as shown in Figure 2-42. Recall that while the gas line is open, the top pressure transducer indicates the gas line pressure and the bottom should reflect the ability of gas to move the 300 millimeter to equilibrate pressure. Once the desired fill pressure was established, the gas line was closed and the rodlet was heated at 5 degrees C/s until the rodlet temperature reached 1,160 degrees C. The rodlet was held at 1,160°C for 85 seconds. The calculated CP-ECR (based on measured rupture strain reported below) was approximately 17 percent.

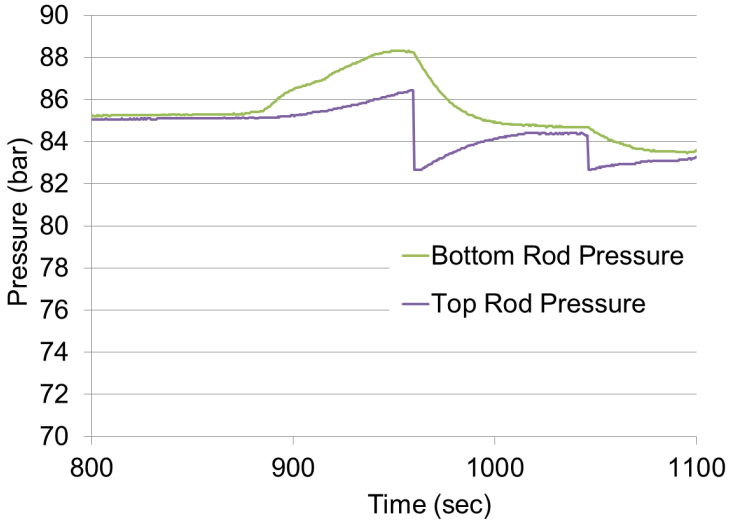

Figure 2-42 Fill pressure adjustment at 300 °C for Test 193, which provides an indication of gas communication

Rupture is estimated to have taken place when the rod internal pressure reached 81 bar and the cladding temperature reached 728 degrees C. The depressurization rate was relatively slow for Test 193; the top pressure gauge recorded a 50 percent reduction in pressure (relative to

81 bar) after 45 seconds and the bottom pressure gauge recorded a 50 percent reduction in pressure after 8 seconds. The temperature and pressure history for Test 193 is shown in Figure 2-43.

Figure 2-43 Temperature and pressure history for Test 193

2.4.3 In-Cell Measurements

After the simulated LOCA transient was complete, the fuel rod was examined. Figure 2-44 provides two photos of the fuel rod after the transient. The rupture opening was measured to be 13.8 millimeters wide and 17.8 millimeters in length.

(a) (b)

Figure 2-44 Rod segment from Test 193 (a) in test rig after transient and (b) a closeup of the rupture opening after the transient

The rod experienced minor distortion (or bending) during the LOCA transient, which can be seen in Figure 2-45. Profilometry measurements were made and they are shown in Figure 2-46. In Figure 2-46, the initial diameter and rupture length are also indicated. The mid-wall rupture strain value for Test 193 was calculated to be 50 percent.

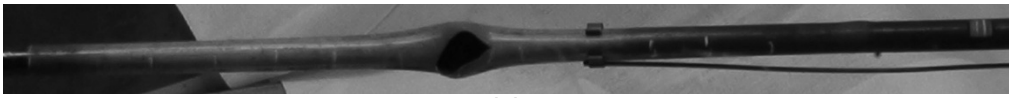

(a)

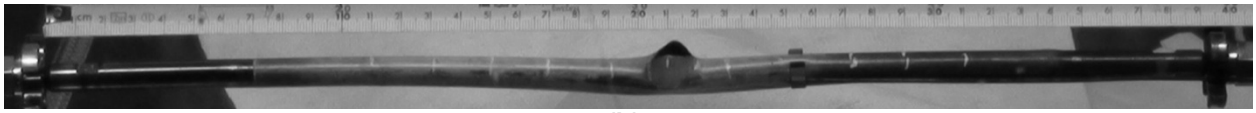

(b)

Figure 2-45 Rod segment from Test 193 showing no significant rod bending (a) in plane with the rupture and (b) minor bending out of plane with the rupture

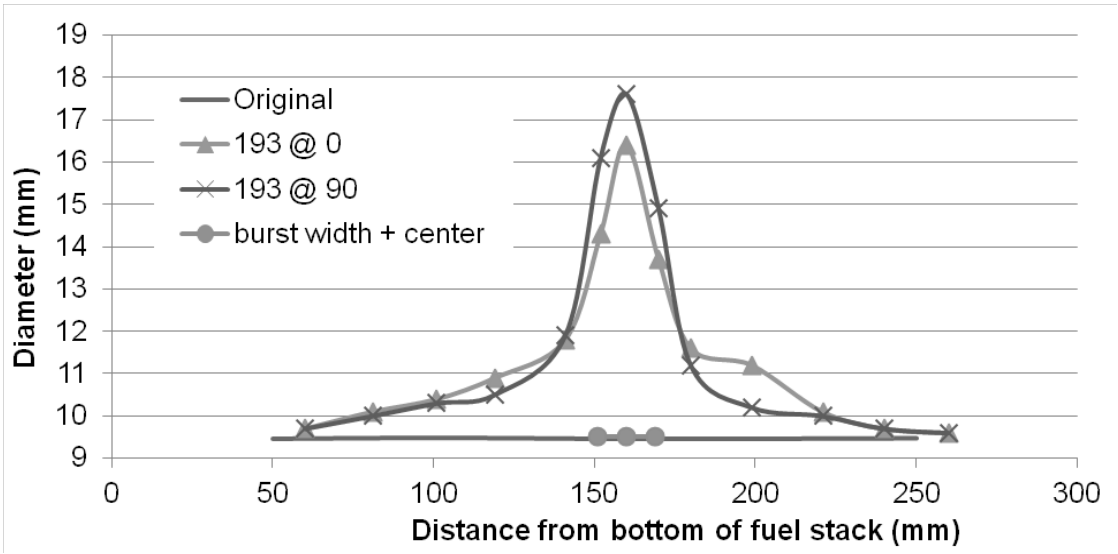

Figure 2-46 Profilometry measurements of segment 193 post-transient. The rupture length is also indicated.

In total, it appears that about half of the fuel fell out of this rod during the simulated LOCA transient test and during shaking. During the wire probe measurement, completed after all experimental steps (LOCA transient, bending and shaking), the probe traveled unobstructed approximately 92 millimeters above and approximately113 millimeters below the rupture center. The mass loss measured following the LOCA test was 105 grams. The mass loss measured following the bend test and after shaking was 41 grams. In total, 146 grams of fuel was lost. Figure 2-47 provides an image of the collected fuel fragments.

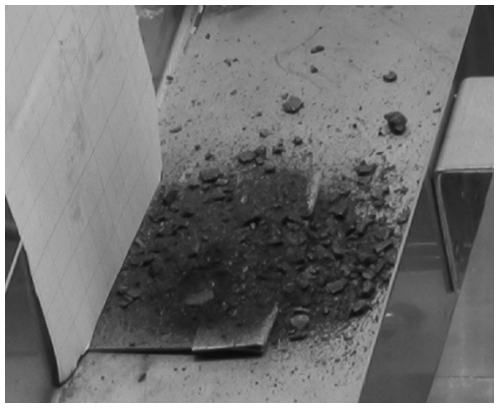

Figure 2-47 Images of fuel collected from Test 193

The fragment size distribution of the fuel dispersed and collected from Test 193 was investigated using sieve analysis. The measured mass of each sieve group is provided in Table 2-10, along with the mass percentage of each group relative to the total fuel analyzed.

Table 2-10 Fragment Size Distribution Results from Test 193

Size	Weight fuel (g)	% of total
< 0.125 mm	18.6	18%
0.125 - 0.25	10.7	10%
0.25 - 0.5 mm	13.7	13%
0.5 - 1 mm	17.4	17%
1 - 2 mm	19.6	19%
2 - 4 mm	20.2	20%
> 4 mm	2.1	2%
Sum:	102.3	100%

2.4.4 Metallography and Hot-Vacuum Extraction

Two metallography examinations were made of the rodlet used in Test 193. The locations of metallography samples are shown in Figure 2-48.

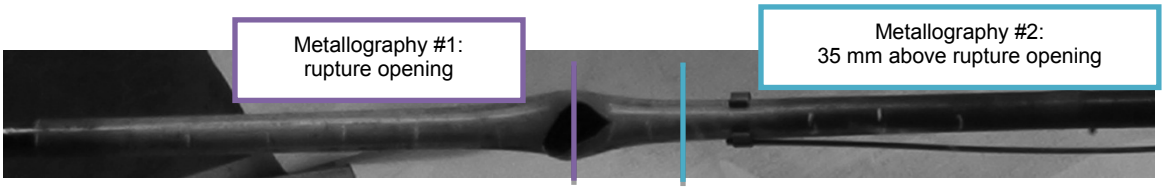

Figure 2-48 Photo of test segment from Test 193, indicating the location of metallography

The metallography sample shown in Figure 2-49 was taken from the rupture opening. Select, high-resolution images from the outer cladding diameter and inner cladding diameter are included in Figure 2-50 and Figure 2-51, respectively.

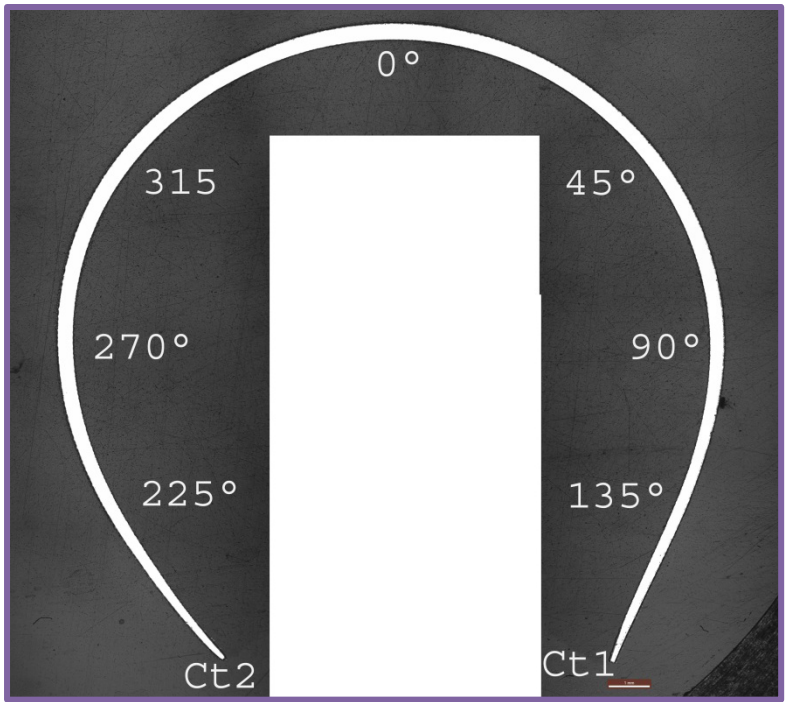

Figure 2-49 Macrograph of cross section from the rupture region of rodlet tested in LOCA Test 193

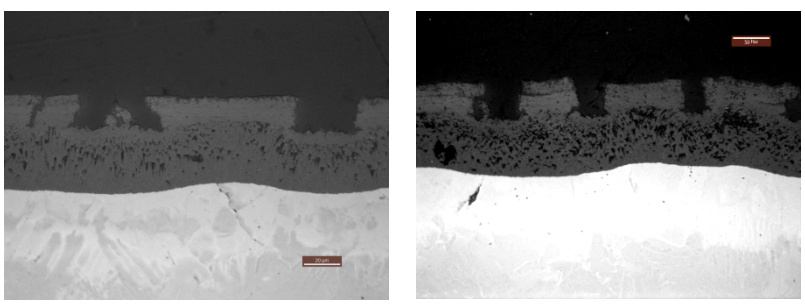

(a) **(b)**

Figure 2-50 Two high-resolution images of the cladding outer diameter from the metallography examination in the rupture region of the rodlet tested in LOCA Test 193 at (a) 90° and (b) 270°

Here, it is useful to recall that for Test 193 the calculated CP-ECR was 17 percent, with a hold time at 1,185°C of 85 seconds. In Figure 2-50, the initial oxide thickness can be seen to have cracked and separated in this high strain (50 percent) area, and the transient oxidation layer is seen beneath this damaged initial oxide layer. In Figure 2-51, it appears that some fuel fragments remain on the inner diameter and that the initial fuel-cladding bonding layer has also cracked and separated. An inner diameter transient oxidation layer is not apparent in these images, although the micrographs indicate some unique microstructure layer that may be an alpha zirconium layer. The absence of an inner diameter transient oxidation layer is somewhat surprising at this location because it is in the rupture node and was held for 85 seconds at high temperature.

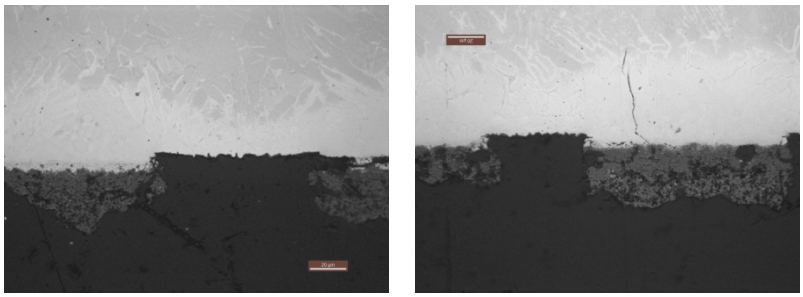

(a) (b)

Figure 2-51 Two high-resolution images of the cladding inner diameter from the metallography examination in the rupture region of the rodlet tested in LOCA Test 193 at (a) 135° and (b) 270°

The metallography sample shown in Figure 2-52 was taken from a section 35 millimeters above the rupture opening. Select, high-resolution images from the outer cladding diameter and inner cladding diameter are included in Figure 2-53 and Figure 2-54, respectively.

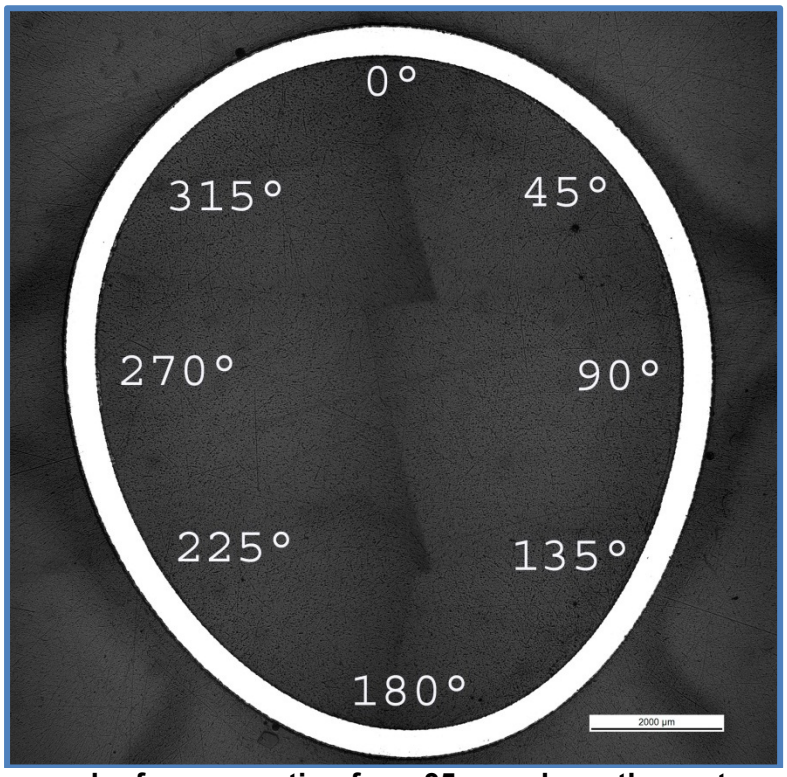

Figure 2-52 Macrograph of cross section from 35 mm above the rupture region of rodlet tested in LOCA Test 193

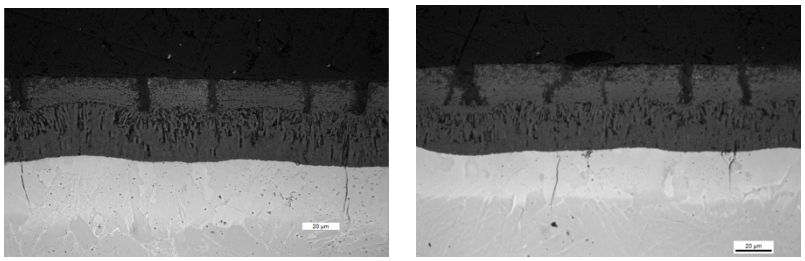

(a) (b)

Figure 2-53 Two high-resolution images of the cladding outer diameter from the metallography examination 35 mm above the rupture region of the rodlet tested in LOCA Test 193 at (a) 45° and (b) 270°

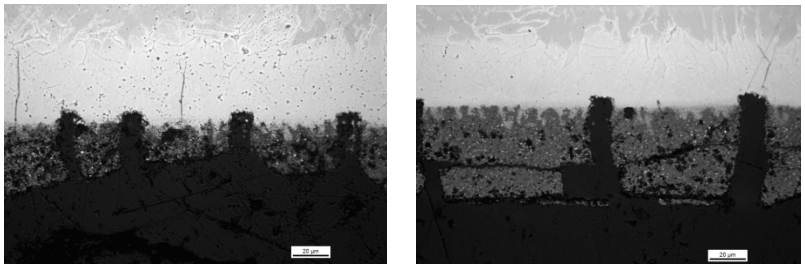

(a) (b)

Figure 2-54 Two high-resolution images of the cladding inner diameter from the metallography examination 35 mm above the rupture region of the rodlet tested in LOCA Test 193 at (a) 135° and (b) 270°

In Figure 2-53, the initial oxide thickness can be seen to have cracked and separated at this location 35 millimeters above the rupture node, and the transient oxidation layer is seen beneath this damaged initial oxide layer. The local strain in this region is approximately 15 to 20 percent. In Figure 2-54, it appears that some fuel fragments remain on the inner diameter and that the initial fuel-cladding bonding layer has also cracked and separated. An inner diameter transient oxidation layer is not apparent in these images, although the micrographs indicate some unique microstructure layer that may be an alpha zirconium layer.

No hydrogen measurements were ordered for this sample; however, metallography was completed on etched samples, which reveals the microstructure and hydrogen features across the cross section. One example is shown in Figure 2-55, which is taken from the M/C sample at the rupture mid-plane.

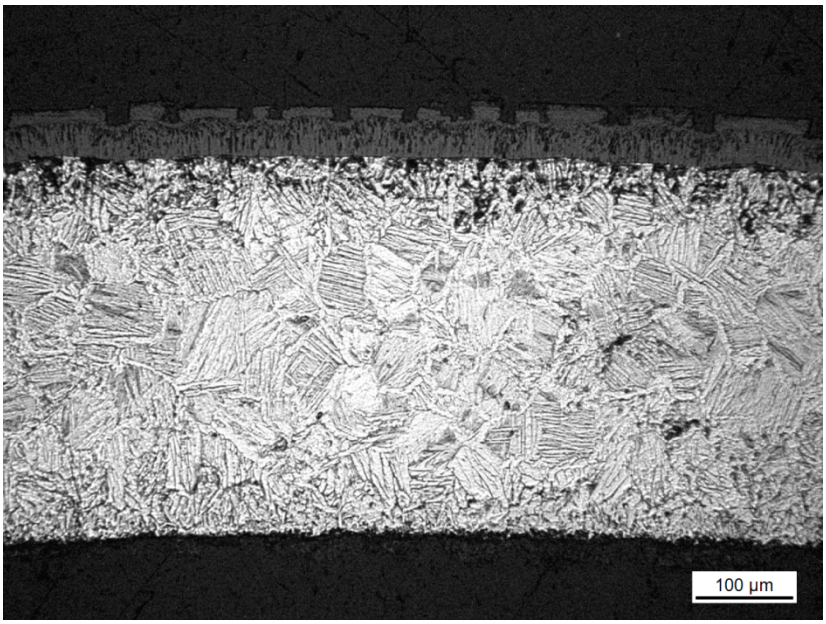

Figure 2-55 Etched cross section revealing hydrogen microstructure in the cladding in the rupture region of Test 193

2.4.5 Gamma Scan Results with Comparison to Profilometry and Initial Wire Probe Measurements

Almost 1 year after the last LOCA tests were completed, emerging questions prompted new PIE investigations. The wire probe measurements performed just after the LOCA tests indicated a long length of empty cladding, but also a significant amount of residual fuel material in some test segments. To investigate the length and condition of the remaining fueled segments, gamma scans were performed. Recall that the rodlet used in Test 193 fractured in the rupture node during the four-point bend test. The two halves of the rodlet were gamma scanned separately and the scans in combination covered almost the entire length of the rodlet, as shown in Figure 2-56.

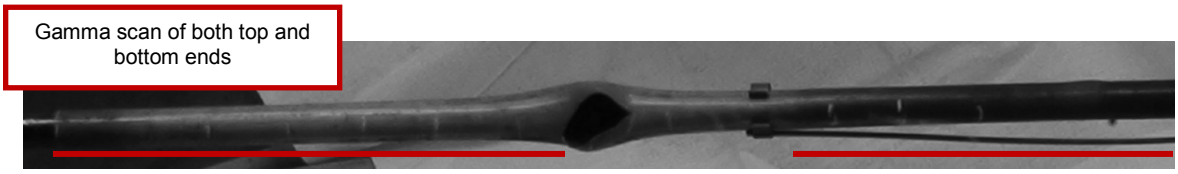

Figure 2-56 Photo of test segment from Test 193, indicating the relative length of gamma scan results

In Figure 2-57, the gamma scan results were plotted together with the profilometry results and the wire probe measurements performed just after the LOCA test (indicated as “post-LOCA” in the figure below) and just after the shaking test (indicated as “final wire probe measurement” in the figure below).

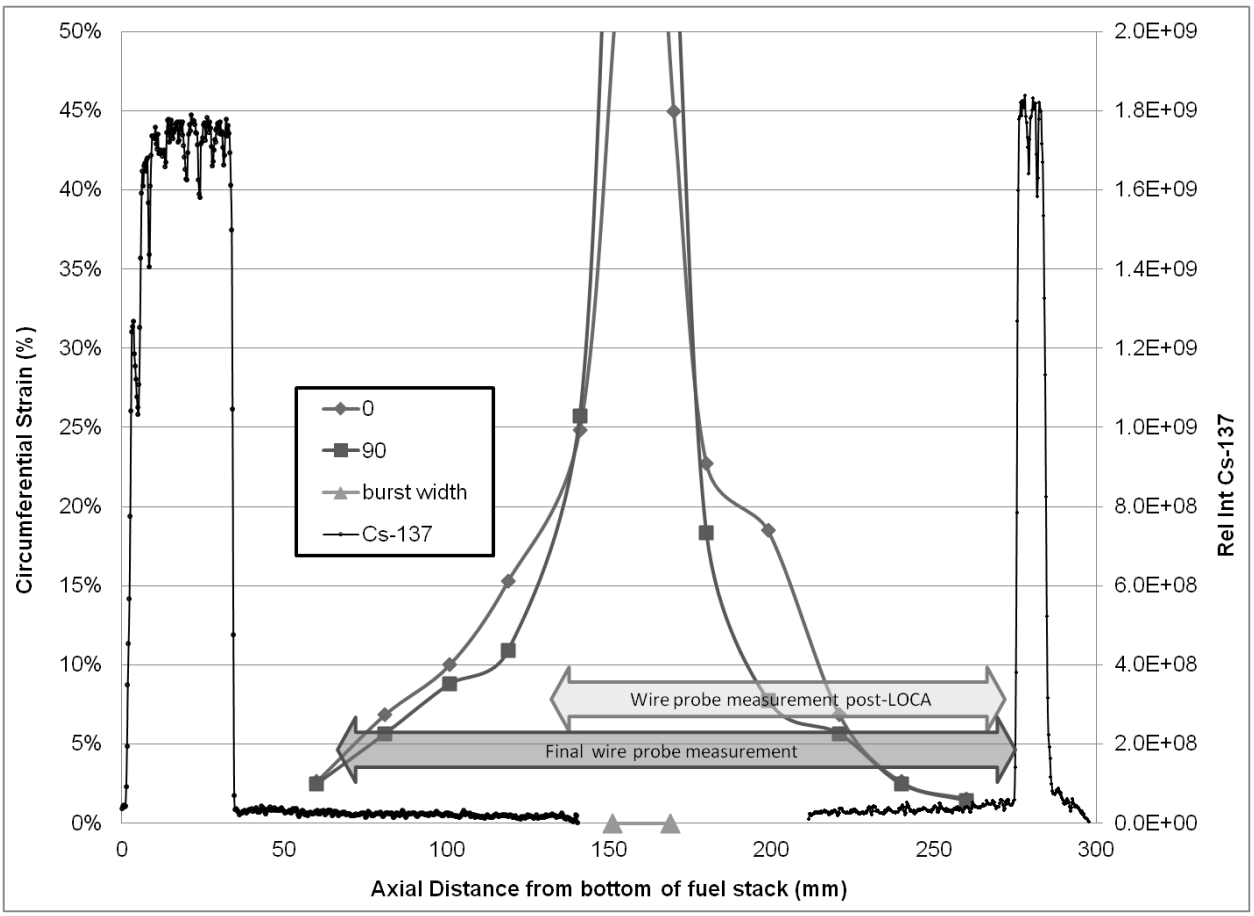

Figure 2-57 Gamma scan results for Test 193 with comparison to profilometry and initial wire probe measurements

As indicated earlier, theses gamma scan results were obtained over 1 year after the LOCA test was performed. In the time between the LOCA test and these gamma scans, the rodlet portions were stored in metal cans in the hot-cell. Some fuel material was found in the metal cans once the rodlet portions were removed for gamma scanning and some addition material fell out after minor shaking. The mass of fuel material found in the can storing the bottom portion of the rodlet was 6.6 grams. A small amount of fuel material was also found in the can storing the top portion of the rodlet. It is important to note that this fuel had fallen out of the rod before the gamma scan. This additional fuel loss during storage is slight less than what would be expected from the difference between the final wire probe measurement and the indication on the gamma scan results of the start of the remaining fuel column on the top rodlet portion.

2.5 Test 196

Table 2-11 summarizes measurements and values that characterize the initial state, transient, and in-cell measurements of Test 196. The initial state, transient information and in-cell measurements will be described further in the following sections. Metallography, hydrogen measurements, and gamma scan results will also be provided.

Table 2-11 Measurements and Values That Characterize the Initial State, Transient, and In-Cell Measurements of Test 196

Initial State	Adjacent H (wppm)	Average Oxide (μm)	Rod Average Burn Up (GWd/MTU)		Rod Internal Pressure at 300°C (bar)	
	149	20	55.2		82	
Transient	Peak Cladding Temperature (°C)	Rupture Temp (°C)	Rupture Pressure (bar)	Time (s) to reach 50% of rupture P for top/bottom gauges	CP-ECR (%)	Quench
	950	686	81	5 / 2	0	Yes
In-Cell Measurements	Max Strain (%)	Length >10% Strain (mm)	Wire Probe Measurement (mm) (Top/Bottom)		Rupture Dimensions (mm) (Width/Length)	
	25	95	90 / 66		0.2 / 1.5	

2.5.1 Initial State

For test 196, a segment of high burnup Westinghouse ZIRLO™ with a Zirconium Diboride Integral Fuel Burnable Absorber (IFBA) coating was used. The segment was taken from a rod that was irradiated at a U.S. PWR power plant and had a rod average burnup of 55.2 GWd/MTU. The operating history for this rod was typical of U.S. power plant operation to this burnup. The pellet enrichment was 4.94 weight percent (wt%) U^{235}. The 300-millimeter segment was taken from the middle section of the fuel rod, approximately 1300 millimeters from the bottom of the full length rod. A hydrogen content of 149 wppm was measured at a location adjacent to the segment. The eddy current measurements indicate that the oxide layer thickness is relatively constant over the length of this segment, averaging about 20 micrometers in thickness.

2.5.2 Transient Information

To begin the transient, the rodlet was heated and maintained at 300 degrees C for approximately 15 minutes to achieve thermal equilibrium. Before initiating the temperature ramp, the desired fill pressure was established at 300 degrees C. For test 196, the rodlet was pressurized to 82 bar (at 300 degrees C). The pressure adjustment procedure provides an indication of gas communication by observing the response time of the lower pressure transducer, as shown in Figure 2-58. While the gas line is open, the top pressure transducer indicates the gas line pressure and the bottom should reflect the ability of gas to move the 300 millimeter segment length to equilibrate pressure. Once the desired fill pressure was established, the gas line was closed and the rodlet was heated at 5 degrees C/s through ballooning and rupture. This was a “ramp-to-rupture” test and therefore the furnace was shut off to terminate the test at 950 degrees C and there was no quench. No significant oxidation was accumulated during this test.

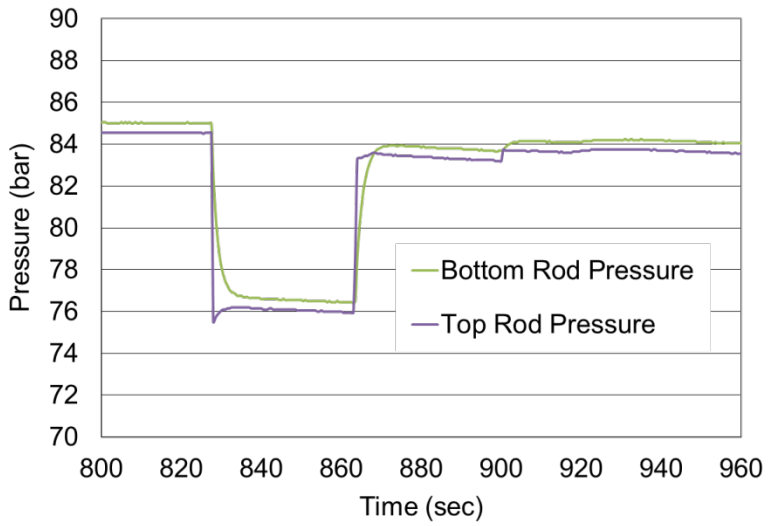

Figure 2-58 Fill pressure adjustment at 300 °C for Test 196, which provides an indication of gas communication

Rupture is estimated to have taken place when the rod internal pressure reached 81 bar and the cladding temperature reached 686 °C (1267 degrees F). The depressurization rate was relatively fast for test 196; the top pressure gauge recorded a 50 percent reduction in pressure (relative to 81 bar) after 5 seconds and the bottom pressure gauge recorded a 50 percent reduction in pressure after 2 seconds. The temperature and pressure history for Test 196 is shown in Figure 2-59.

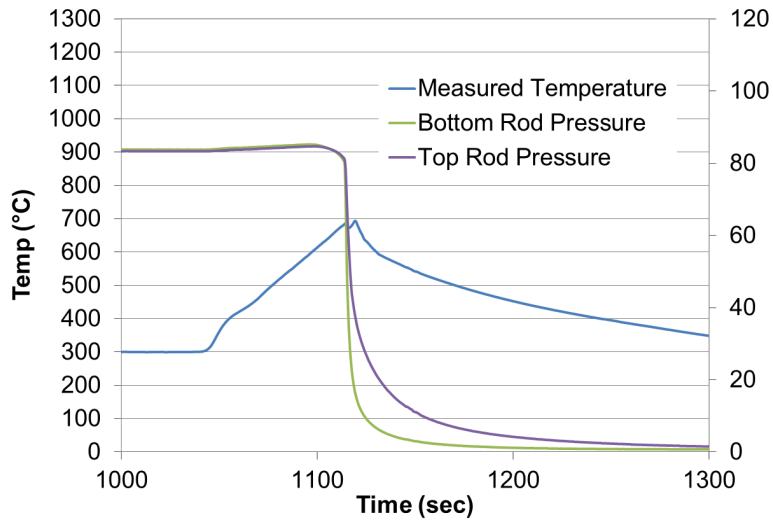

Figure 2-59 Temperature and pressure history for Test 196

2.5.3 In-Cell Measurements

After the simulated LOCA transient was complete, the fuel rod was examined. Figure 2-60 provides two photos of the fuel rod after the transient. The rupture opening was measured to be 0.2 millimeter wide and 1.5 millimeters in length.

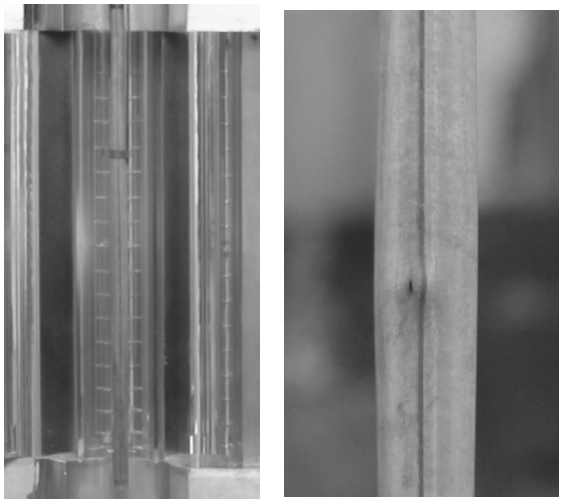

(a) (b)

Figure 2-60 Rod segment from Test 196 (a) in test rig after transient and (b) a closeup of the rupture opening after the transient

The rod did not experience distortion (or bending) during the LOCA transient, which can be seen in Figure 2-61. Profilometry measurements were made and they are shown in Figure 2-62. In Figure 2-62, the initial diameter and rupture length are also indicated. The mid-wall rupture strain value for Test 196 was calculated to be 25 percent.

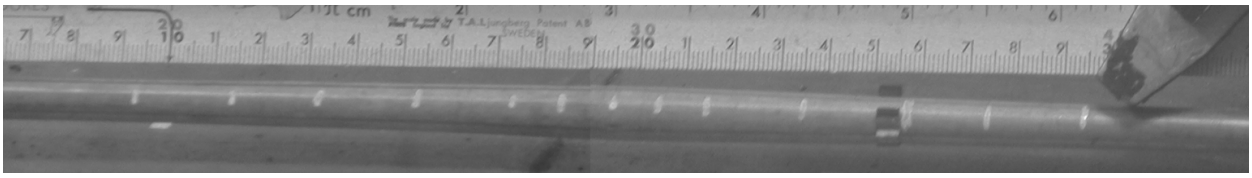

Figure 2-61 Rod segment from Test 196 showing no significant rod bending

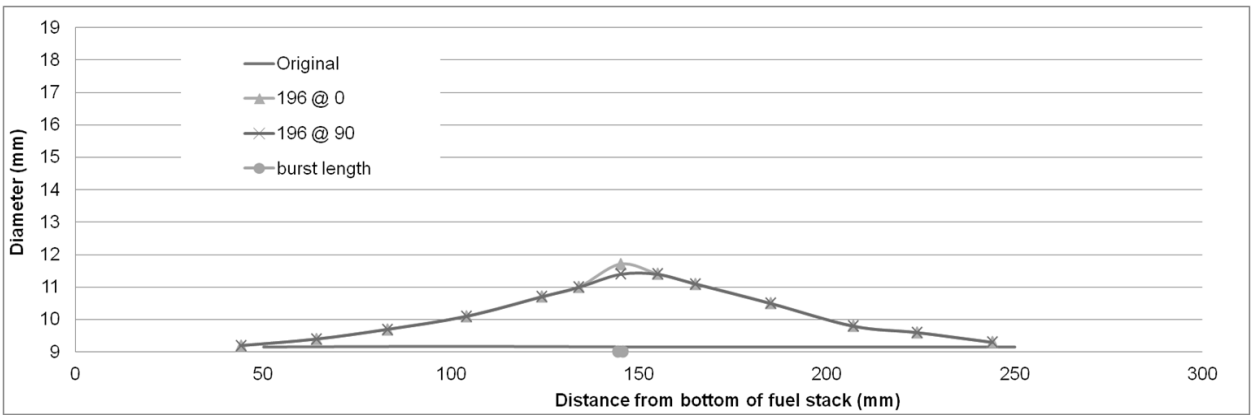

Figure 2-62 Profilometry measurements of segment 196 post-transient. The rupture length is also indicated.

Because this rodlet did not experience significant oxidation and therefore was expected to be highly ductile, there was no bend test performed on this rod. Instead, the rod was manually cut into two pieces, through the rupture node. The two pieces were then shaken and fuel loss was observed. There was no fuel loss measured following the LOCA test; however, it appears that about half of the fuel fell out of this rod during shaking. During the wire probe measurement, completed after shaking, the probe traveled unobstructed approximately 90 millimeters above and approximately 66 millimeters below the rupture center. The mass loss measured following the bend test and after shaking was 77 grams. Figure 2-63 provides an image of the collected fuel fragments.

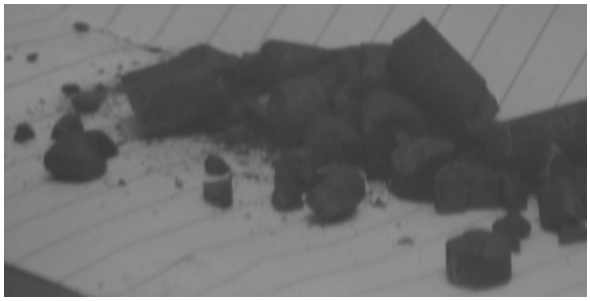

Figure 2-63 Images of fuel collected from Test 196

The fragment size distribution of the fuel dispersed and collected from Test 196 was investigated using sieve analysis. The measured mass of each sieve group is provided in Table 2-12, along with the mass percentage of each group relative to the total fuel analyzed.

Table 2-12 Fragment Size Distribution Results from Test 196

Size	Weight fuel (g)	% of total
< 0.125 mm	0.4	1%
0.125 - 0.25	0.4	1%
0.25 - 0.5 mm	0.3	0%
0.5 - 1 mm	0.3	0%
1 - 2 mm	0.6	1%
2 - 4 mm	9.4	12%
> 4 mm	65.9	85%
Sum:	77.3	100%

2.5.4 Metallography and Hot-Vacuum Extraction

One metallography examination and four hydrogen measurements were made of the rodlet used in Test 196. The locations of metallography and hydrogen measurements are shown in Figure 2-64.

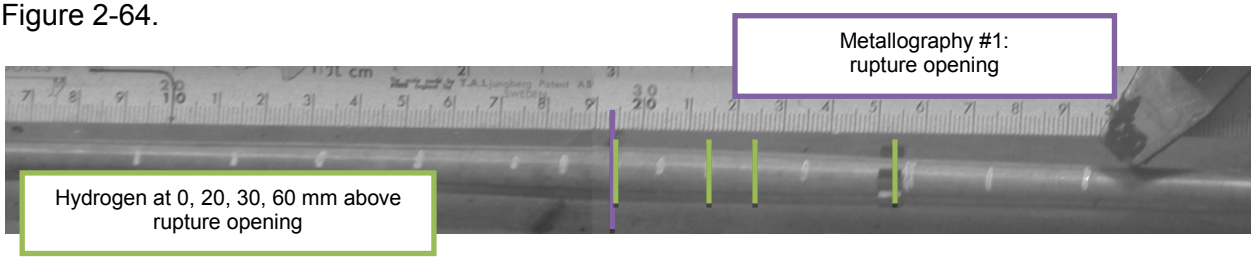

Figure 2-64 Photo of test segment from Test 196, indicating the location of metallography and hydrogen measurements

The metallography sample shown in Figure 2-65 was taken from the rupture opening. Select, high-resolution images from the outer cladding diameter and inner cladding diameter are included in Figure 2-66 and Figure 2-67, respectively.

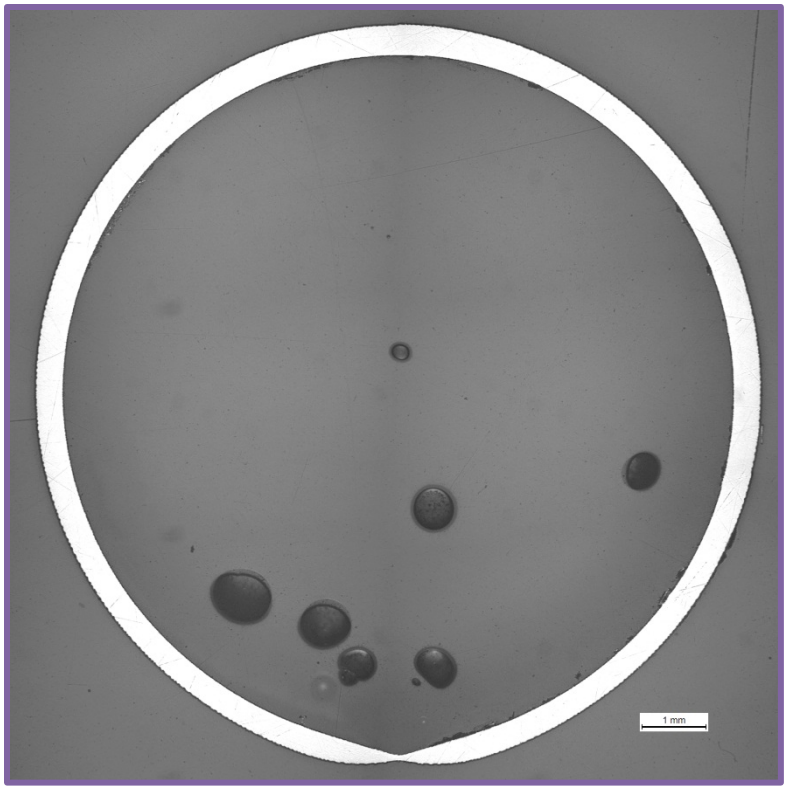

Figure 2-65 Macrograph of cross section from the rupture region of rodlet tested in LOCA Test 196

In Figure 2-66, the initial oxide thickness can be seen to have cracked and separated with the strain of the cladding. The strain at this location was approximately 25 percent. No transient oxidation layer can be observed in these images, which is expected for this test because it was a “ramp-to-rupture” test and did not accumulate significant oxidation. In Figure 2-67, some remnants of a fuel-clad bonding layer can be observed. This layer can be seen to have cracked and separated with the strain of the cladding. Again, this is expected because the test was terminated just after rupture and before significant transient oxidation could accumulate.

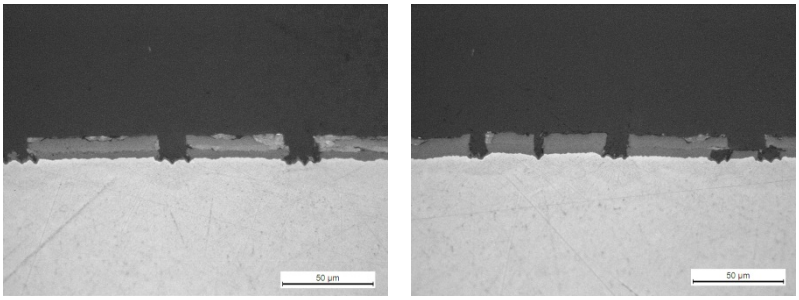

(a) **(b)**

Figure 2-66 Two high-resolution images of the cladding outer diameter from the metallography examination in the rupture region of the rodlet tested in LOCA Test 196 at (a) 90° and (b) 270°

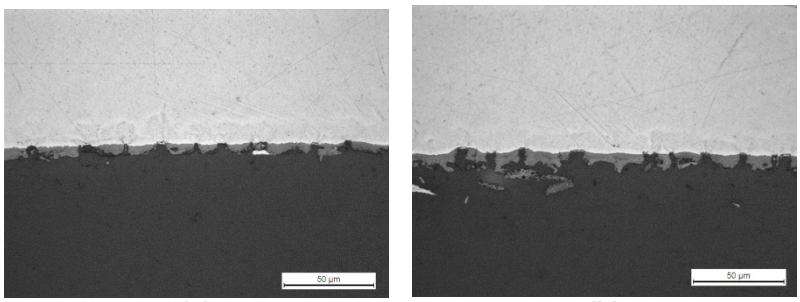

(a) (b)

Figure 2-67 Two high-resolution images of the cladding inner diameter from the metallography examination in the rupture region of the rodlet tested in LOCA Test 196 at (a) 45° and (b) 270°

The location and values of hydrogen content, measured by hot vacuum extraction, are provided in Table 2-13, and illustrated, relative to the segment post-LOCA strain profile and rupture length measurements, in Figure 2-68.

Table 2-13 Hydrogen Measurements for Test 196

Distance above rupture opening (mm)	0	20	30	60
Hydrogen Content (wppm)	137	110	144	131

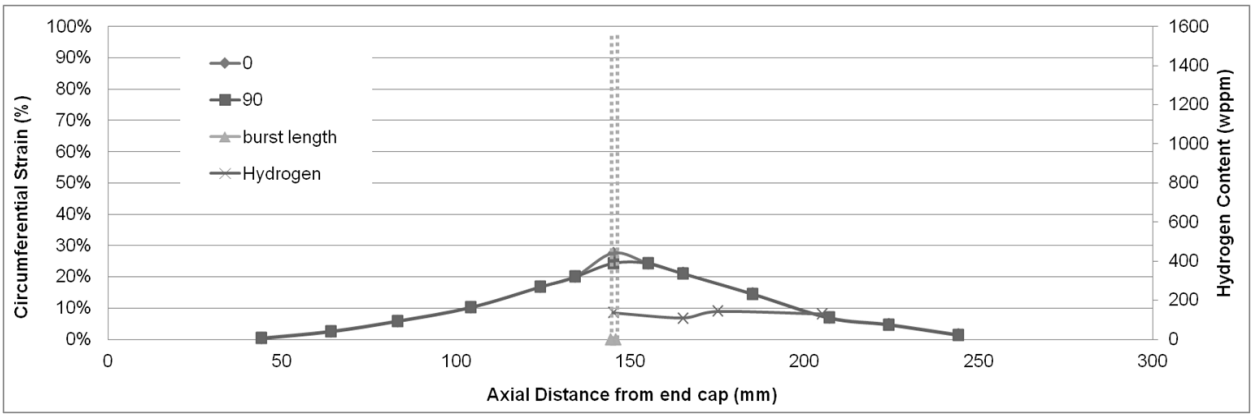

Figure 2-68 Hydrogen measurements from 196 relative to segment strain profile and rupture length

2.5.5 Gamma Scan Results with Comparison to Profilometry and Initial Wire Probe Measurements

Almost 1 year after the last LOCA tests were completed, emerging questions prompted new PIE investigations. The wire probe measurements performed after the shaking test indicated a long length of empty cladding, but also a significant amount of residual fuel material in some test segments. To investigate the length and condition of the remaining fueled segments, gamma scans were performed. Recall that the rodlet used in Test 196 was cut into two pieces and that multiple portions of cladding material were removed for metallography and hydrogen analysis. The remaining portions of the upper and lower portions were gamma scanned separately and

the scans in combination covered a little over half of the length of the rodlet, as shown in Figure 2-69.

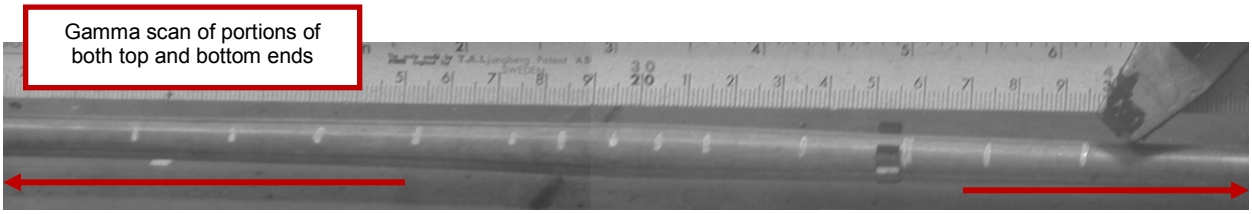

Figure 2-69 Photo of test segment from Test 196, indicating the relative length of gamma scan results

In Figure 2-70, the gamma scan results were plotted together with the profilometry results and the wire probe measurements performed after the shake test (indicated as "final wire probe measurement" in the figure below).

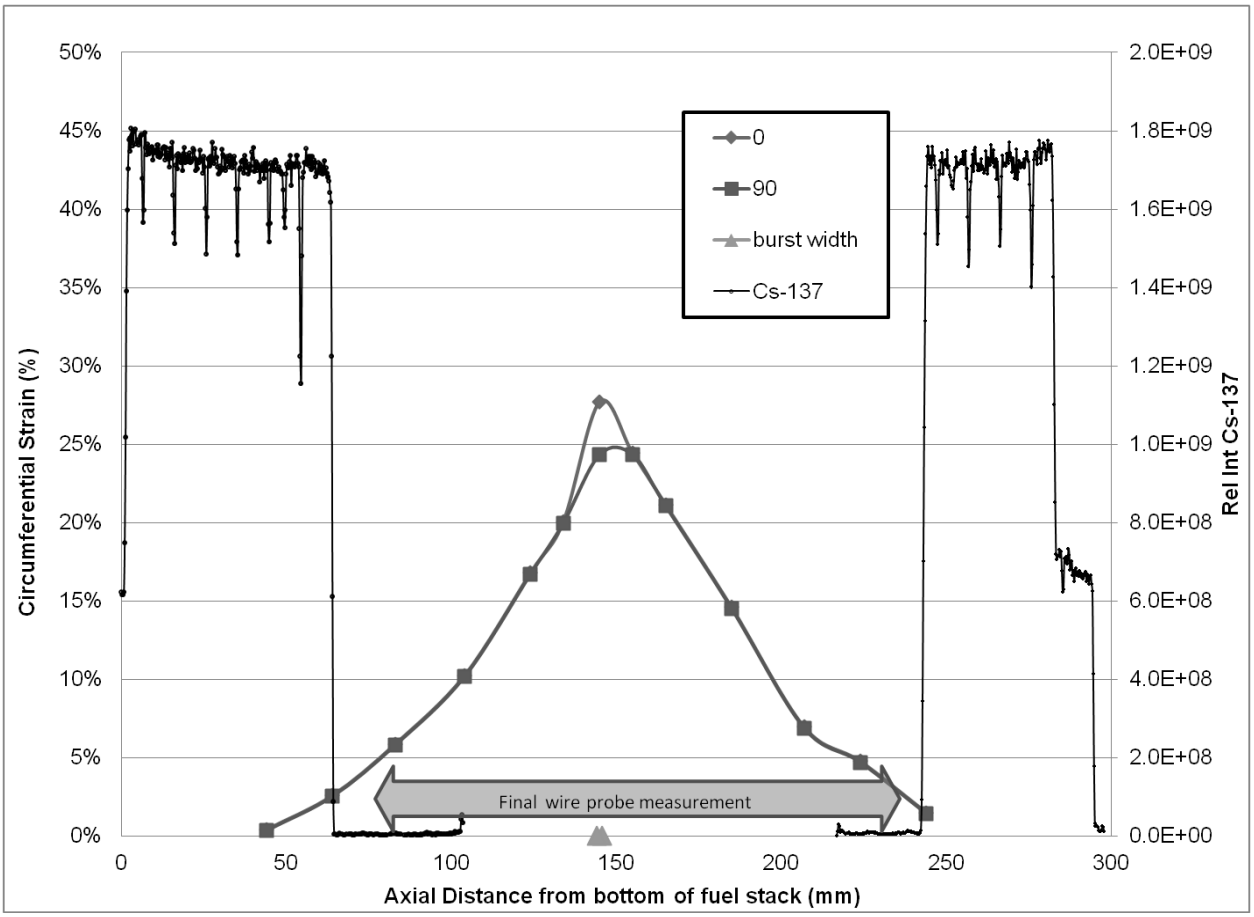

Figure 2-70 Gamma scan results for Test 196 with comparison to profilometry and initial wire probe measurements

As indicated earlier, theses gamma scan results were obtained over 1 year after the LOCA test was performed. In the time between the LOCA test and these gamma scans, the rodlet portions were stored in metal cans in the hot-cell. Some fuel material was found in the metal cans once the rodlet portions were removed for gamma scanning and some addition material fell out after minor shaking. The mass of fuel material found in the can storing the bottom portion of the rodlet was 8.3 grams. A few milligrams of fuel material was found in the can storing the top portion of the rodlet. An image of the fuel material collected from the bottom end of rodlet 196 is shown in Figure 2-71. It is important to note that this fuel had fallen out of the rod before the gamma scan. This additional fuel loss during storage approximately accounts for the difference between the final wire probe measurement and the indication on the gamma scan results of the start of the remaining fuel column on the top rodlet portion.

Figure 2-71 Fuel fragments collected from the bottom of rod 196 after gentle shaking just before gamma scan

Considering the initial wire probe measurements, the fuel fragments collected after the LOCA test and initial shake test (shown in Figure 2-63 and quantified in Table 2-12) likely originated from the middle 150 millimeter region of the fuel rod that was measured to be empty following the LOCA test. However, the fuel fragments shown in Figure 2-71 collected 1 year later after gentle shaking just before the gamma scan likely originated from some span beyond the middle 150 millimeter, possibly in the axial length between the wire probe measurement and the indication of fuel in the gamma scan (approximately 70 to 75 millimeter in Figure 2-70). Additional sieve analysis was performed to characterize the fragment size distribution of the fragments collected and shown in Figure 2-71. The measured mass of each sieve group is provided in Table 2-14, along with the mass percentage of each group relative to the total fuel analyzed. Figure 2-72 provides a comparison of the fuel fragment size distribution from these two regions of segment 196. The comparison suggests that fragmentation size distribution is comparable in these two regions.

Table 2-14 Fragment Size Distribution Results for Fuel Fragments Collected from the Bottom End of Rod 196 after Gentle Shaking Just before Gamma Scan

Size	Weight fuel (g)	% of total
< 0.125 mm	0.01	0%
0.125 - 0.25	0.01	0%
0.25 - 0.5 mm	0.03	0%
0.5 - 1 mm	0.07	1%
1 - 2 mm	0.50	8%
2 - 4 mm	1.77	27%
> 4 mm	4.27	64%
Sum:	6.66	100%

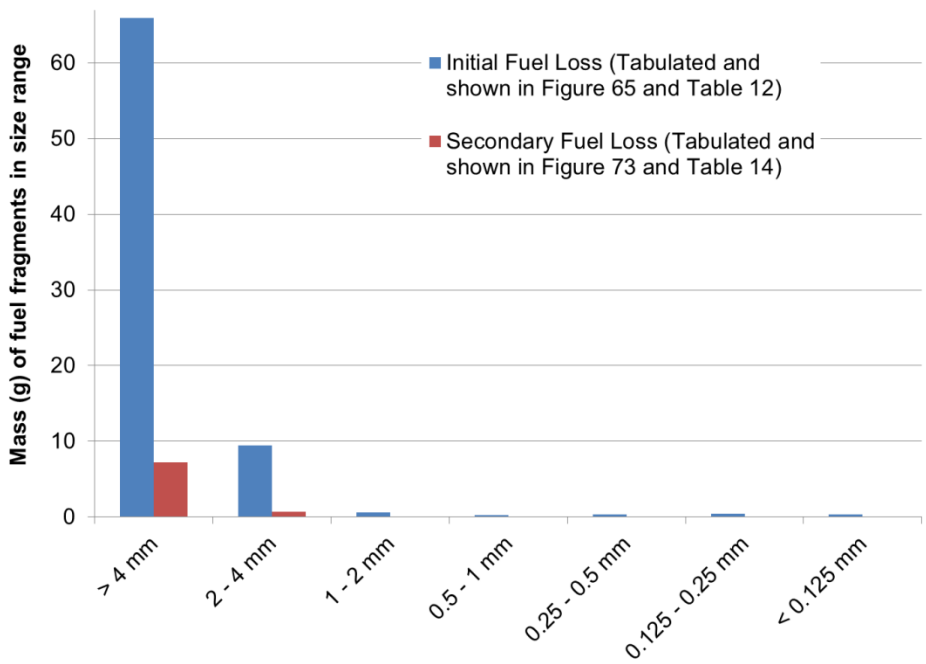

Figure 2-72 Comparison of fuel fragment size distribution from two regions of segment 196

2.6 Test 198

Table 2-15 summarizes measurements and values that characterize the initial state, transient, and in-cell measurements of Test 198. The initial state, transient information and in-cell measurements will be described further in the following sections. Metallography, hydrogen measurements, and gamma scan results will also be provided.

Table 2-15 Measurements and Values That Characterize the Initial State, Transient, and In-Cell Measurements of Test 198

Initial State	Adjacent H (wppm)	Average Oxide (μm)	Rod Average Burn Up (GWd/MTU)		Rod Internal Pressure at 300°C (bar)	
	225	20	55.2		82	
Transient	Peak Cladding Temperature (°C)	Rupture Temp (°C)	Rupture Pressure (bar)	Time (s) to reach 50% of rupture P for top/bottom gauges	CP-ECR (%)	Quench
	1185	693	81	3 / 2	15	Yes
In-Cell Measurements	Max Strain (%)	Length >10% Strain (mm)	Wire Probe Measurement (mm) (Top/Bottom)		Rupture Dimensions (mm) (Width/Length)	
	25	115	55 / 76		1.6 / 11	

2.6.1 Initial State

For Test 198, a segment of high burnup Westinghouse ZIRLO™ fuel with a Zirconium Diboride Integral Fuel Burnable Absorber (IFBA) coating was used. The segment was taken from a rod which was irradiated at a U.S. PWR power plant and had a rod average burnup of 55.2 GWd/MTU. The operating history for this rod was typical of U.S. power plant operation to this burnup. The pellet enrichment was 4.94 wt% U^{235}. The 300-millimeter segment was taken from the middle section of the fuel rod, approximately 2200 millimeters from the bottom of the full length rod. A hydrogen content of 225 wppm was measured below the segment. The eddy current measurements indicate that the oxide layer thickness is relatively constant over the length of this segment, and average about 20 micrometers.

2.6.2 Transient Information

To begin the transient, the rodlet was heated and maintained at 300 degrees C for approximately 15 minutes to achieve thermal equilibrium. Before initiating the temperature ramp, the desired fill pressure was established at 300 degrees C. For Test 198, the rodlet was pressurized to 82 bar (at 300 degrees C). The pressure adjustment procedure provides an indication of gas communication by observing the response time of the lower pressure transducer, as shown in Figure 2-73. Recall that while the gas line is open, the top pressure transducer indicates the gas line pressure and the bottom should reflect the ability of gas to move the 300 millimeter segment length to equilibrate pressure. Once the desired fill pressure was established, the gas line was closed and the rodlet was heated at 5 degrees C/s until the rodlet temperature reached 1,185 degrees C. The rodlet was held at 1,185 degrees C for 85 seconds. The calculated CP-ECR (based on measured rupture strain reported below) was approximately 15 percent.

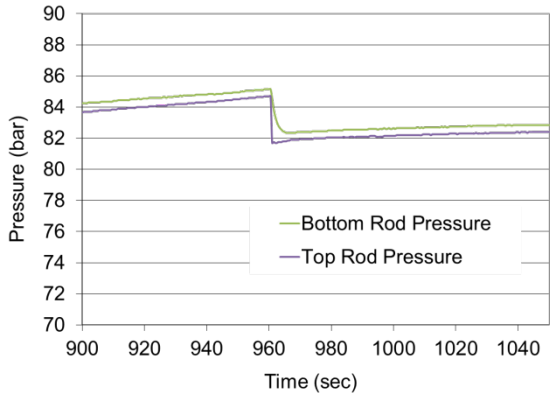

Figure 2-73 Fill pressure adjustment at 300 °C for Test 198, which provides an indication of gas communication

Rupture is estimated to have taken place when the rod internal pressure reached 81 bar and the cladding temperature reached 693 degrees C (1279 degrees F). The depressurization rate was relatively fast for Test 198; the top pressure gauge recorded a 50 percent reduction in pressure (relative to 81 bar) after 3 seconds and the bottom pressure gauge recorded a 50 percent reduction in pressure after 2 seconds. The temperature and pressure history for Test 198 is shown in Figure 2-74.

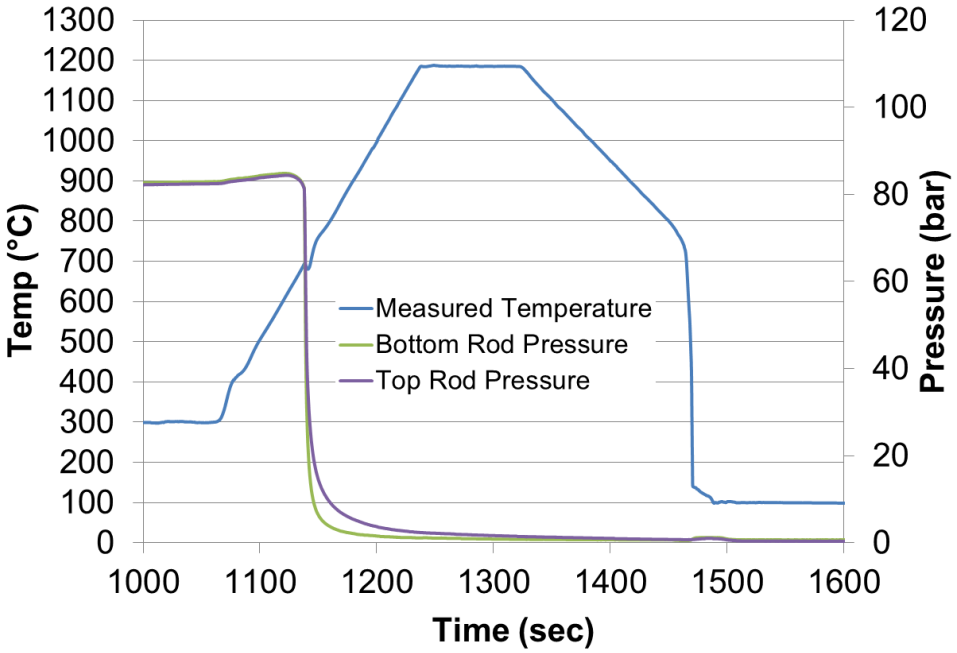

Figure 2-74 Temperature and pressure history for Test 198

2.6.3 In-Cell Measurements

After the simulated LOCA transient was complete, the fuel rod was examined. Figure 2-75 provides a photo of the fuel rod after the transient. The rupture opening was measured to be 1.6 millimeters wide and 11 millimeters in length.

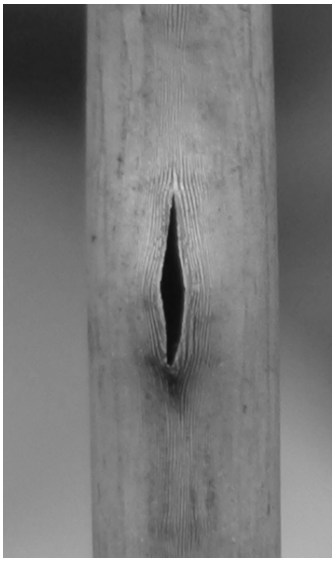

Figure 2-75 Rupture opening after the transient simulation for Test 198

The rod did not experience distortion (or bending) during the LOCA transient, which can be seen in Figure 2-76. Profilometry measurements were made and they are shown in Figure 2-77. In Figure 2-77, the initial diameter and rupture length are also indicated. The mid-wall rupture strain value for Test 198 was calculated to be 25 percent.

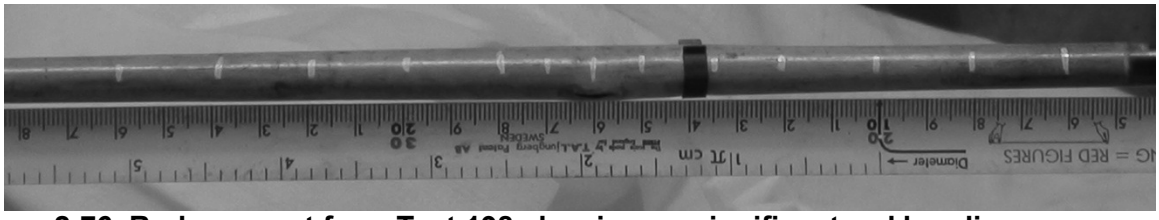

Figure 2-76 Rod segment from Test 198 showing no significant rod bending

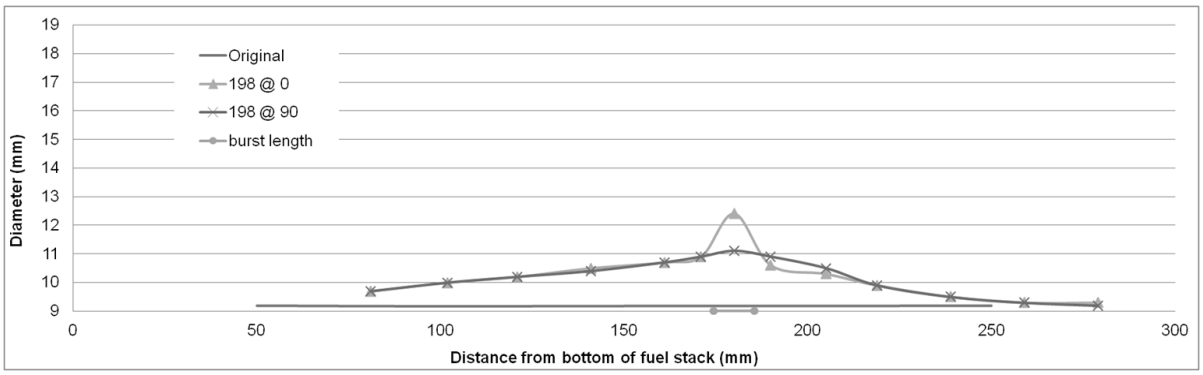

Figure 2-77 Profilometry measurements of segment 198 post-transient. The rupture length is also indicated.

There was no fuel loss measured following the LOCA test, however, it appears that about half of the fuel fell out of this rod during shaking. During the wire probe measurement, completed after shaking, the probe traveled unobstructed approximately 55 millimeters above and approximately 76 millimeters below the rupture center. There was no measured mass loss following the LOCA test. The mass loss measured after shaking was 62 grams. Figure 2-78 provides an image of the collected fuel fragments.

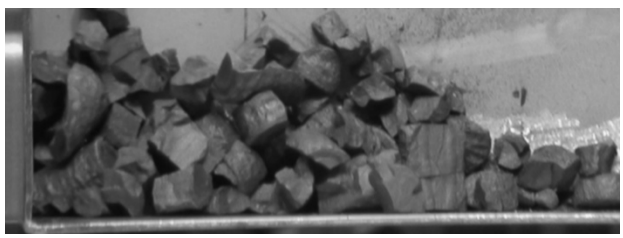

Figure 2-78 Images of fuel collected from Test 198

The fragment size distribution of the fuel dispersed and collected from Test 198 was investigated using sieve analysis. The measured mass of each sieve group is provided in Table 2-16, along with the mass percentage of each group relative to the total fuel analyzed.

Table 2-16 Fragment Size Distribution Results from Test 198

Size	Weight fuel (g)	% of total
< 0.125 mm	0.50	1%
0.125 - 0.25	0.50	1%
0.25 - 0.5 mm	0.50	1%
0.5 - 1 mm	0.40	1%
1 - 2 mm	0.80	1%
2 - 4 mm	17.50	28%
> 4 mm	42.10	68%
Sum:	62.3	100%

2.6.4 Metallography and Hot-Vacuum Extraction

Two metallography examinations and ten hydrogen measurements were made of the rodlet used in Test 198. The locations of metallography and hydrogen measurements are shown in Figure 2-79.

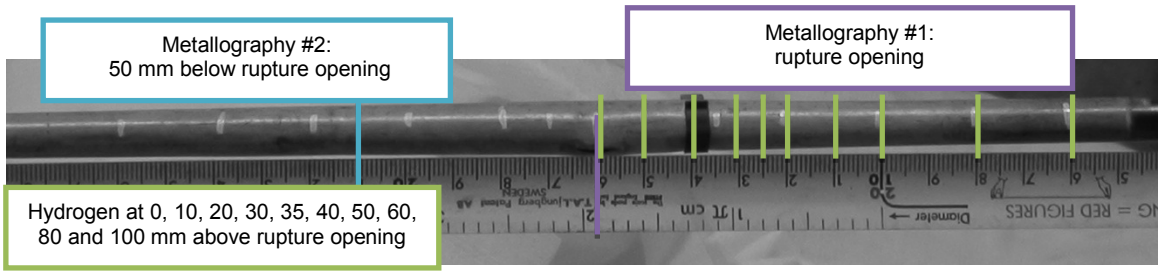

Figure 2-79 Photo of test segment from Test 198, indicating the location of metallography and hydrogen measurements

The metallography sample shown in Figure 2-80 was taken in the rupture opening. Select, high-resolution images from the outer cladding diameter and inner cladding diameter are included in Figure 2-81 and Figure 2-82, respectively.

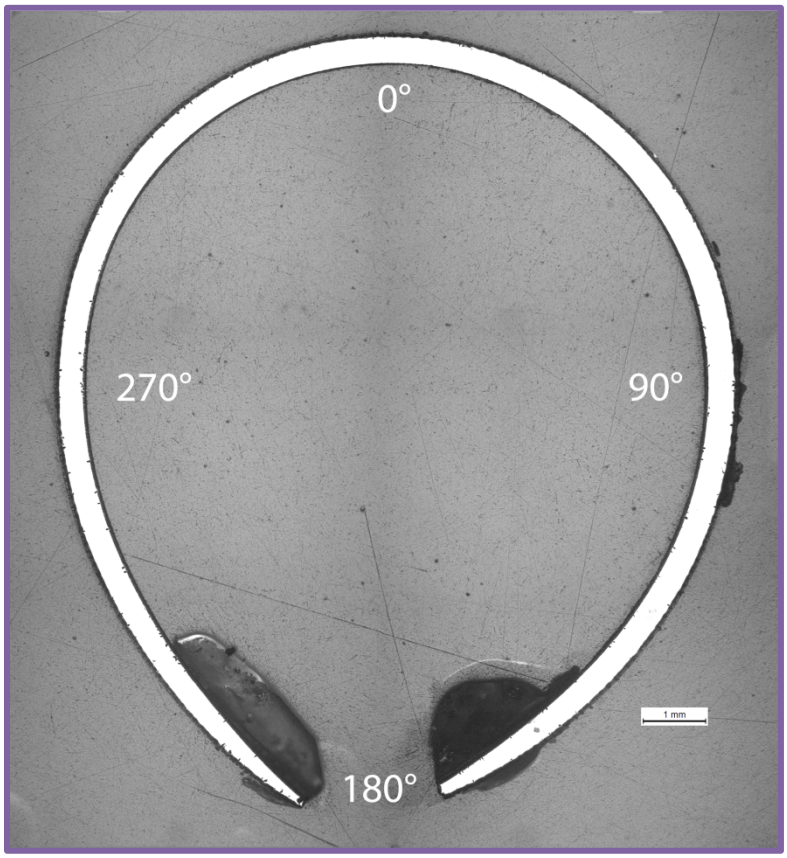

Figure 2-80 Macrograph of cross section from the rupture region of rodlet tested in LOCA Test 198

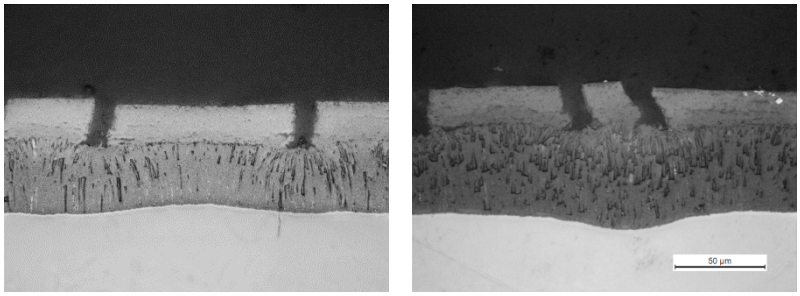

(a) (b)

Figure 2-81 Two high-resolution images of the cladding outer diameter from the metallography examination in the rupture region of the rodlet tested in LOCA Test 198 at (a) 90° and (b) 270°

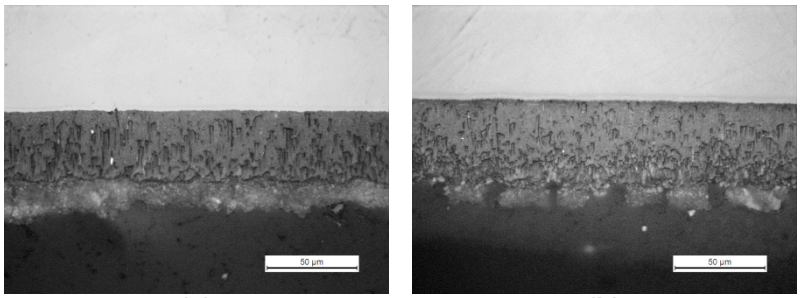

(a) (b)

Figure 2-82 Two high-resolution images of the cladding inner diameter from the metallography examination in the rupture region of the rodlet tested in LOCA Test 198 at (a) 90° and (b) 225°

Here, it is useful to recall that for Test 198 the calculated CP-ECR was 15 percent, with a hold time at 1,185 degrees C of 85 seconds. In Figure 2-81, the initial oxide thickness can be seen to have cracked and separated, and the transient oxidation layer is seen beneath this damaged initial oxide layer. In Figure 2-82, it appears that some fuel fragments remain on the inner diameter and that the initial fuel-cladding bonding layer is somewhat cracked and separated. An inner diameter transient oxidation layer is seen, which appears to be approximately the same thickness at the outer transient oxidation layer. These observations are expected at this location because it is in the rupture node.

The metallography sample shown in Figure 2-83 was taken from a section 50 millimeters below the rupture opening. Select, high-resolution images from the outer cladding diameter and inner cladding diameter are included in Figure 2-84 and Figure 2-85, respectively.

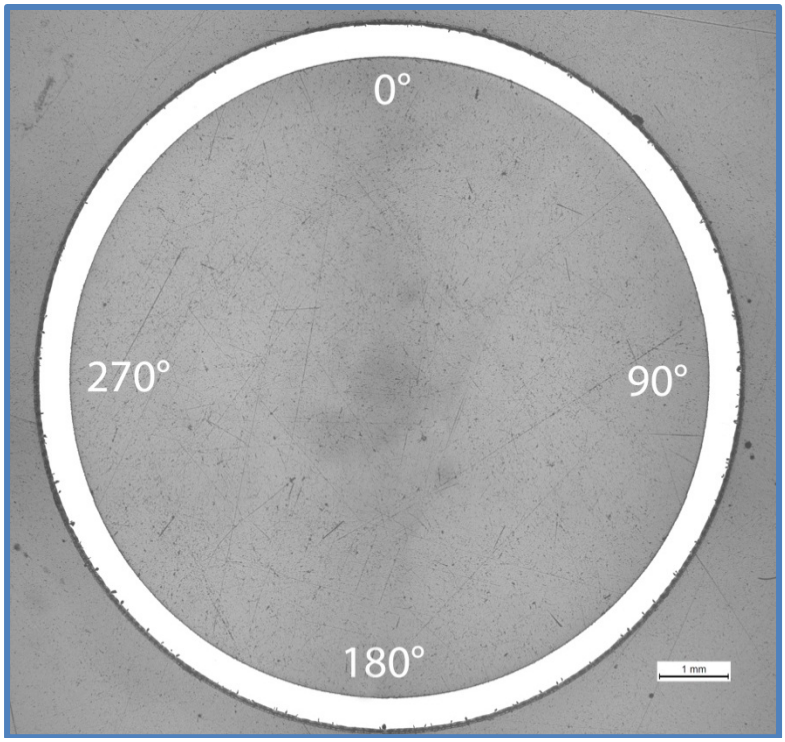

Figure 2-83 Macrograph of cross section from 50 mm below the rupture region of rodlet tested in LOCA test 198

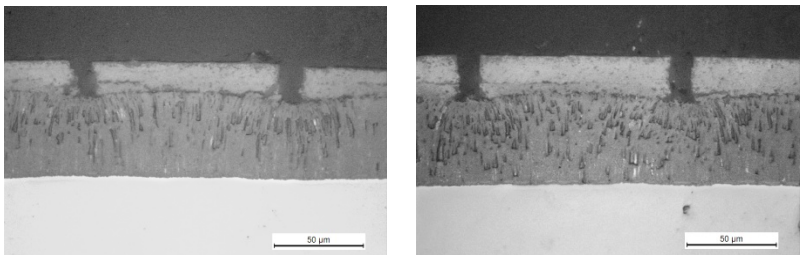

(a) **(b)**

Figure 2-84 Two high-resolution images of the cladding outer diameter from the metallography examination 50 mm below the rupture region of the rodlet tested in LOCA Test 198 at (a) 90° and (b) 180°

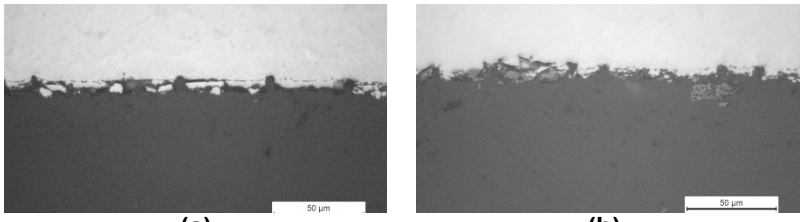

(a) **(b)**

Figure 2-85 Two high-resolution images of the cladding inner diameter from the metallography examination 50 mm below the rupture region of the rodlet tested in LOCA Test 198 at (a) 90° and (b) 225°

In Figure 2-84, the initial oxide thickness can be seen to have cracked and separated, and the transient oxidation layer is seen beneath this damaged initial oxide layer. In Figure 2-85, a few small fuel fragments remain on the inner diameter. An inner diameter transient oxidation layer is not observed at this location 50 millimeters below the rupture opening. These observations are interesting because they suggest this region, 50 millimeters below the rupture node, was not exposed to a steam environment during the transient. The metallography samples were not prepared in such a way to reveal the presence and thickness of an alpha layer and the extent of fuel cladding bonding on this sample has not been characterized.

The location and values of hydrogen content, measured by hot vacuum extraction, are provided in Table 2-17, and illustrated, relative to the segment post-LOCA strain profile and rupture length measurements, in Figure 2-86.

Table 2-17 Hydrogen Measurements from Test 198

Distance above rupture opening (mm)	0	10	20	30	35	40	50	60	80	100
Hydrogen Content (wppm)	733	1531	1155	641	636	442	294	367	247	201

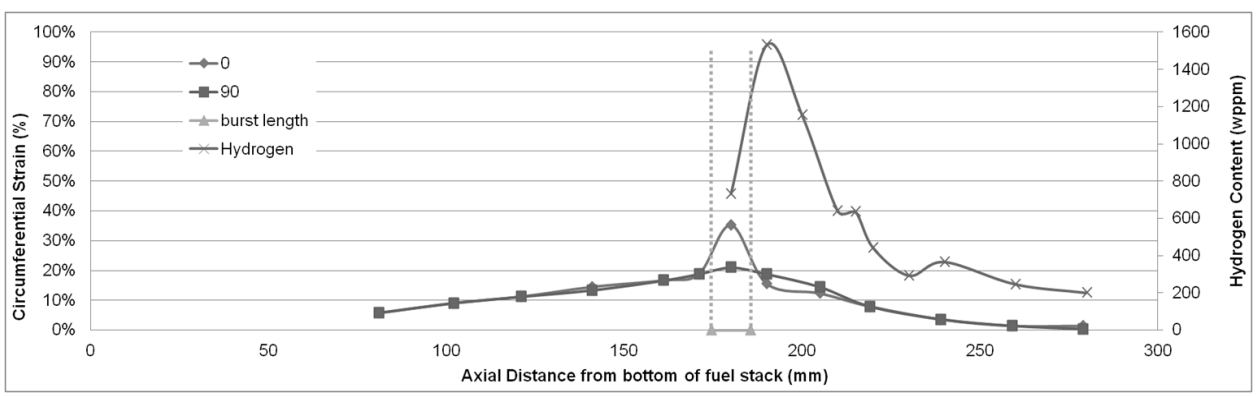

Figure 2-86 Hydrogen measurements from Test 198 relative to segment strain profile and rupture length

2.6.5 Gamma Scan Results with Comparison to Profilometry and Initial Wire Probe Measurements

Almost 1 year after the last LOCA tests were completed, emerging questions prompted new PIE investigations. The wire probe measurements performed after the shaking test indicated a long length of empty cladding, but also a significant amount of residual fuel material in the end regions of the test segments. To investigate the length and condition of the remaining fueled segments, gamma scans and additional M/C examination were performed. Recall that the rodlet used in Test 198 broke into two halves during the four-point bend test and that multiple

portions of cladding material were removed for metallography and hydrogen analysis. The remaining length of the lower portion was gamma scanned, as shown in Figure 2-87. The location of the additional M/C examination is also shown in Figure 2-87.

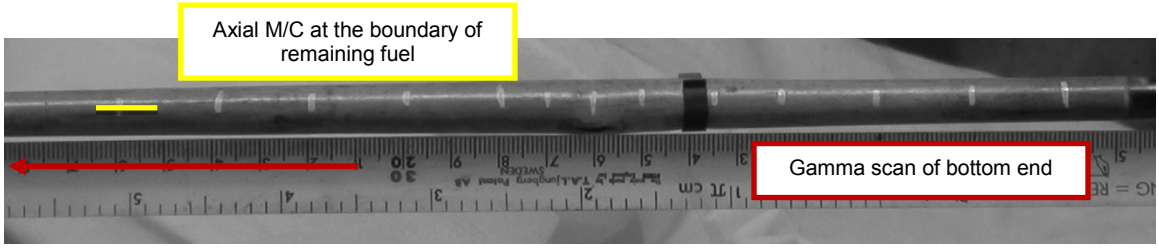

Figure 2-87 Photo of test segment from Test 198, indicating the relative length of gamma scan results and location of an additional M/C examination in the remaining fueled region

In Figure 2-88, the gamma scan results were plotted together with the profilometry results and the wire probe measurements performed after the shaking test (indicated as “final wire probe measurement” in the figure below).

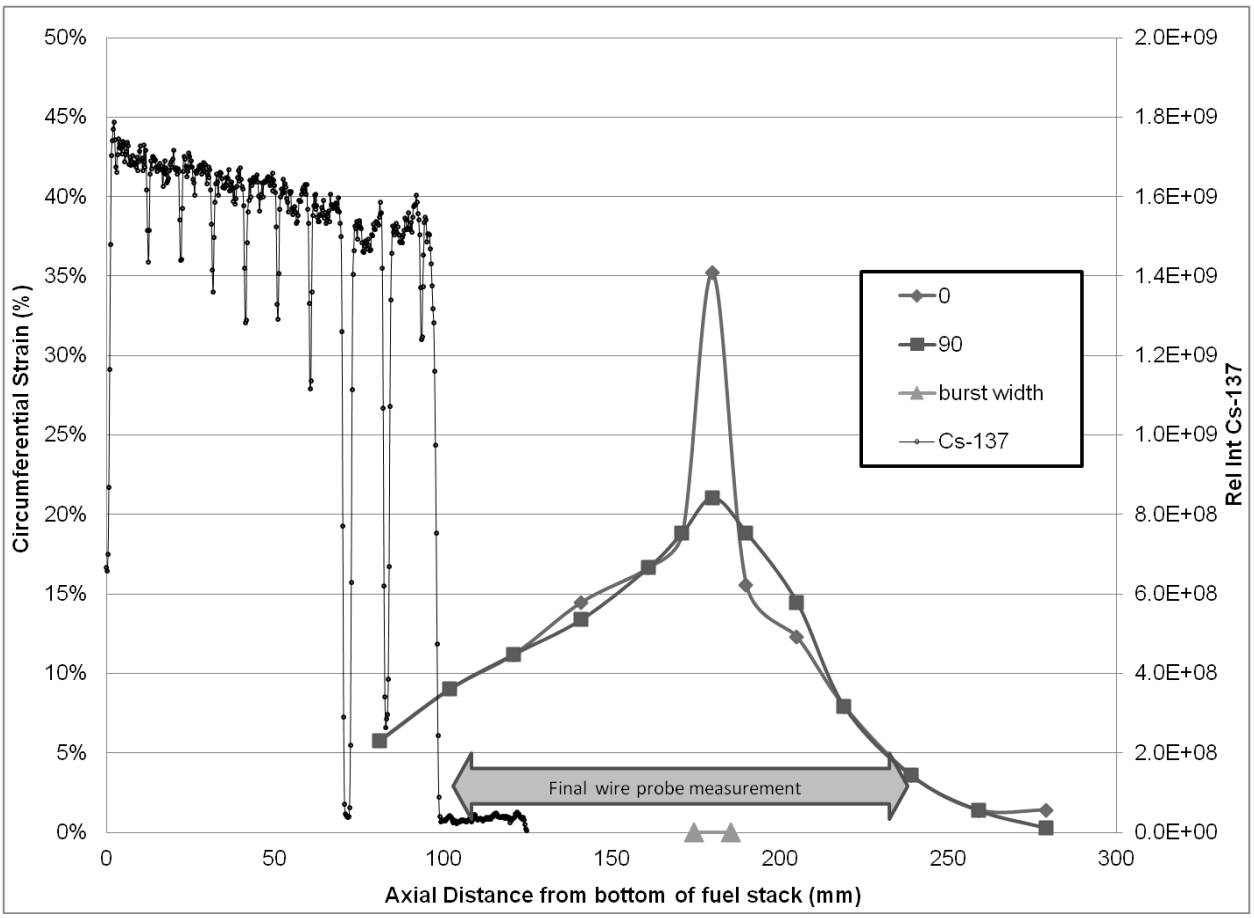

Figure 2-88 Gamma scan results for Test 198 with comparison to profilometry and initial wire probe measurements

As indicated earlier, theses gamma scan results were obtained over 1 year after the LOCA test was performed. In the time between the LOCA test and these gamma scans, the rodlet portions were stored in metal cans in the hot-cell. Some fuel material was found in the metal cans once the rodlet portions were removed for gamma scanning. The mass of fuel material found in the can storing the bottom portion of the rodlet was 6.6 grams. It is important to note that this fuel had fallen out of the rod before the gamma scan. This additional fuel loss during storage approximately accounts for the difference between the final wire probe measurement and the indication on the gamma scan results of the start of the remaining fuel column on the bottom rodlet portion.

An additional M/C examination provides an even more detailed characterization of the remaining fueled region than the gamma scan results. The axial M/C sample shown in Figure 2-89 was taken at the boundary of remaining fuel and empty cladding, covering a span approximately 80-105 millimeters from the segment bottom. The image reveals that the boundary between fueled an empty cladding is rather abrupt, and that the residual fuel is relatively intact. The fuel-clad gap in this image appears rather large and it is somewhat surprising that these fuel pellets did not relocate even after the agitation of the shake test.

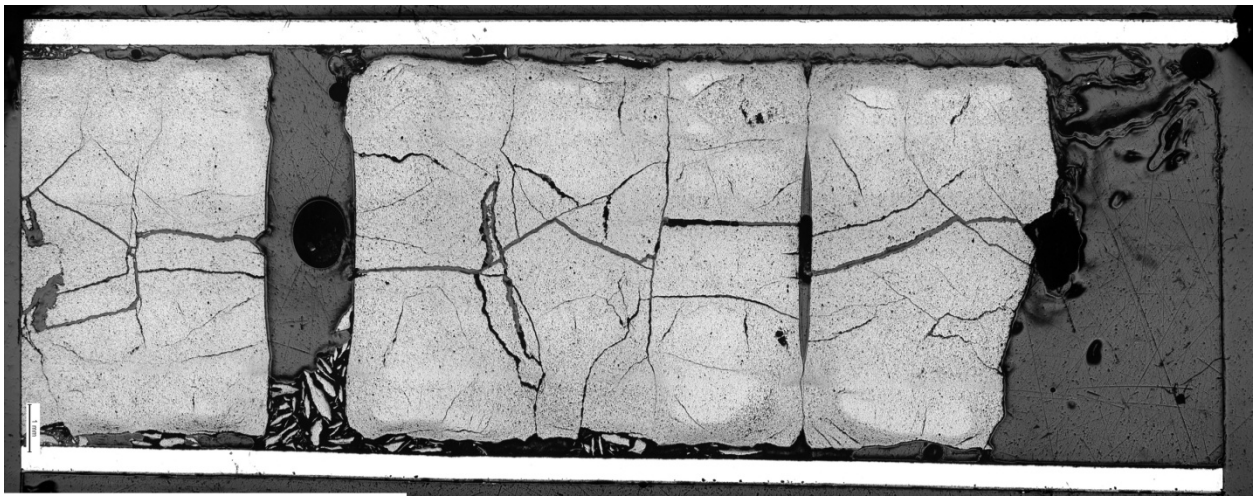

Figure 2-89 Macrograph of axial cross section covering a span approximately 80–105 mm from the segment bottom of the rodlet tested in LOCA Test 198

Select, high-resolution images are included in Figure 2-90 from the inner (a) and outer (b) cladding diameter. These images were near the bottom (left) of the axial M/C, approximately 84 millimeters from the original segment bottom of the rodlet tested in LOCA Test 198.

In Figure 2-90 (a), a thin fuel-clad bond layer and an alpha layer microstructure can be seen on the inner diameter. This region of the test segment remained fueled and was far (more than 100 millimeters) from the rupture location. In Figure 2-90 (c and d), the initial oxide layer and transient oxide layer can be seen. Again, it is useful to recall that for Test 198 the calculated CP-ECR was 15 percent, with a hold time at 1185 degrees C of 85 seconds.

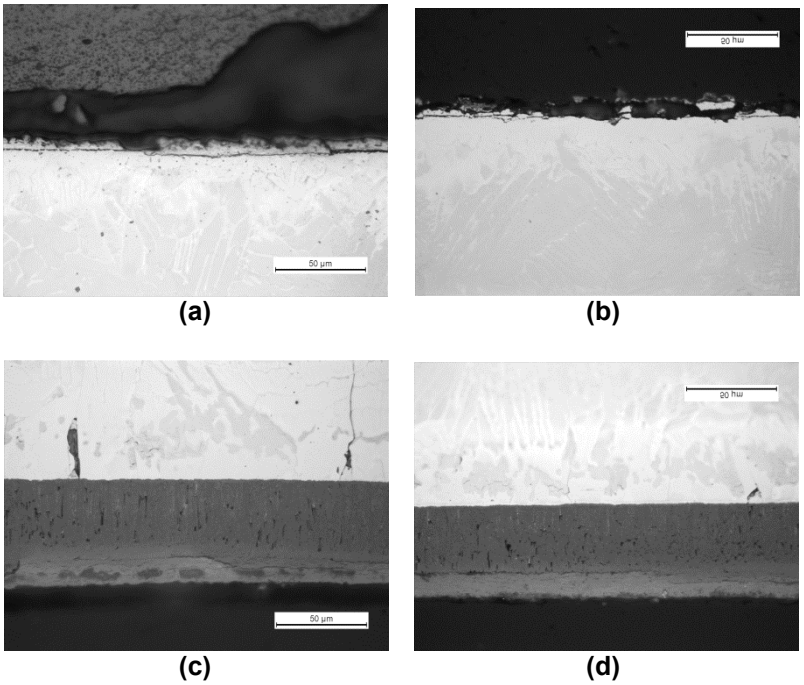

Figure 2-90 High-resolution images of the cladding (a and b) inner and (c and d) outer diameter taken from the axial M/C shown above. These images were near the bottom (left) of the axial M/C, approximately 85 mm from the original segment bottom of the rodlet tested in LOCA Test 198.

3. REVIEW OF TEST RESULTS FOR SPECIFIC PARAMETER COMPARISONS

In this section, the test results presented above will be revisited and grouped for specific parameter comparisons. In addition, new figures will be presented which facilitate the comparison of important parameters between tests. Previous papers have discussed postulated explanations for the observations of each test [4] and future reports are planned to utilize results from this program and others to support a mechanistic understanding of fuel fragmentation, relocation, and dispersal phenomenon [5, 6]. For the purpose of this report however, the test results provided above are simply being revisited to facilitate comparison by the reader.

3.1 Initial State

Table 3-1 provides the burnup value of the segment from each LOCA test, as well as the values of initial hydrogen, oxide thickness, and rod internal pressure. The rod segments for Tests 189 and 191-193 are very similar, as are the rod segments for Tests 196 and 198. The pre-test hydrogen and oxide layers are similar for all six rod segments.

Table 3-1 Summary of All "Initial State" Information from the Six LOCA Tests

Test	Adjacent H (wppm)	Average Oxide (μm)	Rod Average Burn Up (GWd/MTU)	Rod Internal Pressure at 300°C (bar)
189	176	20	68.2	110
191	187, 271	20-30	69.3	110
192	176, 288	25-30	68.2	82
193	187	20	69.3	82
196	149	20	55.2	82
198	225	20	55.2	82

3.2 Transient

Table 3-2 provides the value of peak cladding temperature, rupture temperature and pressure, and depressurization rate (time in seconds for top/bottom pressure gauge to reach 50 percent of rupture pressure) for each test. The pressure response after rupture in the top plenum as a function of time for all six tests is plotted in Figure 3-1. The rupture conditions for all six tests are relatively similar; however, the depressurization rates for Tests 196 and 198 were notably faster than for Tests 189 and 191-192. The depressurization behavior in Test 193 is unique, with a hold up near 40 bar even after 90 seconds. This is assumed to be attributed to fuel fragments clogging the pressure gauge, thus interfering with the accuracy of the measurement. The relatively slow depressurization rates, particularly the rates for 189, 191-192, suggest that the fuel remaining at the rodlet ends induces some gas flow restriction between the gas plenum at the top and bottom of the rods and the rupture opening.

Table 3-2 Summary of All "Transient" Information from the Six LOCA Tests

Test	Peak Cladding Temperature (°C)	Rupture Temp (°C)	Rupture Pressure (bar)	Time (s) to 50% of rupture P for top/bottom gauges	CP-ECR (%)	Quench
189	950	700	109	35 / 7	0	No
191	1185	680	104	21 / 10	13	Yes
192	1185	700	81	13 / 15	11	Yes
193	1185	728	81	45 / 8	17	Yes
196	950	686	81	5 / 2	0	No
198	1185	693	81	3 / 2	15	Yes

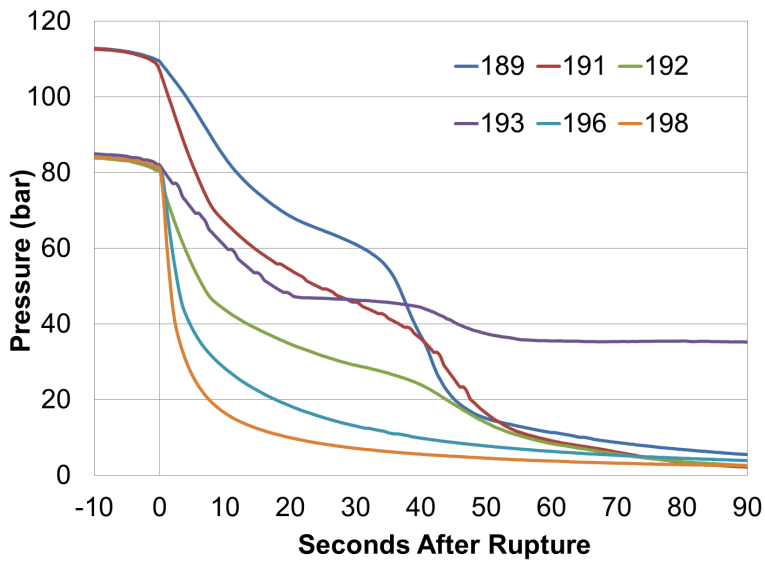

Figure 3-1 Pressure drop after rupture in the top plenum, plotted as a function of time, for all six tests

3.3 In-Cell Measurements

Table 3-3 provides the value of maximum circumferential strain, rupture dimensions and wire probe measurements for each test. In addition, the length of circumferential strain greater than 10 percent was identified for each test and is provided in Table 3-3. Figure 3-2 provides the approximate percentage of fuel loss during each test. In this case, the values provided in the previous section for total mass lost during the LOCA transient and total mass lost during bending and shaking were used to depict mass loss relative to the total segment fuel mass (approximated to be 150 grams).

Table 3-3 Summary of All "In-Cell Measurement" Information from the Six LOCA Tests

Test	Max Strain (%)	Length >10% Strain (mm)	Wire Probe Measurement (mm) (Top/Bottom)	Rupture Dimensions (mm) (Width/Length)
189	48	105	82 / 66	10.5 / 23.9
191	50	70	70 / 55	17.5 / 21.6
192	56	85	85 / 73	9 / 22.7
193	50	100	113 / 91	13.8 / 17.8
196	25	95	90 / 66	0.2 / 1.5
198	25	115	55 / 76	1.6 / 11

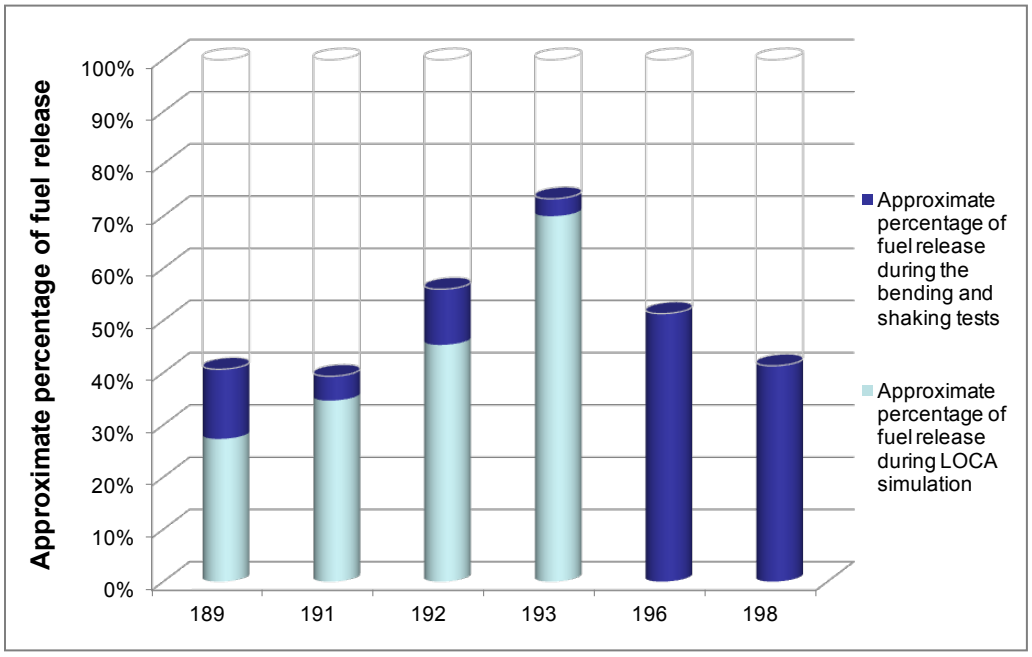

Figure 3-2 Approximate percentage of fuel loss during each test, color-coded by when fuel loss occurred. Note: Measured mass loss was compared to an estimated initial fuel mass of 150 g for the 300-mm segment.

Fuel fragment size measurements were made for the total mass of fuel material found outside of the fuel rod for five of the LOCA tests (the exception is Test 189, which was sent to disposal before fragmentation analysis) and have been tabulated in the previous sections. Figure 3-3 provides the results of the fuel fragment size measurements using a bar chart to more easily depict the distribution of fragments in each test and the comparison of results between tests. One of the first observations that are apparent is a significant difference in distribution between Tests 191-193 and Tests 196 and 198. In Tests 191-193, the fuel was finely fragmented and all fragments measured less than 4 millimeters (except a small amount from Test 193). The mass

of fuel fragments from these tests was approximately evenly distributed between the size groups separated by the six sieves used. In contrast, the fuel in Tests 196 and 198 was not finely fragmented and the fragments measured predominately larger than 4 millimeters.

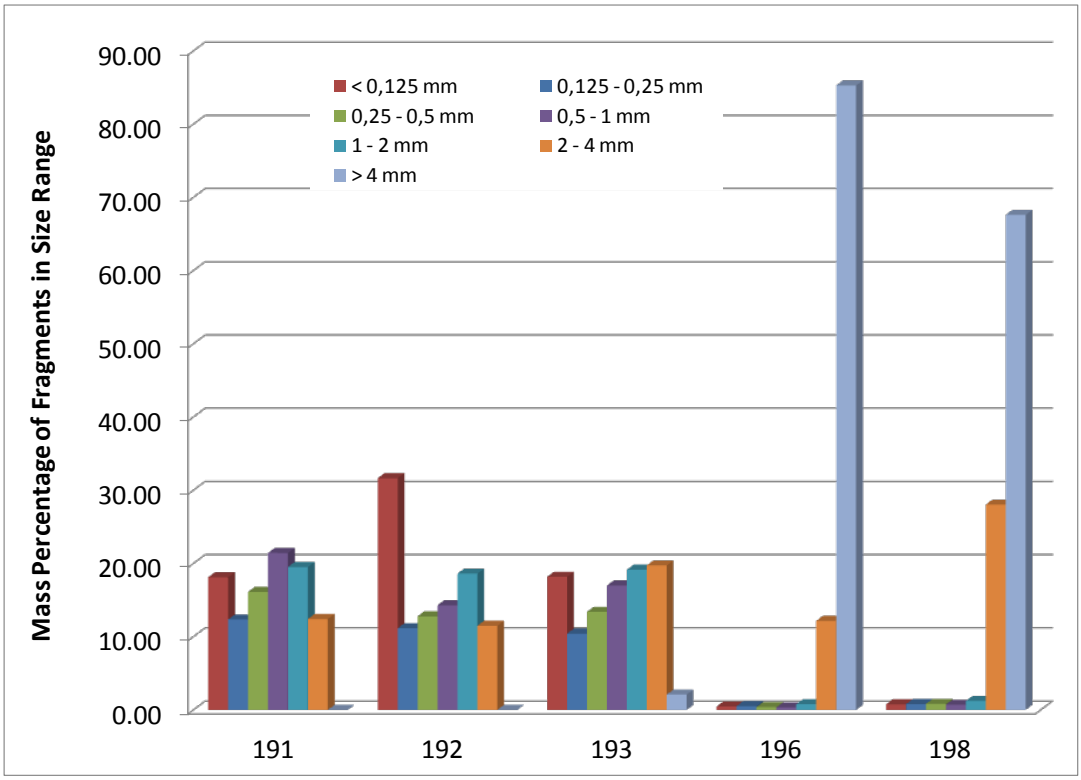

Figure 3-3 Fragment size distribution for each test

4. CONCLUSIONS

This report presented and discussed the results of the U.S. Nuclear Regulatory Commission's (NRC's) integral loss-of-coolant accident (LOCA) testing program conducted at Studsvik Nuclear AB in Sweden, including the test conditions, rodlet response, and post-test examinations for each test. Recently, discussion about the results of LOCA testing in the area of fuel fragmentation, relocation, and dispersal has grown common and rigorous throughout the international community. Therefore, the observations of fuel fragmentation, relocation, and dispersal in this experimental program are likely to be of particular interest for comparison to related or complimentary experimental programs. Previous papers have discussed postulated explanations for the observations of each test [4] and future reports are planned to utilize results from this program and others to support a mechanistic understanding of fuel fragmentation, relocation, and dispersal phenomenon [5, 6].

5. REFERENCES

1. M. Helin, J. Flygare, STUDSVIK/N-11/130, “NRC LOCA Tests at Studsvik, Design and Construction of Test Train Device and Tests with Unirradiated Cladding Material,” Available in USNRC’s ADAMS Public Document Collection, Agencywide Documents Access and Management System Accession No. ML12215A431.

2. M. Flanagan, “NUREG-2119: Mechanical Behavior of Ballooned and Ruptured Cladding,” February 2012.

3. P. Raynaud, “NUREG-2121: Fuel Fragmentation, Relocation, and Dispersal during the Loss-of-Coolant Accident,” March 2012.

4. M. Flanagan, P. Askeljung, “Observations of Fuel Fragmentation, Mobility and Release in Integral, High-Burnup, Fueled LOCA Tests,” Presented at the LOCA workshop of the May 2012 Halden Program Group Meeting in Lyon, France.

5. M. Flanagan, B.C. Oberländer, A. Puranen “Research Efforts in the Area of Fuel Fragmentation, Relocation and Dispersal under LOCA Conditions” Presented at the Enlarged Halden Program Group Meeting, Storefjell, Norway, March 10–15, 2013.

6. M. Flanagan, B.C. Oberländer, A. Puranen “Fuel Fragmentation, Relocation and Dispersal under LOCA Conditions: Experimental Observations” Manuscript prepared for TOPFUEL Conference, Charlotte, NC, September 2013.

NRC FORM 335
(12-2010)
NRCMD 3.7

U.S. NUCLEAR REGULATORY COMMISSION

BIBLIOGRAPHIC DATA SHEET

(See instructions on the reverse)

1. REPORT NUMBER
(Assigned by NRC, Add Vol., Supp., Rev., and Addendum Numbers, if any.)

NUREG-2160

2. TITLE AND SUBTITLE
Post Test Examination Results from Integral, High Burnup, Fueled LOCA Tests at Studsvik Nuclear Laboratory

3. DATE REPORT PUBLISHED

MONTH	YEAR
August	2013

4. FIN OR GRANT NUMBER

5. AUTHOR(S)
Michelle E. Flanagan, United States Nuclear Regulatory Commission
Peter Askeljung, Hot Cell Laboratory, Studsvik Nuclear AB, Sweden
Anders Puranen, Hot Cell Laboratory, Studsvik Nuclear AB, Sweden

6. TYPE OF REPORT
Technical

7. PERIOD COVERED (Inclusive Dates)

8. PERFORMING ORGANIZATION - NAME AND ADDRESS (If NRC, provide Division, Office or Region, U. S. Nuclear Regulatory Commission, and mailing address; if contractor, provide name and mailing address.)
Division of Systems Analysis
Office of Nuclear Regulatory Research
U.S. Nuclear Regulatory Commission
Washington, DC 20555-0001

9. SPONSORING ORGANIZATION - NAME AND ADDRESS (If NRC, type "Same as above", if contractor, provide NRC Division, Office or Region, U. S. Nuclear Regulatory Commission, and mailing address.)
Same as above.

10. SUPPLEMENTARY NOTES

11. ABSTRACT (200 words or less)

This report presents and discusses the results of the U.S. Nuclear Regulatory Commission's integral loss of coolant accident (LOCA) testing program conducted at Studsvik Nuclear AB in Sweden. In this program, refabricated, high burnup irradiated fuel rodlets were subjected to LOCA conditions. In total, six single rod LOCA tests were conducted in the Hot Cell Laboratory at Studsvik Nuclear AB. This report documents the test conditions, rodlet response, and post test examinations for all six tests. The purpose of this document is to make this information available for comparison to related or complementary experimental programs. The observations of fuel fragmentation, relocation, and dispersal in this experimental program may be of particular interest for comparison to related or complementary experimental programs.

12. KEY WORDS/DESCRIPTORS (List words or phrases that will assist researchers in locating the report.)
loss-of-coolant accident, nuclear fuel, fuel fragmentation, fuel relocation, fuel dispersal, Studsvik LOCA tests, high burnup

13. AVAILABILITY STATEMENT
unlimited

14. SECURITY CLASSIFICATION
(This Page)
unclassified
(This Report)
unclassified

15. NUMBER OF PAGES

16. PRICE

Printed
on recycled
paper

Federal Recycling Program

UNITED STATES
NUCLEAR REGULATORY COMMISSION
WASHINGTON, DC 20555-0001

OFFICIAL BUSINESS

NUREG-2160

Post Test Examination Results from Integral, High-Burnup, Fueled LOCA Tests at Studsvik Nuclear Laboratory

August 2013